Gondwana Research xxx (2013) xxx–xxx

Contents lists available at SciVerse ScienceDirect

Gondwana Research

journal homepage: www.elsevier.com/locate/gr

GR Focus Review

# Precambrian greenstone sequences represent different ophiolite types

H. Furnes [a,*], Y. Dilek [b,c], M. de Wit [d]

[a] Department of Earth Science and Centre for Geobiology, University of Bergen, Allégaten 41, 5007 Bergen, Norway
[b] Department of Geology & Environmental Earth Science, Miami University, Oxford, OH 45056, USA
[c] State Key Laboratory of Geological Processes and Mineral Resources, and School of Earth Science and Mineral Resources, China University of Geosciences, Beijing 100083, China
[d] AEON – Africa Earth Observatory Network, and Faculty of Science, Nelson Mandela Metropolitian University 7701, Port Elizabeth, 6031, South Africa

ARTICLE INFO

*Article history:*
Received 14 March 2013
Received in revised form 14 June 2013
Accepted 14 June 2013
Available online xxxx

*Keywords:*
Precambrian greenstone belts
Ophiolite classification
Subduction-related ophiolites
Subduction-unrelated ophiolites
Precambrian plate tectonics

ABSTRACT

We present here a global geochemical dataset from one hundred-and-five greenstone sequences, ranging in age from the Eoarchean through the Archean and Proterozoic Eons that we have examined to identify different ophiolite types (c.f. Dilek and Furnes, 2011) with distinct tectonic origins in the Precambrian rock record. We apply well-established discrimination systematics (built on immobile elements) of basaltic components of the greenstone sequences as our geochemical proxies. The basaltic rocks are classified under two major groups, subduction-related and subduction-unrelated. This analysis suggests that ca. 85% of the greenstone sequences can be classified as subduction-related ophiolites, generated in backarc to forearc tectonic environments. The chemical imprint of subduction processes on the various greenstone sequences is highly variable, but particularly strong for the Archean occurrences, such as the 3.8 Ga Isua (Greenland) and the 3.8–4.3 Ga Nuvvuagittuq (Canada) greenstone belts. Subduction-unrelated greenstone sequences appear to have developed in all phases of ocean basin evolution, through continental rifting, rift–drift tectonics, seafloor spreading, and/or plume magmatism. For the time interval of ca. 3500 million years in the record of Precambrian greenstone evolution, a secular geochemical signature emerges from the oldest to the youngest, in which there is a gradual increase and decrease in the concentrations of incompatible (e.g. Zr) and compatible (e.g. Ni) elements, respectively. The compiled Precambrian greenstone data and our interpretations are consistent with the existence of interactive mantle-lithosphere dynamics, and plate-tectonic-like processes extending back to the Hadean-Archean transition.


**Contents**



* Corresponding author. Tel.: +47 5558 3530; fax: +47 5558 3660.
*E-mail address:* harald.furnes@geo.uib.no (H. Furnes).

1342-937X/$ – see front matter © 2013 International Association for Gondwana Research. Published by Elsevier B.V. All rights reserved.
http://dx.doi.org/10.1016/j.gr.2013.06.004

## 1. Introduction

There is no simple definition of a greenstone belt (de Wit, 2004), but it is a term generally used to describe elongated to variably-shaped terranes of variable length and width, consisting of spatially and temporally related, Archean to Proterozoic intrusive and extrusive ultramafic, mafic to felsic rocks commonly associated with variable amounts and types of metasedimentary rocks, and intruded by granitoid plutons. The term *greenstone* relates to the variety of green minerals such as serpentine, chlorite, epidote, actinolite and hornblende that comprise the main volume of the mafic rocks, showing that they represent low- to medium-grade (most commonly), or even granulite-facies metamorphic rock assemblages. There are about 250 such greenstone belts worldwide; their areal extent varies significantly from small (e.g. Isua, Greenland – 75 $km^2$) to large (e.g. the Lapland Greenstone belt – 50,000 $km^2$), and their mafic component is predominantly tholeiitic basalt, though in some (e.g. the Hattu schist belt, encompassing the many greenstone belts of the Karelian Craton; Rasilainen, 1996) the Mg-rich komatiitic rock may reach ca. 25% (de Wit and Ashwal, 1995, 1997a,b; Hunter and Stove, 1997). For detailed description of the early earth geology, and greenstone belts world-wide, the reader is directed to books and collections of papers in: Windley (1995), Kröner (1981), Condie (1994), Goodwin (1996), de Wit and Ashwal (1995, 1997a), Eriksson et al. (2004), Kusky (2004), and Van Kranendonk et al. (2007a).

The usage of the term "ophiolite" has been rather restricted in connection with Precambrian greenstone belts (de Wit and Ashwal,

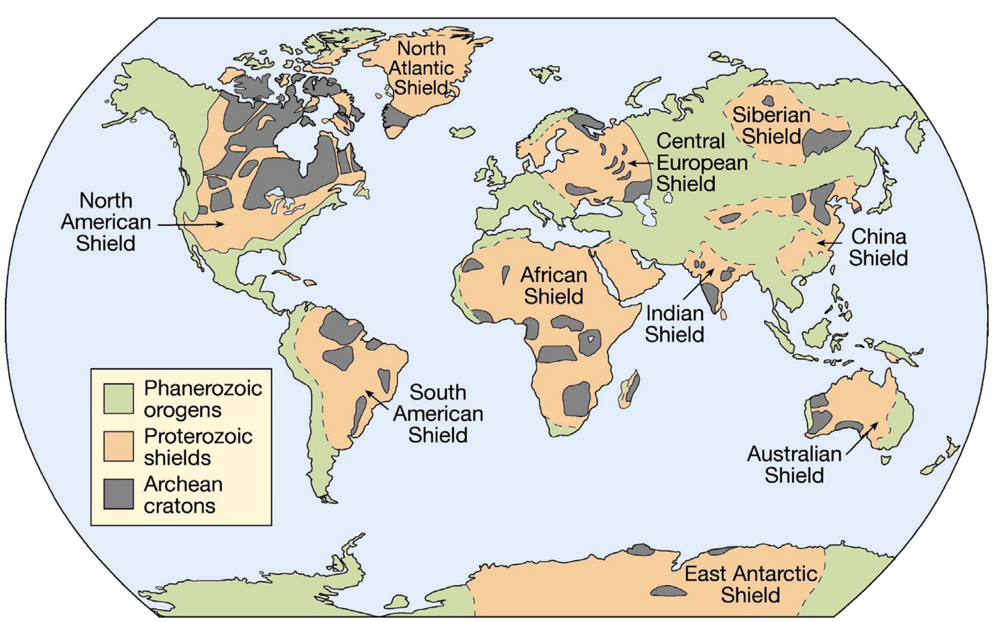


**Fig. 1.** Map showing the World distribution of Phanerozoic rocks, Proterozoic Shields and Archean cratons. Modified from Marshak (2005), Whitmeyer and Karlstrom (2007).

Please cite this article as: Furnes, H., et al., Precambrian greenstone sequences represent different ophiolite types, Gondwana Research (2013), http://dx.doi.org/10.1016/j.gr.2013.06.004

**Table 1**
Summary of selected greenstone sequences.

| Magmatic sequence | Age (Ga) | Lithological components | Suggested tectonic setting | Main reference to geochemical data, geology, and tectonic setting |
|---|---|---|---|---|
| 1. Nuvvuagittuq (NE Canada) | 4.3?–3.8 | Mafic volcanics | Mantle sources metasomatically modified. Suprasubduction ? | O'Neil et al., 2011; Adam et al., 2012 |
| 2. Isua (SW Greenland) | 3.8 | Pillow lavas and volcaniclastics, sheeted dyke complex, gabbro, mantle peridotites | Plume to suprasubduction | Polat et al., 2002; Polat and Hofmann, 2003; Komiya et al., 2004; Furnes et al., 2007, 2009 |
| 3. Pilbara Supergroup (NW Australia) Warrawoona Group | 3.53–3.43 | Mainly basaltic pillow lava, minor felsic and ultramafic lavas, chert layers | Plume magmatism | Van Kranendonk and Pirajno, 2004; Van Kranendonk et al., 2007a,b |
| 4. Pilbara Supergroup (NW Australia) Kelly Group | 3.35–3.29 | Mainly basaltic pillow lava, minor felsic and ultramafic lavas, chert layers | Plume magmatism | Van Kranendonk and Pirajno, 2004; Van Kranendonk et al., 2007a,b |
| 5. Southern Iron Ore Group, (Singhbhum Craton, NE India) | 3.51 | Basaltic pillow lavas, overlain by dacitic volcanic rocks | Suprasubduction zone | Mukhopadhyay et al., 2012 |
| 6. Barberton–Komati Complex (South Africa) | 3.48 | Komatiite to basaltic lavas and intrusive rocks | 1. Oceanic mantle plume 2. Suprasubduction | Dann, 2000; Chavagnac, 2004; Furnes et al., 2012 |
| 7. Barberton–Hooggenoeg Complex (South Africa) | 3.47 | Mainly basaltic pillowed and massive lava, minor komatiitic lava, dyke swarms, mafic-ultramafic intrusions | Suprasubduction | de Wit et al., 2011; Furnes et al., 2011, 2012 |
| 8. Barberton–Kromberg Complex (South Africa) | 3.45 | Basaltic pillowed and massive lava, mafic–ultramafic intrusions, sill swarms | Suprasubduction | de Wit et al., 2011; Furnes et al., 2011, 2012 |
| 9. Barberton–Mendon Complex (South Africa) | 3.33 | Basaltic to komatiitic lava, mafic–ultramafic intrusions | Suprasubduction | Byerly, 1999; de Wit et al., 2011; Furnes et al., 2011, 2012 |
| 10. Nondweni (South Africa) | 3.4 | Ultramafic to mafic flows | Ensialic backarc basin, adjacent to a continental margin | Hofmann and Wilson, 2007 |
| 11. Pietersburg Complex (South Africa) | 3.4 | Pillow lava, gabbro, peridotite | Oceanic-like crust | de Wit et al., 1992 |
| 12. Sargur Group (SW India) | 3.35 | Komatiitic to tholeiitic lava | Plume-arc | Jayananda et al., 2008 |
| 13. Commondale (South Africa) | 3.33 | Komatiite flows and minor intrusives | Subduction-related | Wilson, 2003 |
| 14. Regal Formation (W Australia) | 3.2 | Pillowed and massive lava, hyaloclastite, dykes, BIF/bedded chert, volcaniclastics | Spreading ridge | Ohta et al., 1996; Hickman, 2004; Van Kranendonk et al., 2007b; Hickman, 2012 |
| 15. Whundo Group (Pilbara Craton, NW Australia) | 3.12 | Boninites, interlayered tholeiites, and calc-alkaline volcanic rocks | Introceanic arc setting | Smithies et al., 2005 |
| 16. Ivisaartoc (SW Greenland) | 3.075 | Pillow basalt, gabbros and anorthosite, ultramafic intrusions | Suprasubduction-related oceanic crust | Polat et al., 2008 |
| 17. Ujarassuit (SW Greenland) | 3.07 | Basalts, minor andesites and boninites | Suprasubduction, forearc-backarc | Ordóñez-Calderon et al., 2009 |
| 18. Storø, lower part (SW Greenland) | 3.06 | Basalt lava, minor andesitic volcaniclastics, ultramafics and anorthosite | Subduction-related, no continental contamination | Ordóñez-Calderon et al., 2009 |
| 19. Tartoq Group (SW Greenland) | 3.0 | Tholeiitic pillow lava, sills, dykes, and ultramafic rocks | Suprasubduction | Szilas et al., 2013 |
| 20. Koolyanobbing greenstone (Yilgarn Craton, SW Australia) | 3.0 | Komatiite, boninite, tholeiitic basalt | Suprasubduction | Angerer et al., 2013 |
| 21. Olondo (Siberia, Russia) | 3.0 | Basalt lava and gabbro, ultramafic to mafic sills | Suprasubduction | Puchtel, 2004 |
| 22. Fiskenæsset (SW Greenland) | 2.97 | Thol. basalt, mafic/ultramafic intrusions | Oceanic subduction | Polat et al., 2011 |
| 23. Vedlozero-Sergozero (Karelia, Russia) | 2.921 | Komatiite and tholeiite pillowed and massive lava | Deep (210–240 km) mantle plume | Svetov et al., 2001 |
| 24. Belingwe (Zimbabwe) | 2.9–2.7 | Intrusive and extrusive komatiites, tholeiitic basalt | 1. Intra-oceanic mantle plume 2. Ensialic rift above mantle plume 3. Backarc oceanic crust | Kusky and Kidd, 1992 Bolhar et al., 2003 Hofmann and Kusky, 2004 |
| 25. Kostomuksha (Karelia, Russia) | 2.843 | Komatiite and basalt | Oceanic plateau | Puchtel et al., 1998 |
| 26. Storø, upper part (SW Greenland) | 2.8 | Basaltic flows, minor andesitic volcaniclastics, ultramafics and anorthosite | Intraoceanic suprasubduction | Ordóñez-Calderon et al., 2011 |
| 27. Khizovaara-Iringora (North Karelia, Russia) | 2.8 | Tholeiitic and boninitic lavas, gabbro, rare felsic dykes, metaperidotite bodies | Suprasubduction | Shchipansky et al., 2004 |
| 28. Meekatharra-Cue (Yilgarn, SW Australia) | 2.8–2.76 | Komatiite, komatiite basalt, boninite, tholeiitic basalt, andesite and felsic volcanic and intrusive rocks | Subduction-related magmatism from depleted mantle plume | Wyman and Kerrich, 2012 |
| 29. Tikshozero (Karelia, Russia) | 2.785 | Mainly tholeiite and rare komatiite | Backarc and initial island arc | Mil'kevich et al., 2007 |
| 30. Rio das Velhas Greenstone Belt (Brazil) | 2.772 | Basalt lava, volcaniclastic sediments, BIF, and minor felsic volcanic rocks | Submarine plateau (plume), and island arc/backarc basin | Zucchetti et al., 2000; Baltazar and Zucchetti, 2007; Noce et al., 2007 |
| 31. Carajas Greenstone Belt Grão Pará Group (Brazil) | 2.76 | Basalt lava, dykes/sills and gabbro, jaspilites and some rhyolites | Attenuated continental crust, in backarc setting | Zucchetti, 2007 |
| 32. Taishan (China) | 2.747 | Komatiite–tholeiitic volcanic rocks | 1. Plume-craton interaction 2. Formation at stable continental margin | Polat et al., 2006 Wang et al., 2013 |
| 33. Kushtagi-Hungund (Southern India) | 2.746 | High-Mg pillow basalts and boninites, adakites and rhyolite | Plume-fed oceanic slab, subducted in intraoceanic setting | Naqvi et al., 2006 |

(continued on next page)

**Table 1** (*continued*)

| Magmatic sequence | Age (Ga) | Lithological components | Suggested tectonic setting | Main reference to geochemical data, geology, and tectonic setting |
|---|---|---|---|---|
| 34. Wawa (Superior Province, Southern Canada) | 2.75–2.65 | 1. Tholeiitic and komatiitic lava 2. Calc-alkaline basalt to dacite | 1. Plume<br>2. Island arc | Polat and Kerrich, 2000<br>Polat and Kerrich, 2000 |
| 35. Abitibi (SE Canada) | 2.735–2.670 | Felsic lavas and dykes; subordinate mafic flows and gabbro (lower part); basalt and komatiite flows and gabbro in upper part | Oceanic arc and plume magmatism | Xie et al., 1993; Kerrich et al., 1998; Wyman, 1999a; Sprole et al., 2002; Mueller et al., 2009; Dostal and Mueller, 2013 |
| 36. Yellowknife (Slave Craton, NW Canada) | 2.722–2.658 | Massive and pillowed thol. basalt, gabbro, anorthosite, minor felsic volcanic rocks | 1. Continental margin rift, or 2. backarc setting | Isachsen and Bowring, 1994; Cousens, 2000 |
| 37. Kalgoorlie (Yilgarn Craton, SW Australia) | 2.71 | Basalt and komatiite pillowed & massive flows, gabbro, peridotite | Mantle plume below continental crust | Bateman et al., 2001 |
| 38. Gindalbie & Kurnalpi (Yilgarn Craton, SW Australia) | 2.7 | Mainly basalt and andesite, minor basalt, andesite, dacite and rhyolite | Intra-arc to mature arc-rift | Barley et al., 2008 |
| 39. Wind River (N America) | 2.7 | Basaltic pillow lava, sheeted dykes, gabbro, ultramafic cumulates | Oceanic crust | Harper, 1985; Wilks and Harper, 1997 |
| 40. Gadwal greenstone (Southern India) | 2.7–2.5 | Tholeiitic pillow lavas intercalated with boninites | Intraoceanic subduction, interaction with mantle plume | Manikyamba et al., 2005 |
| 41. Suomussalmi (Baltica, Finland) | 2.65 | Lower komatiites and tholeiitic basalt, upper andesite and felsic volcanic rocks | No suggestion | Jahn et al., 1980 |
| 42. Kuhmo-Tipasjarvi (Baltica, Finland) | 2.65 | Lower komatiites and tholeiitic basalt | No suggestion | Jahn et al., 1980 |
| 43. Bastar greenstone (central eastern India) | 2.6 | Sub-alkaline basalt, basaltic andesite, and boninitic volcanic rocks | Stable continental rift setting | Srivastava et al., 2004 |
| 44. Hutti greenstone (Southern India) | 2.6 | Metabasalts, Mg-andesites, felsic flows | Intra-oceanic subduction | Manikyamba et al., 2009 |
| 45. Zanhuang Complex (China) | 2.5 | Pillow lava, gabbro and ultramafic rocks as blocks in melange | Suprasubduction | Deng et al., 2013 |
| 46. Dongwanzi (China) | 2.5 | Pillow basalt, sheeted dyke complex, gabbro, peridotite | Suprasubduction | Huson et al., 2004 |
| 47a. Krasnaya Rechka structure (Central Karelia, Russia) 47b. Semch structure (Central Karelia, Russia) | 2.5 | Massive and pillowed basalts | Andean continental margin | Svetov et al., 2004; Svetov et al., 2009 |
| 48. Arvarench (Kola, Russia) | 2.429 | Ultramafic to felsic intrusive and volcanic rocks | Intracratonic rifting | Vrevsky, 2011 |
| 49. Kholodnikan greenstone (Siberia, Russia) | 2.41 | Lower komatiite and basalt, upper calc-alk. basalt, andesite, dacite and rhyolite | Ascending mantle plume, followed by secondary melting | Lavrik and Mishkin, 2010 |
| 50. Mazaruni & Barama greenstone (South America) | 2.25 | Lower tholeiitic basalt pillow lava and gabbro, upper part of intermediate and felsic volcanic rocks and minor basalt | Incipient arc or marginal basin | Renner and Gibbs, 1987 |
| 51. Birimian terrane (Western Africa) | 2.1 | Mainly tholeiitic pillow lava, dolerite, gabbro, calc-alkaline andesite-rhyolite | Backarc Immature arc on oceanic crust | Abouchami and Boher, 1990; Sylvester and Attoh, 1992; Vidal and Alric, 1994 |
| 52. Karasjok belt (Baltica, Norway) | 2.1 | Komatiites and tholeiitic basalts | Rift tectonic setting | Pharaoh et al., 1987 |
| 53. Jeesiorova (Baltica, Finland) | 2.056 | Mainly komatiites and komatiitic basalt | Mantle plume | Hanski et al., 2001 |
| 54. Peuramaa (Baltica, Finland) | 2.056 | Mainly basalts, minor basaltic komatiites | Mantle plume | Hanski et al., 2001 |
| 55. Narracoota Formation (W Australia) | 2.0 | Pillow basalt, sheeted dyke complex, layered mafics and ultramafics, boninites | Spreading center in back-arc | Pirajno et al., 1998 |
| 56. Purtuniq ophiolite (Cape Smith Belt, NE Canada) | 2.0 | Pillow basalt, sheeted dyke complex, gab-bro, tr.hjemite, mafic/ultramafic cumulates | Oceanic spreading center | Scott et al., 1991 |
| 57. Nuttio (Baltica, Finland) | 2.0 | Serpentinites, cut by boninitic, tholeiitic to calc-alkaline dykes | Forearc basin in island arc | Hanski, 1997 |
| 58. Pilguyärvi Formation (Pechenga, Russia) | 1.97 | Tholeiitic pillowed and massive basalts, minor felsic volcanic rocks | Red Sea type | Skruf'in and Theart, 2005 |
| 59. Jormua (Baltica, Finland) | 1.95 | Pillow lava, sheeted dyke complex, plagio-granite, gabbro and mantle peridotite | Red Sea type | Peltonen et al., 1996 |
| 60. Birch Lake (Cape Smith Belt, South Canada) | 1.9 | Mainly tholeiitic and bonititic volcanism, mafic–ultramafic intrusions | Juvenile arc setting | Wyman, 1999b |
| 61. Flin Flon (Cape Smith Belt, South Canada) | 1.9 | Tholeiitic, calc-alkaline, alkaline and boninitic subaqueous volcanic rocks | Primitive to mature oceanic arc | Stern et al., 1995 |
| 62. Outokumpu (Baltica, Finland) | 1.9 | Peridotite, gabbro, dykes | Red Sea type, early stage | Peltonen et al., 2008 |
| 63. Kandra (SE India) | 1.85 | Pillow basalt, sheeted dyke complex, layered and isotropic gabbro | Chilean type backarc basin | Vijaya Kumar et al., 2010 |
| 64. Payson (N America) | 1.73 | Pillow lava, sheeted dyke complex, gabbro | Intra-arc basin, followed by sea-floor spreading | Dann, 1992 |
| 65. Chewore ophiolite Kalahari-Congo (Africa) | 1.4 | Pillow lava, sheeted dyke complex, gabbro, serpentinized ultramafic rocks | Marginal basin | Johnson and Oliver, 2000 |
| 66. Bas Draa (Morocco) | 1.38 | Mafic dykes | Rift magmatism | El Bahat et al., 2013 |
| 67. Fraser Complex (SW Australia) | 1.3 | A stack of thrust sheets of mainly pyroxene granulite, garnet amphibolite and metagabbro | Oceanic arc or arcs | Condie and Myers, 1999 |
| 68. Leerkrans Formation (South Africa) | 1.3 | Massive, amygdaloidal basalt and quartz porphyry | Continental back-arc basin | Bailie et al., 2011 |
| 69. Coal Creek Domain (Grenville, North America) | 1.33–1.28 | Serpentinite, gabbro, dykes | Island arc setting | Garrison, 1981, 1985 |
| 70. Queensborough Complex (Grenville, North America) | 1.25 | Pillow lava, dykes and gabbro, cumulate peridotite and pyroxenite | Backarc basin environment | Smith and Harris, 1996 |
| 71. Pie de Palo (South America) | 1.118 | Lava, gabbro and diorite, serpentinite | Suprasubduction | Vujovich and Kay, 1998; Ramos et al., 2000 |

Please cite this article as: Furnes, H., et al., Precambrian greenstone sequences represent different ophiolite types, Gondwana Research (2013), http://dx.doi.org/10.1016/j.gr.2013.06.004

**Table 1** (*continued*)

| Magmatic sequence | Age (Ga) | Lithological components | Suggested tectonic setting | Main reference to geochemical data, geology, and tectonic setting |
|---|---|---|---|---|
| 72. Phulad (NW India) | 1.012 | Pillow lava, sheeted dyke complex, gabbro, harzburgite | Forearc | Volpe and Macdougall, 1990; Shamim Khan et al., 2005 |
| 73. Dunzhugur ophiolite (Siberia, Russia) | 1.02 | Pillow lava, sheeted dyke complex, gabbro and ultramafic cumulates, and mantle tectonites | Suprasubduction, forearc rifting | Khain et al., 2002 |
| 74. Daba & Kui (NW India) | 1.00 | Mafic (gabbroic) bodies | Subduction-related | Pandit et al., 2011 |
| 75. Miaowan (China) | 1.0 | Pillow lava, sheeted dyke complex, gabbro, peridotites | Arc/forearc | Peng et al., 2012 |
| 76. Longsheng ophiolite (China) | 0.977 | Pillow lava, dykes, gabbro, peridotites | Suprasubduction | Li, 1997 |
| 77. Anhui & Jiangxi ophiolites (China) | 0.970 | Pillow basalt and andesite, dolerite, gabbro, diorite, keratophyre and peridotites | Anhui: oceanic crust in continental margin basin<br>Jiangxi: oceanic crust in inter-arc basin | Zhou, 1989; Li et al., 1997<br>Zhou, 1989; Li et al., 1997 |
| 78. Jebel Thurwah (Arabian Shield) | 0.870 | Pillow lava, sheeted dyke complex, vari-textured gabbro, layered mafic and ultra-mafic rocks, harzburgite and dunite | Suprasubduction | Nassief et al., 1984 |
| 79. Darb Zubaydah (Arabian Shield) | 0.830 | Basaltic to andesitic pillow lava and tuff, gabbro and ultramafic cumulates | Intra-arc rifting | Quick, 1990 |
| 80. Bir Umq (Arabian Shield) | 0.838 | Pillow lava, sheeted dyke complex, layered ans isotropic gabbro, basal harzburgite, dunite and pyroxenite | Suprasubduction | Ahmed and Hariri, 2008 |
| 81. Onib (Nubian Shield, Egypt) | 0.808 | Pillow lava, sheeted dyke complex, isotropic gabbro with plagiogranite, layered cumulates, basal peridotites | Suprasubduction | Hussein et al., 2004 |
| 82. Manamedu Complex (India) | 0.800 | Sheeted dyke complex, pl.granite, gabbro and anorthosite, pyroxenite and dunite | Suprasubduction | Yellappa et al., 2010 |
| 83. Older Basement Unit (Republic of Georgia) | 0.800 | Tholeiitic basalt, intruded by gabbro and diorites, harzburgite | Suprasubduction, initiation of island arc | Zakariadze et al., 2007 |
| 84. Fawakhir (Nubian Shield, Egypt) | 0.80–0.70 | Pillow lava, sheeted dyke complex, isotropic gabbro, serpentinized ultramafic rocks | Intra-oceanic subduction zone (incipient arc–forearc) | Abd El-Rahman et al., 2009 |
| 85. Southern Ethiopia | | | | |
| i) Megado | 0.790 | Pillow lava (amphibolites) and gabbro | Suprasubduction, forearc | Yibas et al., 2003 |
| ii) Moyale-El Kur | 0.700–0.660 | Pillow lava (amphibolites) and gabbro | Suprasubduction, forearc | Yibas et al., 2003 |
| 86. Yanbu (Jabal Ess, Al 'Ays) (Arabian Shield) | 0.789 | Volcanic rocks, sheeted dyke complex, plagiogranite, layered cumulate dunite, wehrlite, tectonite harzburgite | Small ocean basin | Ahmed and Hariri, 2008 |
| 87. Tasriwine (Morocco) | 0.762 | Dyke complex, gabbro, pyroxenite, wehrlite, dunite, harzburgite | Arc-related | Samson et al., 2004 |
| 88. Burin Group (Newfoundland, Canada) | 0.760 | Pillowed and massive basalt, minor pyroclastics, abundant gabbro, diabase dykes and sills, peridotite | Oceanic terrane ensimatic arc | O'Driscoll et al., 2001 Murphy et al., 2008 |
| 89. Gabal Gerf (Nubian Shield, Egypt) | 0.750 | Pillow basalt, sheeted diabases, gabbro, serpentinites | Major ocean basin or backarc basin | Zimmer et al., 1995 |
| 90. Wadi Ghadir (Nubian Shield, Egypt) | 0.750 | Pillow basalt, sheeted diabases, gabbro, serpentinites | Backarc basin basalts, contaminated by continental crust | Basta et al., 2011 |
| 91. Wizer (Nubian Shield, Egypt) | 0.750 | Volcanic rocks, gabbros, serpentinites | Forearc | Farahat, 2010 |
| 92. Abu Meriewa (Nubian Shield, Egypt) | 0.750 | Pillow lava, sheeted dyke complex, gabbro, serpentinites | Backarc basin | Farahat, 2010 |
| 93. Wadi Kareim (Nubian Shield, Egypt) | 0.750 | Basalt, diabase, gabbro, and pyroclastic rocks | Backarc basin | Ali et al., 2009 |
| 94. Wadi El Dabbah (Nubian Shield, Egypt) | 0.750 | Basalt and andesite, gabbro, tuffs | Volcanic arc | Ali et al., 2009 |
| 95. Tulu Dimtu (Ethiopia) | 0.750 | Pillowed and massive lava, sheeted dyke complex, gabbroic and ultramafic cumulates, mantle peridotites | Backarc basin | Tadesse and Allen, 2005 |
| 96. Siroua Massif (Morocco) | 0.743 | Pillow lava, sheeted dyke complex, plagiogranite, gabbroic and ultramafic cumulates, peridotites | Marginal sea/island arc | El Boukhari et al., 1992 |
| 97. Jabal al Wask (Arabian Shield) | 0.743 | Massive and pillowed lava, gabbro and trondhjemite, peridotite | Backarc basin | Bakor et al., 1976 |
| 98. Halaban (Arabian Shield) | 0.700 | Mainly gabbro, local massive basalt and trondhjemite | Ensialic backarc basin, suprasubduction | Al-Saleh and Boyle, 2001 |
| 99. Bou Azzer ophiolite (Morocco) | 0.697 | Pillow lava and diabase, keratophyre | Island arc/forearc | Naidoo et al., 1991 |
| 100. Enganepe (Polar Urals, Russia) | 0.670 | Aphyric basalt, overlain by pillow lava intruded by diabase dykes. Blocks of harzburgite, gabbro and plagiogranite in associated melange | Oceanic island arc | Scarrow et al., 2001 |
| 101."Marich" ophiolite (Kenya) | 0.663 | Pillow lava and volcaniclastics, sheeted dyke complex, layered gabbro, serpentinite, dunite, pyroxenite | Arc-related | Ries et al., 1992 |
| 102. Bayankhongor (Mongolia) | 0.647 | Pillow basalt, sheeted dykes, gabbro and plagiogranite, ultramafic cumulates | Mid-ocean ridge | Buchan et al., 2001; Jian et al., 2010 |
| 103. Pirapora (South America) | 0.628 | Pillow lavas, sheeted dyke complex, gabbroic and dunite cumulates | Mature backarc basin | Tassinari et al., 2001 |

(continued on next page)

Please cite this article as: Furnes, H., et al., Precambrian greenstone sequences represent different ophiolite types, Gondwana Research (2013), http://dx.doi.org/10.1016/j.gr.2013.06.004

**Table 1** (*continued*)

| Magmatic sequence | Age (Ga) | Lithological components | Suggested tectonic setting | Main reference to geochemical data, geology, and tectonic setting |
|---|---|---|---|---|
| 104. Chaya Massif, Baikal-Muya (Siberia, Russia) | 0.627 | Peridotites and gabbronorite | Suprasubduction | Amelin et al., 1997 |
| 105. Cele (Turkey) | >0.590 | Diabase, gabbros (anorthosite–troctolite), dunite, lherzolite, wehrlite, ol-websterite | Suprasubduction (arc to backarc) | Yiğitbaş et al., 2004; Bozkurt et al., 2008 |
| 106. Matchless (Namibia) | 0.600 | Pillow lava, sheeted dyke complex, gabbro and serpentinites | Rift-related — Red Sea type | Breitkoff and Maiden, 1988; Klemd et al., 1989 |
| 107. Agardagh Tes-Chem (Mongolia) | 0.569 | Massive and pillowed basalt and basaltic andesite, microgabbro, sheeted dyke complex, ultramafic rocks | Intra-oceanic island arc system and associated backarc basin | Pfänder et al., 2002 |
| 108. Tcherni Vrah & Deli Jovan (Bulgaria/Serbia) | 0.563 | Pillow lava, dykes, gabbro, peridotites | Mid-ocean ridge | Savov et al., 2001 |
| 109. Marlborough (E Australia) | 0.560 | Dolerite, gabbro, harzburgite | Backarc basin | Bruce et al., 2000 |
| 110. Frolosh/Struma (Bulgaria) | 0.560 | Mafic tuff, diabase, diorite, gabbro | Frolosh-basement ophiolite, Struma Diorite (magmatic arc) | Kounov et al., 2012 |
| 111. North Qilian Suture (China) | 0.517 | Lower tholeiitic massive lava and overlying boninitic pillow lava, dykes, gabbro | Suprasubduction initiation at 517 Ma, backarc extension at 487 Ma | Xia et al., 2012 |

Abbreviations: Thol. = tholeiitic; calc-alk. = calc-alkaline; pl.granite = plagiogranite; ol-websterite = olivine-websterite.

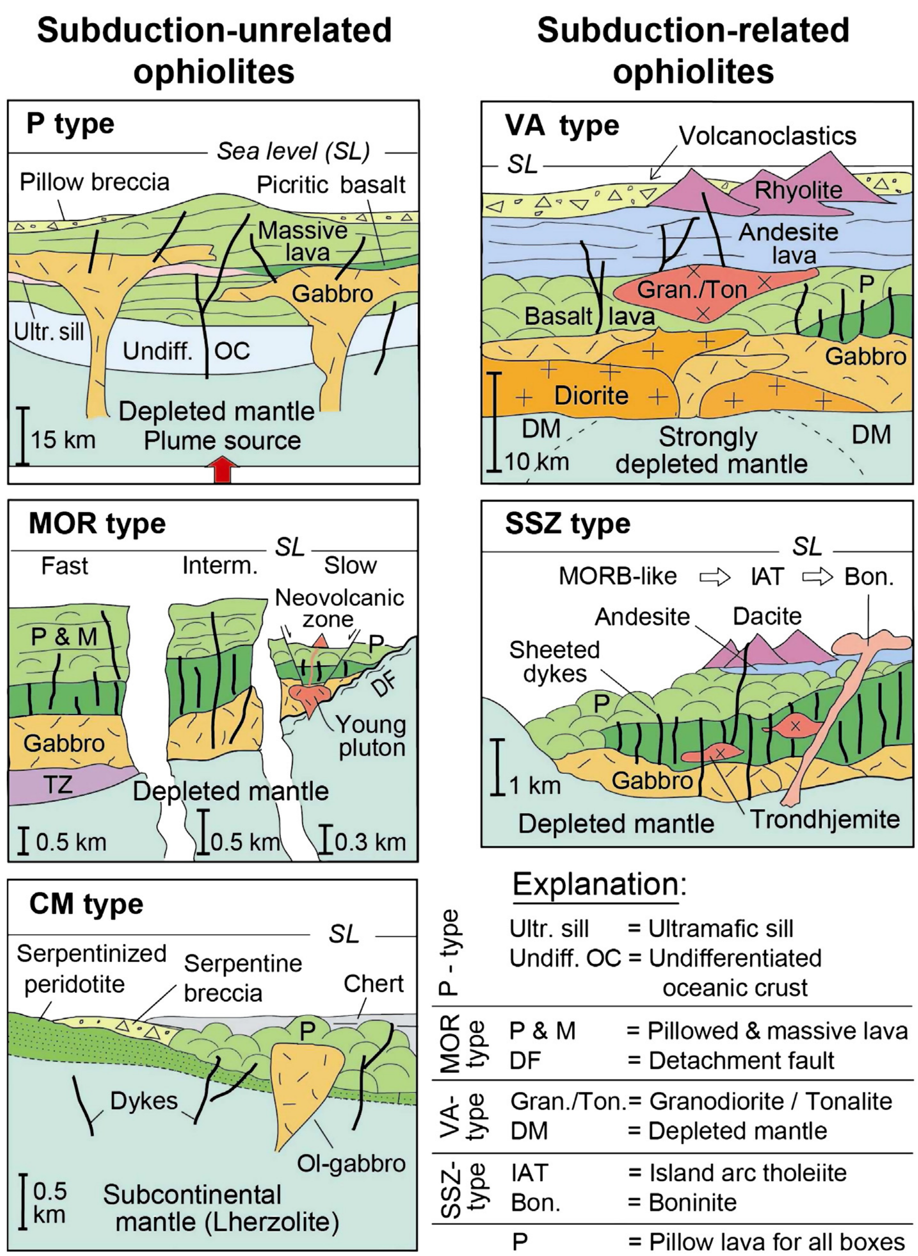


**Fig. 2.** Ophiolite types.
Modifed from Dilek and Furnes (2011), and Furnes et al. (in press).

1997a,b), and the debate as to whether greenstone belts contain ophiolites has been ongoing for some time. Some authors (e.g. Bickle et al., 1994; Hamilton, 1998, 2011) argue that no ophiolites are represented in Precambrian greenstone belts, whereas others (e.g. Dann, 1991; Dann and Bowring, 1997; de Wit and Ashwal, 1997b; St-Onge et al., 1997; Sylvester et al., 1997; Kusky, 2004; Furnes et al., 2007; Dilek and Polat, 2008; Furnes et al., 2009, 2012) report different lines of evidence for their representation. It has been widely accepted that there are well-preserved ophiolites in the Proterozoic rock record that are structurally and geochemically reminiscent of their Phanerozoic counterparts (Windley, 1995). The middle Proterozoic Jormua Complex (1950 Ma) in central Finland contains, for example a well-defined sheeted dyke complex as part of a Penrose-style complete ophiolite sequence (Kontinen, 1987; Peltonen et al., 1998). Later, a 2505 Ma purported example was reported from the North China craton, represented by the Dongwanzi ophiolite complex associated with a large, thick melange zone (Kusky et al., 2001; Kusky and Li, 2002; Li et al., 2002). However, the Dongwanzi Complex as a representative of an ophiolite has been questioned since its components may not be all cogenetic (Zhai et al., 2002; Zhao et al., 2007). The oldest possible Precambrian ophiolite is represented by the ca. 3.8 Ga mafic-ultramafic rocks of the Isua supracrustal belt in Southwest Greenland (Furnes et al., 2007, 2009). Metabasalts and komatiitic rocks of the 3.5–3.3 Ga Barberton greenstone belt in the Makhonjwa Mountains (South Africa) may also represent a section of Archean oceanic crust (de Wit et al., 1987). Much of the Archean ophiolite controversy appears to have stemmed from a common misconception among the greenstone belt community as to the lithological make-up of an idealized ophiolite pseudostratigraphy (de Wit, 2004). Similarly, many ophiolite scientists have divided views about the igneous make-up of the greenstone belts, which are commonly perceived, unlike modern ophiolites, as being dominated by komatiites, although they are not (de Wit and Ashwal, 1997b, and many authors therein).

In this paper we present geochemical data from one hundred-and-five globally distributed greenstone sequences (about 42% of all known greenstone belts) dated from the late Hadean–early Archean through the Proterozoic and into Cambrian (Fig. 1), a range of more than 3500 million years of Earth history, and interpret them in light of the new ophiolite classification system introduced earlier by Dilek and Furnes (2011). We present a brief description of the hundred-and-four examined greenstone belts, their ages and inferred tectonic environment of origin in Table 1. This systematic survey of the Precambrian greenstone belts has significant implications for the understanding and interpretation of the tectonic evolution of the early Earth.

## 2. Ophiolite classification

Ophiolites preserve records of the evolution and destruction of ancient oceanic lithosphere, and are thus important archives for our understanding of the evolution of both accretionary and collisional orogenic belts (Dilek, 2006). Lithological, geochemical and petrological descriptions of Phanerozoic ophiolites are extensive, and the field relations and geochemical characteristics documented in the last 40 years have shown that these fragments of fossil oceanic lithosphere are generated in different tectonic environments (Dilek, 2003; Dilek and Robinson, 2003). The 1972 Penrose definition (Anonymous, 1972) was primarily based on the knowledge at that time of the structural and stratigraphic architecture of the Tethyan (Semail — Oman, Troodos — Cyprus, and the Bay of Islands — Newfoundland, Canada) ophiolites, without any

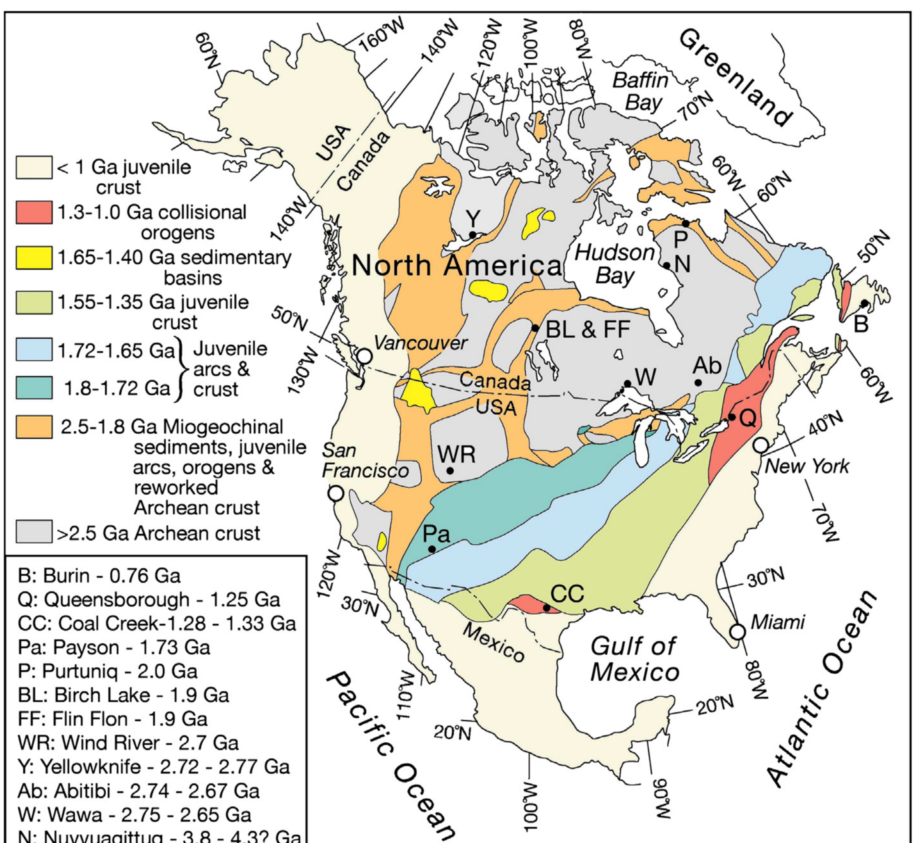


**Fig. 3.** Simplified tectonic map of North America and Canada, showing the locations of investigated greenstone sequences. Modified from Whitmeyer and Karlstrom (2007).

Please cite this article as: Furnes, H., et al., Precambrian greenstone sequences represent different ophiolite types, Gondwana Research (2013), http://dx.doi.org/10.1016/j.gr.2013.06.004

significance attached to the geochemical signature of the ophiolitic units or the tectonic settings of their igneous origin. An idealized, Penrose-type and complete ophiolite section was considered to include from bottom to top: an upper mantle section of peridotites (tectonized harzburgite, lherzolite, dunite), mafic and ultramafic cumulate rocks (gabbro and pyroxenites), isotropic gabbros and plagiogranites, mafic sheeted dykes, a mafic extrusive sequence consisting of pillow and massive lava flows, and pelagic deposits as a sedimentary cover. This ophiolite sequence was regarded to have an approximate layer-cake pseudostratigraphy (Dilek and Eddy, 1992), as a result of seafloor spreading at a mid-ocean ridge setting.

This model has become too simplistic as our knowledge of ophiolites has significantly improved on the basis of our advanced knowledge of the structural architecture and geochemical make-up of different ophiolites and in-situ oceanic crust in the suprasubduction zone environments in different oceans (Dilek, 2003). The seminal paper by Miyashiro (1973) on the island arc origin of the Troodos ophiolite was the first geochemical approach to defining ophiolites and proposed that ophiolites might have formed in other tectonic environments beside mid-ocean ridges. This was a paradigm shift in the ophiolite concept, and led to the definition of suprasubduction zone ophiolites in the early-1980s (Pearce, 1982; Pearce et al., 1984). Systematic petrological and geochemical studies from the 1980s up to now have demonstrated the significance of subduction-derived fluids in the evolution of ophiolitic magmas, indicating that the fossil oceanic crust preserved in most ophiolites may have formed in the upper plate of convergent margins (Dilek and Flower, 2003; Dilek and Robinson, 2003; Flower and Dilek, 2003; Dilek and Thy, 2009). Major differences in the internal structure and stratigraphy of ophiolites and the extreme variations in the geochemistry of their lavas, dykes and upper mantle peridotites, as well as their mode of tectonic emplacement clearly show the 1972 Penrose definition of ophiolites is too restrictive to reflect the herterogeneity in their structure and composition.

Dilek and Furnes (2011) recently defined ophiolites as “suites of temporally and spatially associated ultramafic to felsic rocks related to separate melting episodes and processes of magmatic differentiation in particular oceanic tectonic environments”. In this definition, the geochemical characteristics, internal structure, and thickness of ophiolites vary with the spreading rate, proximity to plumes or trenches, mantle temperature, mantle fertility, and the availability of fluids during their igneous development. These variations are interpreted to have resulted, to the largest extent, from the presence or the lack of subduction influence in ophiolite melt evolution, and thus ophiolites divided into subduction-unrelated and subduction-related categories (Dilek and Furnes, 2011). These two groups are further subdivided, in which the subduction-unrelated ophiolites include continental-margin-, mid-ocean-ridge- (*plume-proximal*, *plume-distal*, and *trench-distal* subtypes), and plume (*plume-proximal ridge* and *oceanic plateaux* subtypes) type ophiolites. The subduction-related ophiolites include suprasubduction-zone type (*backarc to forearc*, *forearc*, *oceanic backarc*, and *continental backarc* subtypes) and volcanic arc type. The first group of ophiolites represents the constructional (rift–drift to seafloor spreading) stage of oceanic crust formation and reflect predominantly mid-ocean-ridge basalt chemical affinities, whereas the second group of ophiolites represents the destructive stages of ocean floor recycling. In this case, ophiolitic units are characterized by variable subduction-related geochemical fingerprints. A compilation of the lithological and structural build-up of the different ophiolite types is shown in Fig. 2.

## 3. Selected greenstone sequences

We describe in this section the hundred-and-five greenstone belts from which the data have been collected, and the general geological setting in which they occur, and report on hundred-and-eleven selected sequences within these identified greenstone belts. We show the regional geology of the major greenstone belts on simplified geological maps in Figs. 3 through 13. Table 1 provides the pertinent literature and our data sources for the greenstone sequences that we describe in this paper. When referring to the subdivisions of the Archean and Proterozoic eons, we have used the time constraints of Walker et al. (2013): Hadean (>4.0 Ga); Eoarchean (4.0–3.6 Ga); Paleoarchean (3.6–3.2 Ga); Mesoarchean (3.2–2.8 Ga); and Neoarchean (2.8–2.5 Ga); Paleoproterozoic (2.5–1.6 Ga); Mesoproterozoic (1.6–1.0 Ga); and Neoproterozoic (1.0–0.541 Ga).

According to this new time scale of Walker et al. (2013), 104 of the hundred-and-five examined greenstone belts are of Precambrian age; only one, the ophiolitic sequence of the North Qilian Suture, China (517 Ma, see Table 1, no. 111) is of Cambrian age.

### *3.1. North America/Canada*

Several Archean and Paleoproterozoic greenstone belts occur in the North American/Canadian shield (Fig. 3). The Eoarchean Nuvvuagittuq greenstone belt in eastern Canada with rocks as old as 4.3 Ga (Table 1, no. 1) represents the oldest one among these North American greenstone belts (O'Neil et al., 2008). The recent detrital zircon dating of

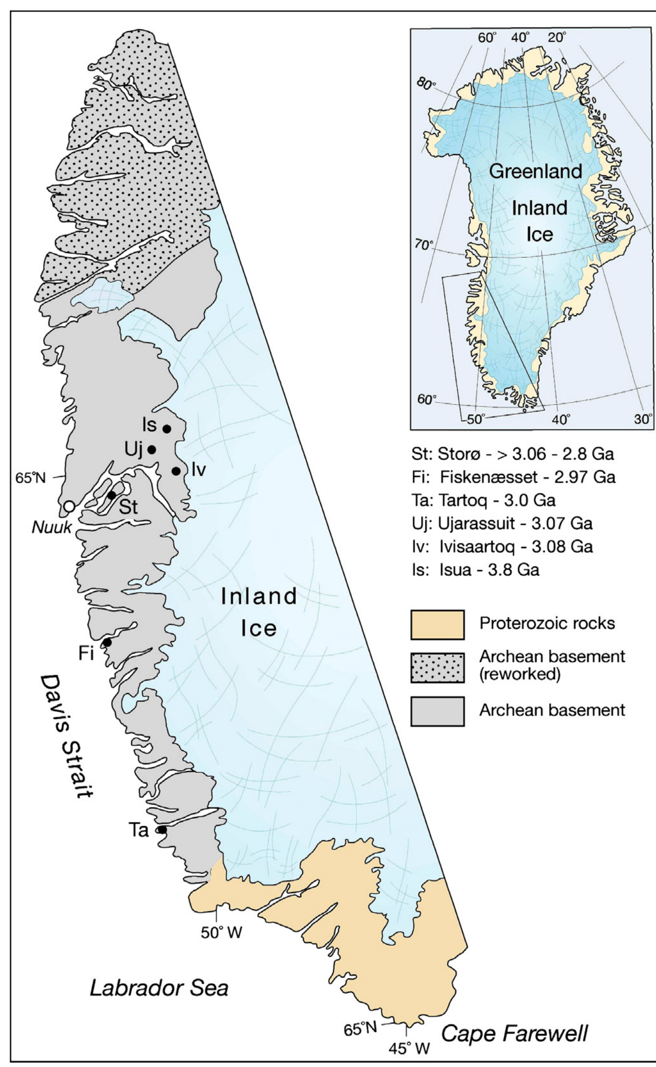


**Fig. 4.** Simplified tectonic map of SW Greenland showing the locations of investigated greenstone sequences.
Modified from Henriksen et al. (2009).

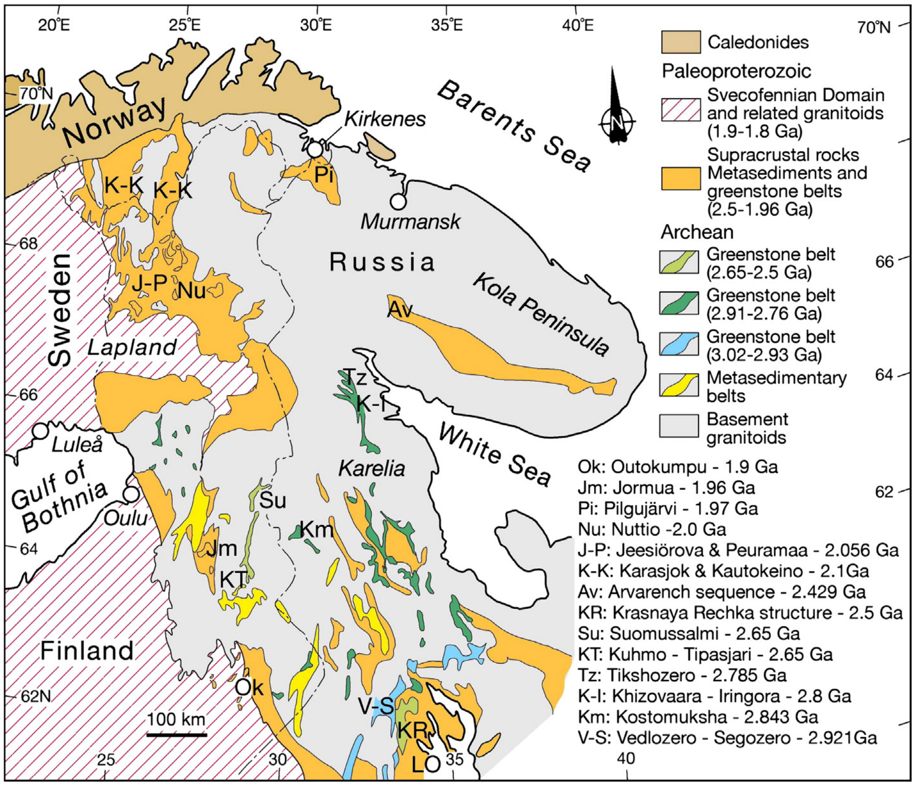


**Fig. 5.** Simplified tectonic map of Baltica showing the locations of investigated greenstone sequences. Karelia area: modified from Heilimo et al. (2010); Lapland area: modified from Hanski et al. (2001); Kola Peninsula: modified from Skruf'in and Theart (2005).

quartzites and quartz-schist in this belt has yielded the ages around 3.8 Ga age (Cates et al., 2013), younger than the previously reported ages of ~4.3 Ga. Four of the investigated sequences are around 2.7 Ga (Fig. 3, Table 1. nos. 34–36, 39). The northernmost of these is the 2.722–2.658 Ga Yellowknife greenstone belt of the southern Slave Province in Canada (Isachsen and Bowring, 1994, 1997), and its dominant lithology comprises volcanic and plutonic rocks of the 2.722–2.701 Ga Kam Group (Cousens, 2000; Corcoran et al., 2004). The ca. 2.7 Ga Schreiber–Hemlo greenstone belts within the Wawa Subprovince (2750 to 2650 Ma) of the Superior Province in Canada include

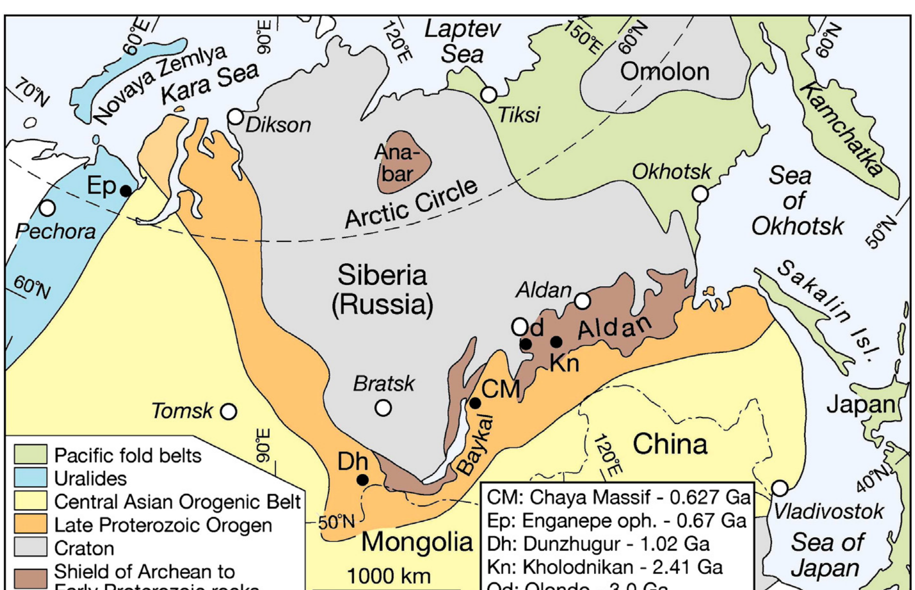


**Fig. 6.** Simplified tectonic map of Siberia and the northern part of the Uralides the locations location of investigated greenstone sequences. Modified from Jahn (2004).

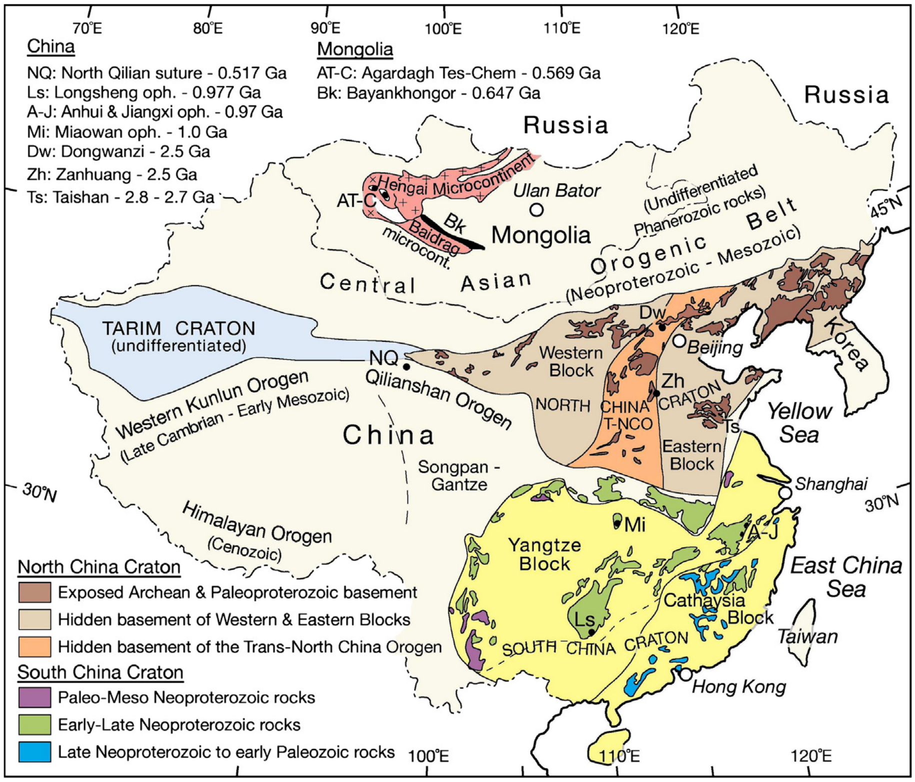


**Fig. 7.** Simplified tectonic map of China and Mongolia showing the distribution of investigated greenstone sequences. China: modified from Zhao and Cawood (2012); Mongolia, modified from Jian et al. (2010).

two distinct extrusive rock associations (Polat et al., 1998, 1999; Polat, 2009). The early volcanic complex (2750–2725 Ma) consists mainly of voluminous tholeiitic basalts and Al-undepleted komatiites that are capped by basaltic lavas transitional to alkaline compositions and Al-depleted komatiites. The extensive Abitibi greenstone belt in the southeastern part of Canada developed during the time span 2.735–2.67 Ga (e.g. Corfu, 1993; Mueller et al., 2009). The oldest part of the sequence (the Hunter Mine Group) consists mainly of felsic subaqueous flows and intrusions and gabbro, whereas the stratigraphically higher parts (the Stoughton-Roquemaure Group) are dominated by pillowed and massive mafic to ultramafic lava flows and intrusions (Scott et al., 2002; Mueller et al., 2009; Dostal and Mueller, 2013). The Wind River

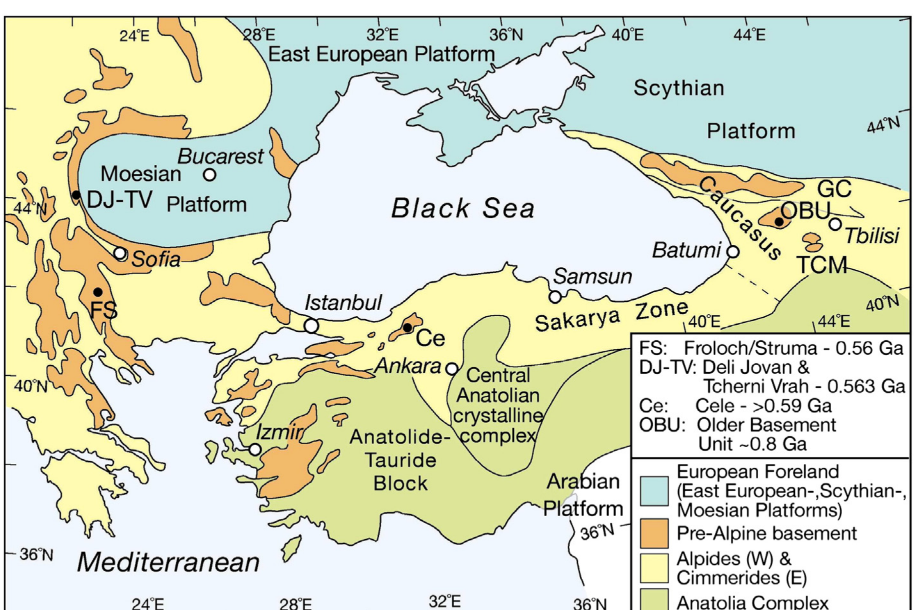


**Fig. 8.** Simplified tectonic map of southeast Europe showing the distribution of investigated greenstone sequences. GC: Great Caucasus; TCM: Transcaucasian Massif. Modified from: Şengör et al. (1984), Zakariadze et al. (2007), Okay et al. (2008), Kounov et al. (2012).

Please cite this article as: Furnes, H., et al., Precambrian greenstone sequences represent different ophiolite types, Gondwana Research (2013), http://dx.doi.org/10.1016/j.gr.2013.06.004

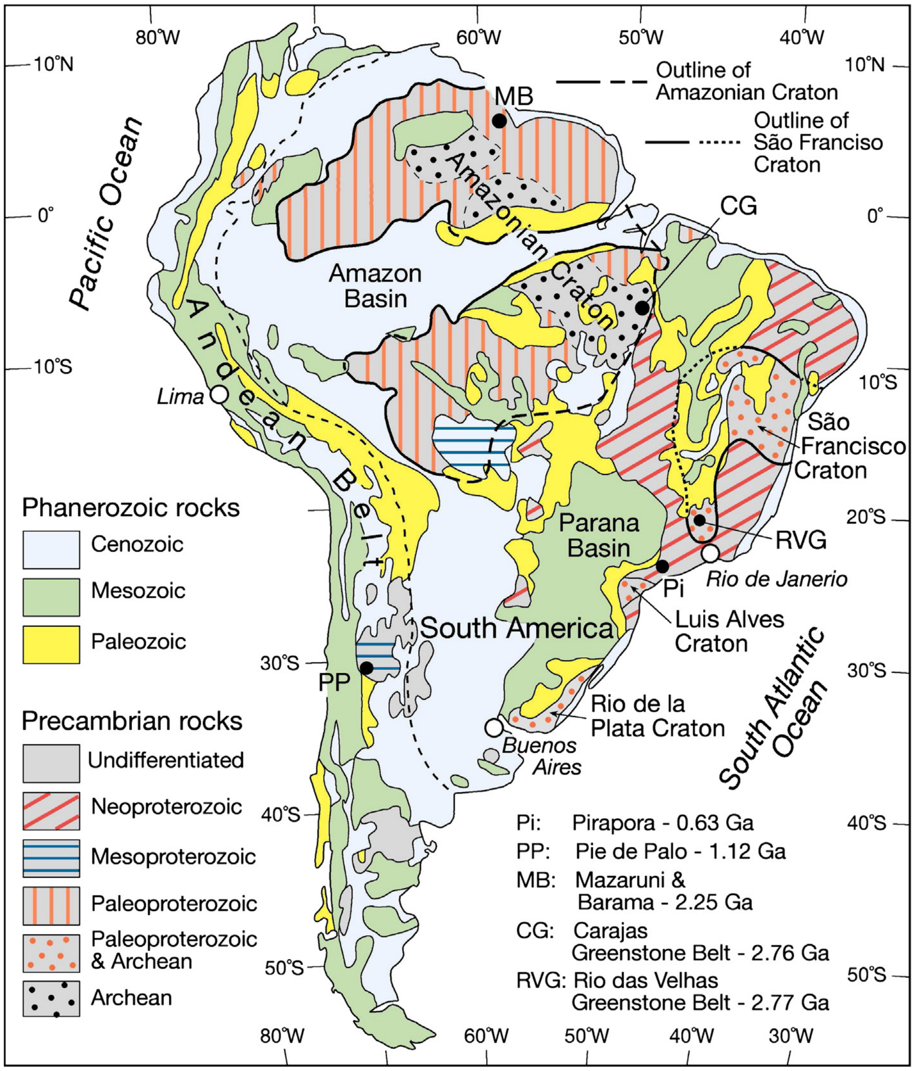


**Fig. 9.** Simplified tectonic map of South America showing the distribution of the two major cratons (Amazonian and São Francisco Cratons) and investigated greenstone sequences. Modified from: Baars (1997), Tassinari (1997), Tassinari and Macambira (1999), Cordani et al. (2000, 2009), Sato et al. (2003), Baltazar and Zucchetti (2007), Oyhantçabal et al. (2011). The outline of the Amazonian and São Francisco Cratons are from Cordani et al. (2009).

Mountains in Wyoming (USA) contains mafic volcanic and plutonic rocks along the margin of a 2.7 Ga granodiorite batholith (Fig. 3). This mafic rock assembly has been interpreted previously as an Archean ophiolite (Harper, 1985; Wilks and Harper, 1997).

The three greenstone sequences represented by the Paleoproterozoic (2.0 to 1.9 Ga) Purtuniq (Cape Smith Belt), Birch Lake and Flin Flon complexes (Fig. 3, Table 1, nos. 56, 60, 61) are all part of the Trans-Hudson Orogen, representing one of the most significant crustal building events in the evolution of North America (e.g. Wyman, 1999a,b). The Paleoproterozoic (1.73 Ga) Payson ophiolite (Fig. 3, Table 1, no. 64), situated within the Mazatzal crustal block in Arizona (USA), contain all the mafic volcanic and plutonic components of a Penrose-type ophiolite (Dann, 1992, 1997). The Mesoproterozoic Queensborough (1.25 Ga) and the Coal Creek (1.28–1.33 Ga) are part of the Grenville province of the eastern USA (Fig. 3, Table 1, nos. 70 and 69, respectively). The youngest Proterozoic magmatic sequence in North America that we consider in this study is the Burin Group (0.76 Ga) in the Avalon Zone of the southeast Newfoundland Appalachians (Fig. 3, Table 1, no. 88).

### 3.2. Greenland

Fig. 4 shows the distribution of the six major greenstone sequences in southwest Greenland. The oldest of these is the 3.7–3.8 Ga Isua supracrustal belt. Despite strong polyphase deformation and amphibolite grade metamorphism, the primary seafloor spreading features in the Isua rocks are still recognizable. The Isua greenstone contains all the components of a Penrose-type ophiolite (Furnes et al., 2007, 2009). Detailed descriptions of this greenstone belt, both in terms of field observations and the geochemistry of its magmatic units are given in Rosing et al. (1996), Nutman et al. (1997), Polat et al. (2002), Polat and Hofmann (2003), Komiya et al. (1999, 2004), and Furnes et al. (2009). The other five greenstone sequences in SW Greenland (Ivisaartoq, Ujarassuit, Tartoq, Fiskenæsset, and Storø), are all around 3 billion years old and include fragments of oceanic lithosphere that formed in (see references in Table 1, nos. 16–19, 22) arc, forearc, and/or backarc tectonic settings (Polat et al., 2008; Ordóñez-Calderon et al., 2009; Polat et al., 2011; Szilas et al., 2013). They hence represent SSZ-type ophiolites (Dilek and Furnes, 2011).

### 3.3. Baltica (NW Russia, Finland, Norway)

Fig. 5 depicts the occurrence and distribution of the fourteen investigated Precambrian greenstone sequences from the Fennoscandian shield of Baltica. The main part of the exposed Archean magmatic rocks occurs within the Karelian region (eastern Finland and northwestern Russia). The Paleoproterozoic rocks included in this study are from

Please cite this article as: Furnes, H., et al., Precambrian greenstone sequences represent different ophiolite types, Gondwana Research (2013), http://dx.doi.org/10.1016/j.gr.2013.06.004

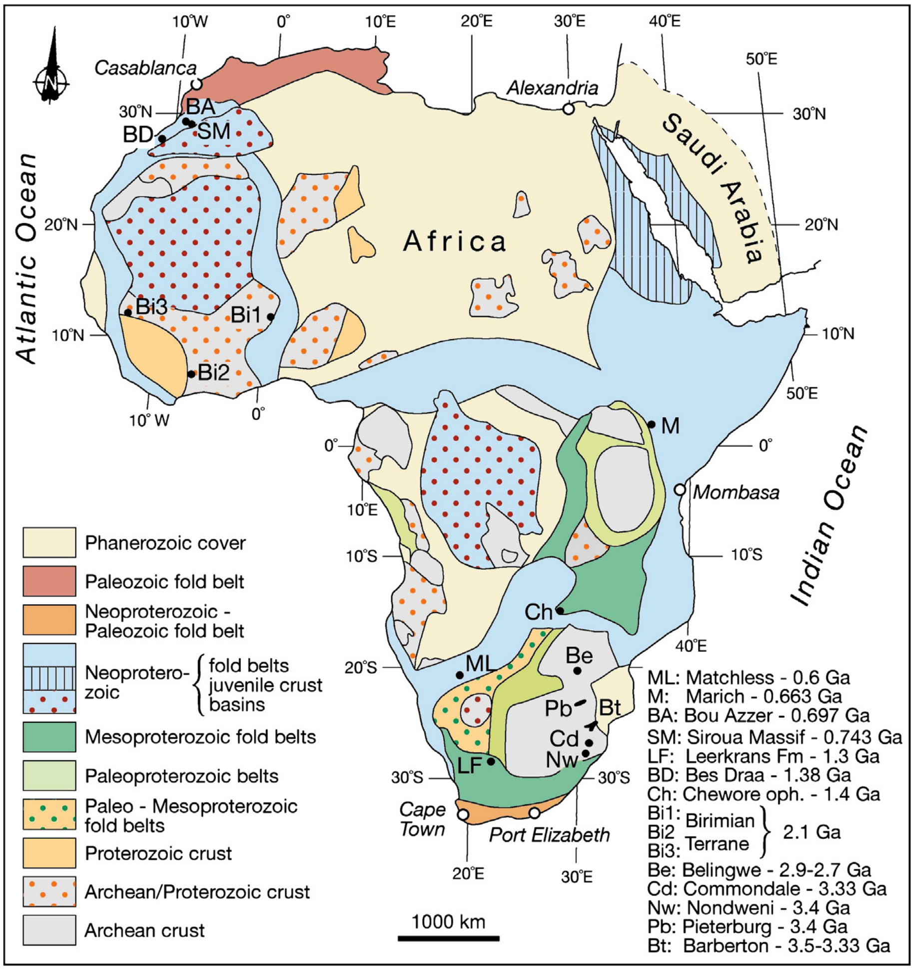


**Fig. 10.** Simplified tectonic map of Africa showing the distribution of investigated greenstone sequences. Modified from Begg et al. (2009).

the western and northwestern parts of Finland, north Norway, and the Kola Peninsula (Fig. 5). Six of these Baltica greenstone sequences are of Archean age (2.9–2.65 Ga), and all occur in the Karelian region. They consist of komatiitic and tholeiitic extrusive and intrusive rocks with plume to suprasubduction zone affinities (see description in Table 1, nos. 23, 25, 27, 29, 41, 42). Two of the Baltica greenstone sequences (Table 1, nos. 46 and 47) straddle the Archean–Proterozoic boundary (2.5–2.4 Ga). Of the six remaining Paleoproterozoic greenstone sequences (2.1–1.9 Ga) four occur in Finland, one in Norway, and one in the NW Kola Peninsula (Fig. 5, and description in Table 1, nos. 52–54, 57–59). These Paleoproterozoic volcanic and intrusive sequences are predominantly of tholeiitic basalt type.

### 3.4. Siberia (Russia)

The location and the general geological setting of five greenstone complexes in Siberia are shown in Fig. 6. The Archean to early Proterozoic Aldan Shield includes the 3.0 Ga Olondo and the 2.41 Ga Kholodnikan greenstone belts (Table 1, nos. 21 and 49) in the southern margin of the Siberian Craton (Fig. 6). The Olondo greenstone belt is the larger of these two in the Aldan Shield, and contains an assortment of well-preserved mafic to ultramafic rocks (Puchtel, 2004). The Kholodnikan greenstone belt consists of a lower-amphibolite unit of volcanic komatiites and basaltic rocks, and an upper calc-alkaline volcanic–sedimentary unit (Lavrik and Mishkin, 2010). The late Proterozoic Dunzhugur (1.02 Ga) and Chaya magmatic complexes (0.627 Ga) occur in the northern part of the Central Asian Orogenic Belt (CAOB) (Fig. 6, Table 1, nos. 73 and 104), and are bounded by the Siberian and North China cratons (Jahn, 2004). The CAOB was formed by a series of successive accretions of island arc complexes in the early Paleozoic. The Dunzhugur complex includes genetically related volcanic, intrusive and upper mantle rocks, and represents a complete Penrose-like ophiolite complex (Khain et al., 2002). The Chaya Massif includes only gabbros and peridotites (Amelin et al., 1997).

The Neoproterozoic 0.67 Ga Enganepe magmatic complex is located in the Polar Urals (Fig. 6, Table 1, no. 100), and comprises a volcanic sequence (mainly pillow lavas) that is intruded by mafic dykes; a melange unit composed of blocks of peridotite, gabbro and plagiogranites is spatially associated with this complex (Scarrow et al., 2001). These rocks in the melange are thought to have once made up the upper mantle and crustal units of a complete ophiolite complex.

### 3.5. China and Mongolia

Fig. 7 shows a simplified tectonic map of China and Mongolia. The three oldest examined greenstone belts (Archean), are the 2.5 Ga Dongwanzi and Zanhuang complexes and the 2.7 Ga Taishan complex (Table 1, nos. 32, 45, 46), located in the North China Craton (Fig. 7).

Please cite this article as: Furnes, H., et al., Precambrian greenstone sequences represent different ophiolite types, Gondwana Research (2013), http://dx.doi.org/10.1016/j.gr.2013.06.004

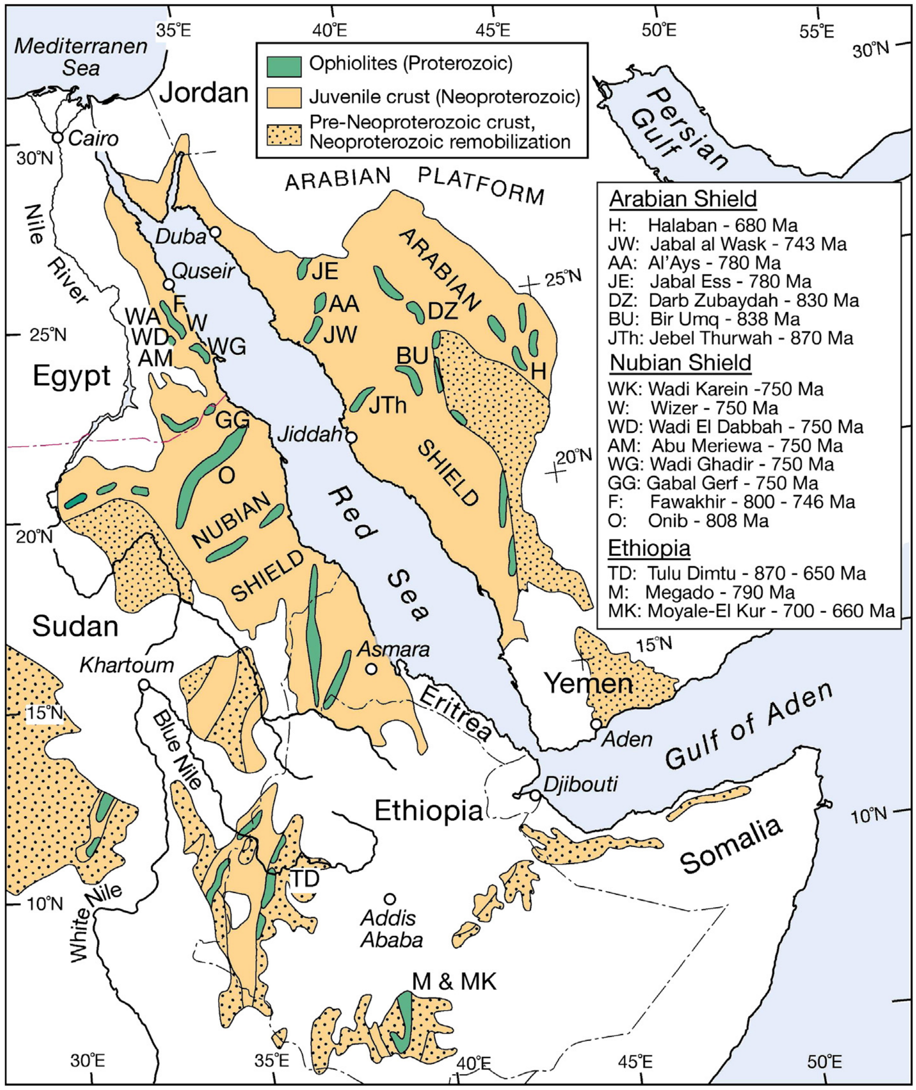


**Fig. 11.** Simplified tectonic map of the Arabian–Nubian Shield showing the distribution of investigated greenstone sequences. Modified from Dilek and Ahmed (2003) and Yibas et al. (2003).

The Taishan complex is situated in the eastern termination of the Eastern Block, whereas the Dongwanzi and Zanhuang complexes are part of the Trans-North China orogen (Fig. 7). The Dongwanzi complex is controversial because U–Pb zircon dating of its mafic and ultramafic units has yielded Mesozoic ages around 300 Ma (Zhao et al., 2007), although it was reported earlier as an Archean ophiolite complex (Kusky et al., 2001), a conclusion still maintained by Kusky and Zhai (2012). The Proterozoic mafic–ultramafic rocks, represented by the Miaowan, Longsheng and Anhui/Jiangxi sequences are all located within the Yangtze Block of the South China Craton (Fig. 7, Table 1, nos. 75–77). We included in this study the Cambrian sequence in the North Qilian suture which is situated at the boundary between the Tarim Craton and the North China Craton, as part of the Qilianshan Orogen (Fig. 7, Table 1, no. 111).

We have used the late Proterozoic Bayankhongor and the Agardagh Tem-Chem complexes in Mongolia (e.g. Buchan et al., 2001, 2002; Pfänder et al., 2002; Jian et al., 2010) in our database for this study (Table 1, nos. 102 and 107). They both occur in the western part of Mongolia, and are part of the Central Asian Orogenic Belt (Fig. 7). The Bayankhongor area hosts two ophiolites of different ages, a late Proterozoic (660–640 Ma) ophiolite as reported here, and a Permo-Triassic (ca. 298–210 Ma) ophiolite, as documented by Jian et al. (2010). According to Wilhem et al. (2012), the late Proterozoic ophiolite formed during the evolution of the Altaids, whereas the Permo-Triassic ophiolite developed in a narrow rift at the eastern end of the Mongol–Okhotsk Ocean.

### 3.6. Southeast Europe

We have examined four Neoproterozoic (0.56–0.8 Ga) greenstone sequences with ophiolite fragments around the Black Sea that constitute part of the Pre-Alpine basement (Fig. 8; Savov et al., 2001; Bozkurt et al., 2008; Kounov et al., 2012). The Transcaucasian Massif in the Greater Caucasus also includes MORB-like metabasic rocks, described as part of a ca. 0.8 Ga Proterozoic ophiolite (OBU; Fig. 8; Zakariadze et al., 2007). For more details, see Table 1, nos. 83, 105, 108, and 110.

### 3.7. South America

Fig. 9 shows the five greenstone sequences investigated in South America that we have examined in this study. The three oldest ones include the Neoarchean (2.77 Ga) and Paleoproterozoic (2.25 Ga) rocks of the Amazonian and Sao Francisco Cratons (Fig. 9) and

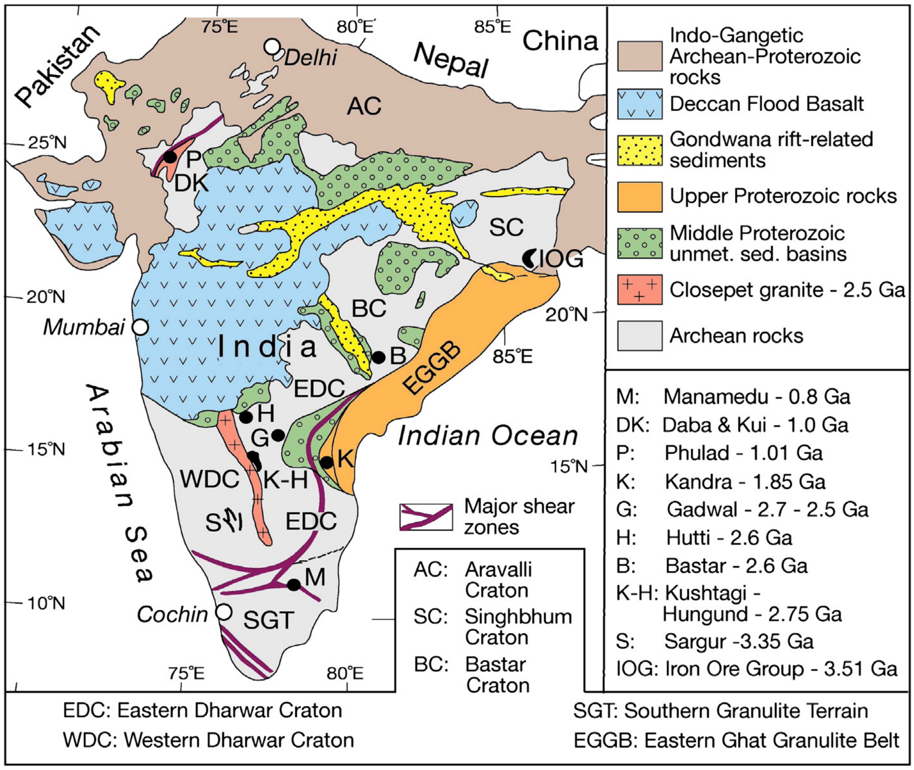


**Fig. 12.** Simplified tectonic map of India showing the distribution of investigated greenstone sequences.
Modified from: Naqvi and Rogers (1987), Shamim Khan et al. (2005), Santosh and Sajeev (2006), Meert et al. (2010), Yellappa et al. (2010), Dharma Rao et al. (2011).

consist of basalt lavas, gabbroic dykes and sills, minor intermediate to felsic lavas, volcanoclastics and BIF/jaspers deposits (Renner and Gibbs, 1987; Zucchetti et al., 2000; Baltazar and Zucchetti, 2007; Noce et al., 2007; Zucchetti, 2007) (Table 1, nos. 30, 31, no. 50). A Mesoproterozoic (1.12 Ga) greenstone sequence composed of mafic lavas and intrusive rocks occurs in the western Sierras Pampeanas (Argentina) of the Andean Belt (Fig. 9, Table 1, no. 71). The youngest, a Neoproterozoic (0.63 Ga) sequence with a complete Penrose-type ophiolite stratigraphy (Table 1, no. 103) occurs along the eastern coast of Brazil (Fig. 9).

### 3.8. Africa

Several Archean greenstone belts occur within the Kaapvaal Craton of the southern part of Africa (Fig. 10). In this study we have examined the Paleoarchean Barberton (~3.5–3.3 Ga), Pietersburg and Nondweni (~3.4 Ga), Commondale (~3.3 Ga) and the Mesoarchean (Belingwe ~2.9–2.7 Ga) greenstone belts (e.g. de Wit et al., 1987; Armstrong et al., 1990; de Wit et al., 1992; Lopez- Martinez et al., 1992; Kröner et al., 1996; Parman et al., 1997; Byerly, 1999; Lowe and Byerly, 1999; Lowe et al., 1999; Dann, 2000; Chavagnac, 2004; Dann and Grove, 2007; Lowe and Byerly, 2007; de Wit et al., 2011; Furnes et al., 2011, 2012, 2013). These greenstone belts, and in particular the well-preserved volcanic and intrusive rocks of the Barberton greenstone belt (BGB), have been the focus of numerous studies over several decades. These include inter alia the classical work of Viljoen and Viljoen (1969), in which the volcanic sequence of the BGB was subdivided into formations (currently redefined as Complexes, de Wit et al., 2011), collectively now defined as the Onverwacht Suite. Although the existing tectonic models regarding the origin and evolution of the Archean greenstone belts in Africa vary considerably, the subduction zone involvement in their formation is widely accepted (see Table 1, nos. 6–11, 13, 24).

The Paleoproterozoic Birimian greenstone sequence in the southern part of the West African Shield (Fig. 1) comprises mainly tholeiitic basaltic lavas and intrusive rocks, and calc-alkaline intermediate to felsic rocks (Table 1, no. 51). The Mesoproterozoic greenstone units are represented by the basaltic lava sequences of the 1.3 Ga Leerkrans Formation of the Wilgenhoutsdrif Group (Bailie et al., 2011), the Chewore ophiolite of the Zambezi/Irumbide Belt of southern Africa, and the Bas Draa rift-related dykes in northwest Africa (Figs. 1 and 10; Table 1, nos. 65, 66, 68). The Neoproterozoic greenstone sequences (0.6–0.73 Ga) are from the Matchless belt in Namibia, the Marich sequence in Kenya, and the Bou Azzer and Siroua Massif in Morocco (Fig. 10, Table 1, nos. 96, 101, 106).

### 3.9. Arabian/Nubian Shield

The Arabian–Nubian Shield comprises a large number of Neoproterozoic greenstone belts with ages between 0.6 and 0.8 Ga, but mainly around 0.75 Ga (Fig. 11). The greenstone sequences from the Nubian Shield are summarized in Table 1, nos. 81, 84, 85, 89–95, and those for the Arabian Shield in Table 1, nos. 78–80, 86, 97, and 98. These greenstone belts are allochthonous and mark various suture zones and sites of tectonic amalgamation of disparate island arc complexes (Stern et al., 1990; Harms et al., 1994; Stern, 1994; Küster and Liégeois, 2001; Abdelsalam et al., 2002; Stern, 2002; Abdelsalam et al., 2003; Stern and Johnson, 2010; Johnson et al., 2011). Structural and geochemical studies (see summary in Dilek and Ahmed, 2003) have shown that some of these arc complexes represent suprasubduction zone oceanic lithosphere.

### 3.10. India

Fig. 12 is a simplified tectonic map of India showing the ten greenstone sequences we have examined in this study. Six of these are of Archean age (Fig. 10). The Iron Ore Group and Sargur sequences are of Paleoarchean age, whereas the Kushtagi-Hungund, Bastar, Hutti, and Gadwal sequences are of Neoarchean age (Table 1, nos. 5, 12, 33,

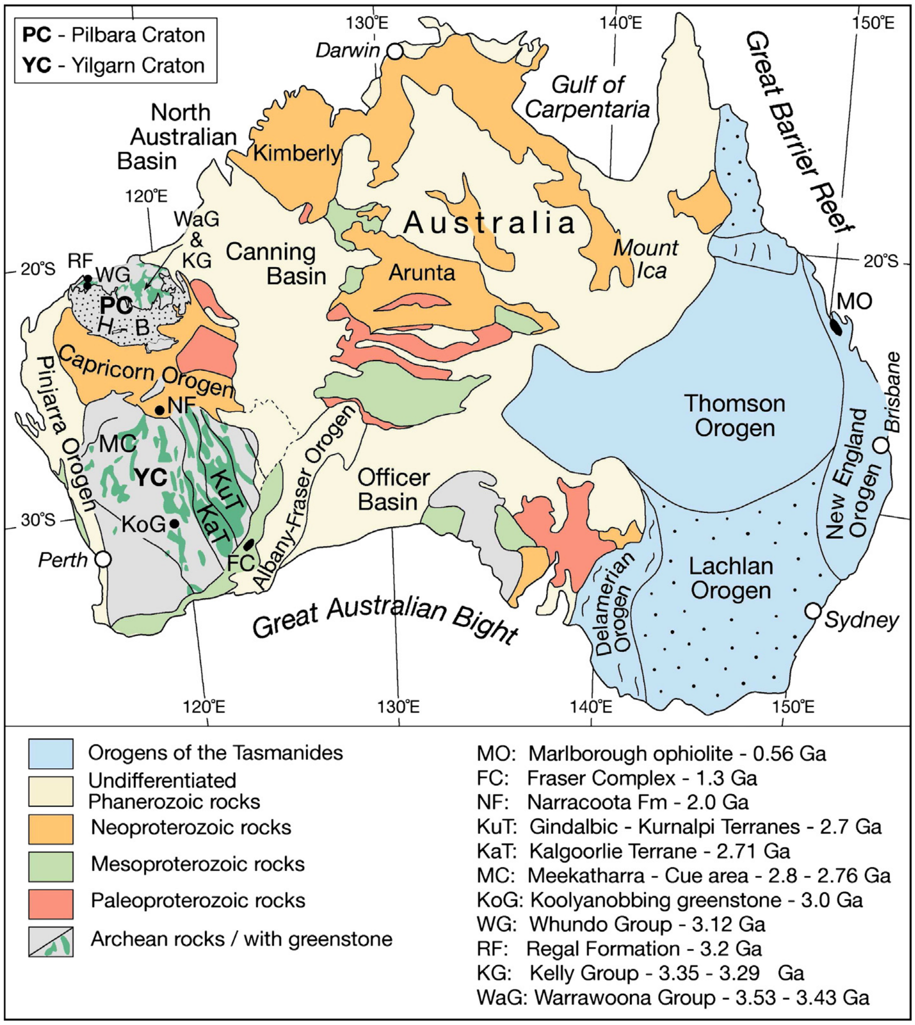


**Fig. 13.** Simplified tectonic map of Australia showing the distribution of investigated greenstone sequences. H-B (of the Pilbara Craton) stands for: Hammersley Basin. Modified from: Pirajno et al. (1998), Condie and Myers (1999), Pirajno and Occhipinti (2000), Van Kranendonk et al. (2001), Fitzsimons (2003), Cawood and Tyler (2004), Glen (2005), Van Kranendonk et al. (2007b), Barley et al. (2008), Kemp et al. (2009), Czarnota et al. (2010), Spaggiari et al. (2011), Hickman (2012), Pawley et al. (2012).

40, 43 and 44). The Paleoproterozoic Kandra, the Mesoproterozoic/Neoproterozoic Phulad and Daba/Kui, and the Neoproterozoic Manamedu greenstone sequences make up the other significant occurrences. The Paleoarchean sequences are dominated by basaltic and komatiitic volcanic units, whereas the Neoarchean sequences consist mainly of tholeiitic basalts and boninites (see Table 1). The Proterozoic sequences Kandra, Phulad and Manamedu (Table 1, nos. 63, 72, 82) are characterized by basaltic lavas, sheeted dyke complexes, gabbros, and peridotites, representing typical Penrose-type ophiolites, whereas the Daba & Kui sequence consists of gabbro (Table 1, no. 74).

### 3.11. Australia

Fig. 13 is a simplified tectonic map of Australia, showing the ten investigated greenstone sequences that range in age from 3.12 Ga to 0.56 Ga. Of the eight Archean examples the Warrawoona (3.53–3.43 Ga), and Kelly (3.35–3.29 Ga) Groups are the oldest (Paleoarchean) in the Pilbara Supergroup (Table 1, nos. 3 and 4) (Van Kranendonk et al., 2007b), whereas the three next oldest, the Whundo, Regal and Koolyanobbing complexes, are of Mesoarchean age (Table 1, nos. 14, 15 and 20). The three others are Neoproterozoic in age (Table 1, nos. 28, 37, 38). The oldest of the Proterozoic sequences is the Paleoproterozoic Narracoota Formation (2.0 Ga) within the Capricorn Orogenic belt (Table 1, no. 55), whereas the Mesoproterozoic Fraser Complex (1.3 Ga) is part of the Albany-Fraser Orogenic belt (Fig. 13, Table 1, no. 67). The much younger Marlborough complex (0.56 Ga) is part of the New England Orogen, which is part of the Tasmanides (Fig. 13, Table 1, no. 109). The geochemical composition of the magmatic rocks in all these complexes is dominated by tholeiitic basaltic pillow lavas; boninitic compositions are reported from most of the complexes (even the oldest Whundo complex), as well as calc-alkaline mafic to felsic rocks in some (see Table 1).

The Pilbara Craton of (Fig. 2) is one of the classical areas for contrasting views concerning the origin of its Paleoarchean greenstone sequences, i.e. whether they formed as a result of horizontal versus vertical tectonic processes. The eastern greenstone sequences of the Pilbara Craton are interpreted to have experienced collision and terrane accretion analogous to the Phanerozoic orogenic belts (e.g. Kloppenburg et al., 2001; Blewitt, 2002), as well as diapiric rise of granitoid domes resulting in convective overturn of the middle to upper crust (e.g., Hickman, 2004; Van Kranendonk et al., 2007b).

### 3.12. Stratigraphic columns

Fig. 14 shows the composite stratigraphic columnar sections of a selection of eleven Archean and seven Proterozoic greenstone sequences that we have examined in this study. For comparison three Phanerozoic

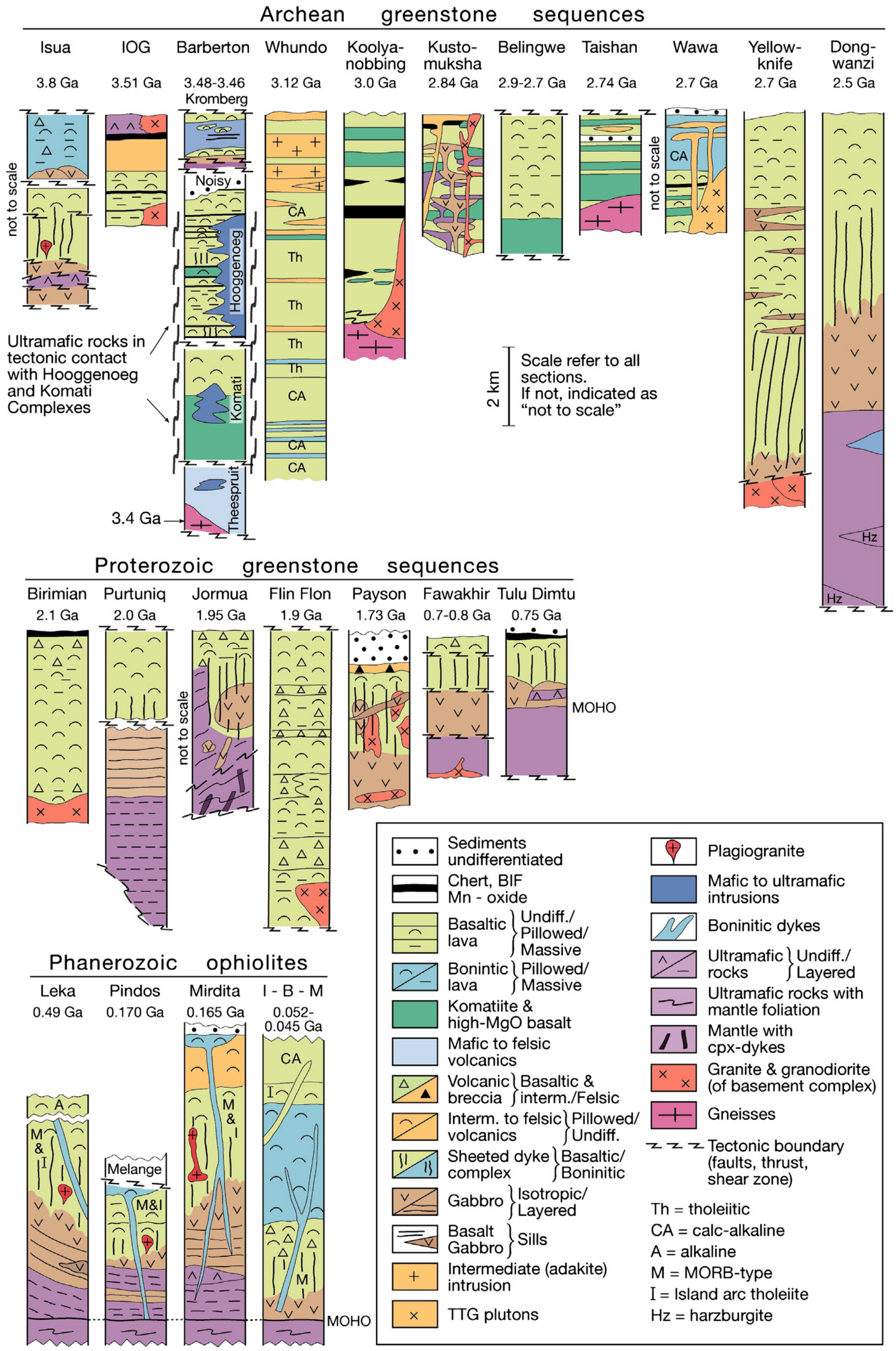


**Fig. 14.** Stratigraphic columnar sections of a selection of 11 Archean and 7 Proterozoic greenstone belts, and three Phanerozoic ophiolite complexes and the Izu-Bonin-Mariana sequence for comparison.

Data from: Isua, Greenland (Furnes et al., 2009); IOG, India (Mukhopadhyay et al., 2012); Barberton, South Africa (de Wit et al., 2011; Furnes et al., 2012); Whundo, Australia (Smithies et al., 2005); Koolyanobbing, Australia (Angerer et al., 2013); Kustomuksha, Karelia, Russia (Puchtel et al., 1998); Belingwe, South Africa (Hofmann and Kusky, 2004); Taishan, China (Polat et al., 2006); Wawa, Canada (Polat et al., 1998); Yellowknife, Canada (Corcoran et al., 2004); Dongwanzi, China (Kusky et al., 2001); Birimian, West African Craton (Sylvester and Attoh, 1992); Purtuniq, Canada (Scott et al., 1992); Flin Flon, Canada (Lucas et al., 1996); Jormua, Finland (Peltonen et al., 1996); Payson, North America (Dann, 1997); Fawakhir, Egypt (Abd El-Rahman et al., 2009); Tulu Dimtu, Etiopia (Tadesse and Allen, 2005); Leka, Norway (Furnes et al., 1988); Mirdita, Albania and Pindos, Greece (Dilek and Furnes, 2009); Izu-Bonin-Mariana (Ishizuka et al., in press).

ophiolites, and one in-situ oceanic crustal sequence, represented by the Izu-Bonin-Mariana system, are also shown. The Precambrian greenstone sequences are highly variable with respect to their thicknesses, ranging from less than 2 km (Taishan) to more than 12 km (Dongwanzi). However, the original thickness for these sequences is unknown, since the basal parts, and in many cases the upper parts, are commonly defined by faults

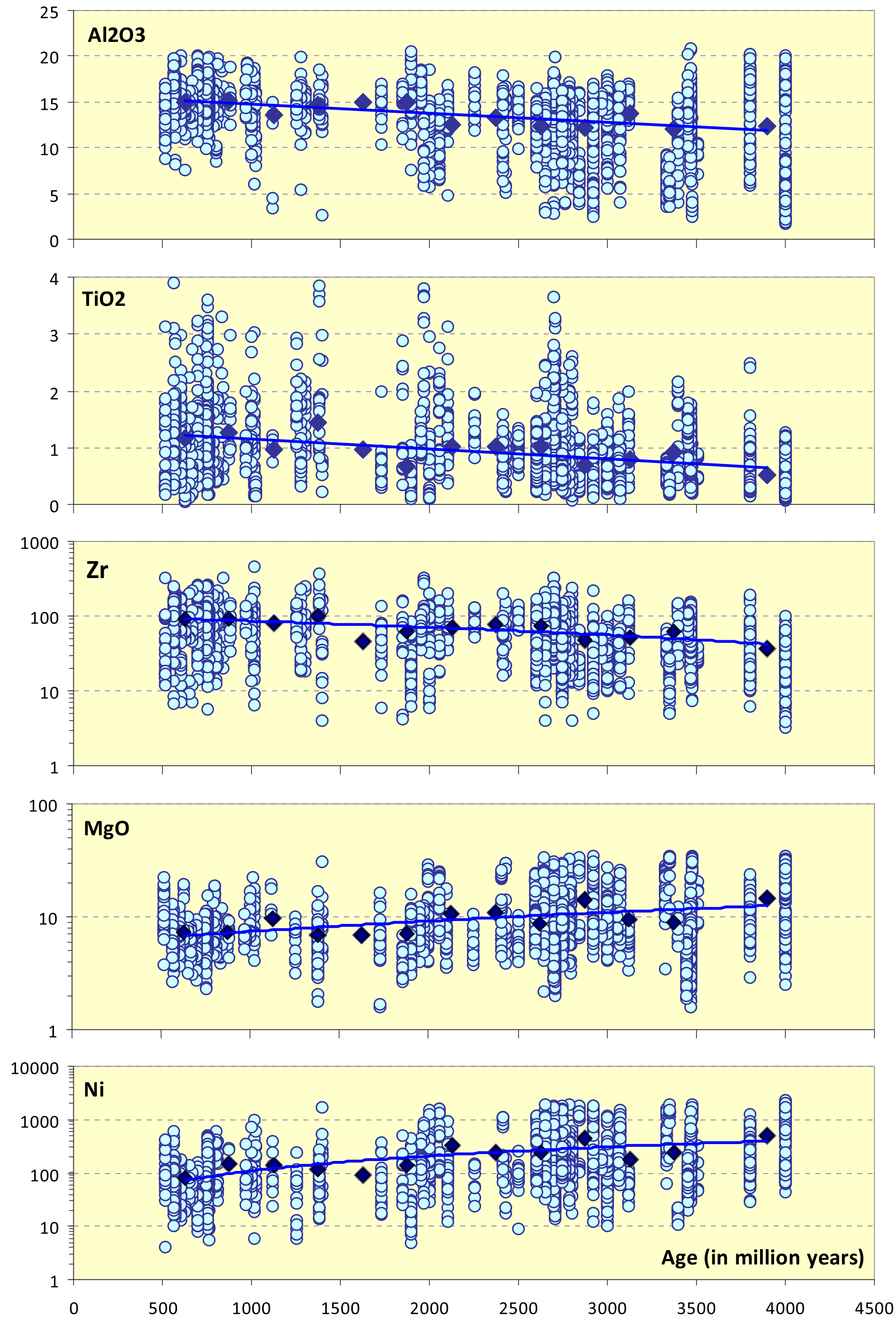


**Fig. 15.** All geochemical data ($Al_2O_3$, $TiO_2$, MgO, Zr and Ni) plotted against age.

(Fig. 14). Most of the Precambrian greenstone belts are composed dominantly of pillowed to massive basaltic lava units that are locally associated with hyaloclastites and volcanic breccias. Komatiites and high-MgO basalts (komatiitic basalts) are common, albeit in minor amounts in the 2.7 Ga and older sequences. However, some exceptions occur, as in the Taishan greenstone sequence (China), and in the lower part of the Komati Complex of the Barberton greenstone belt, where komatiites and high-MgO basalts predominate (Fig. 14). Boninite-like rocks are uncommon in the Precambrian greenstone sequences, but they have been reported from the 3.8 Ga Isua (SW Greenland) and the 3.12 Ga Whudo (W Australia) greenstone sequences (see Table 1 and Fig. 14).

Most Precambrian oceanic basalts, komatiitic basalts and komatiites, and Phanerozoic ophiolites include oceanic sediments (Fig. 14), which provide important information about the tectonic environments of their origin, such as a major ocean, backarc or forearc basin, or a rift basin. The pelagic and turbiditic sedimentary sequence associated with the 3.8 Ga Isua complex (Komiya et al., 1999), and the abundant occurrences of silicified chert associated with the mafic volcanic lavas of the 3.5–3.3 Ga Onverwacht Suite of the Barberton Greenstone Belt (e.g. de Wit et al., 2011, and Fig. 14) represent some of the oldest sedimentary units in the Archean greenstone record. Although we acknowledge the importance of these sedimentary packages associated with the

Please cite this article as: Furnes, H., et al., Precambrian greenstone sequences represent different ophiolite types, Gondwana Research (2013), http://dx.doi.org/10.1016/j.gr.2013.06.004

Precambrian greenstone sequences, we do not discuss their role in our classification of the greenstone belts here since this topic is beyond the scope of this paper.

The topic of the origin of komatiite formation is a subject of controversy. In one model, komatiites are envisioned to have been formed by high degrees of melting of dry peridotites through mantle plume activity (e.g. Arndt et al., 2008). The other model assumes partial melting of a wet, depleted mantle above subduction zones (e.g. Parman and Grove, 2004); in this latter model komatiites are regarded as the Archean equivalent of modern boninites. Thus, if some of the komatiitic rocks are interpreted as the counterparts of modern boninites, the magmatic evolution of the Archean greenstone sequences may not be much different from that of the Proterozoic subduction-related ophiolites, in which boninites are common (see Fig. 14).

Intermediate to felsic volcanic products may occur as the extrusive counterparts of granodioritic intrusions in some of the greenstone sequences, such as in the Wawa greenstone belt in Canada (Fig. 14). Chert and BIFs are commonly interlayered with the lava piles of the 3.0 Ga and older greenstone sequences. Sheeted dyke complexes are common in the 2.7 Ga and younger greenstones, and they also occur in the much older greenstones such as the 3.8 Ga Isua belt. Dyke and sill swarms, together with abundant mafic to ultramafic intrusions occur in the 3.5 Ga Barberton greenstone belt (Fig. 14). Upper mantle peridotites exist in the 3.5 Ga Barberton and the 2.5 Dongwanzi (China) greenstone belts, but their origin and significance in the petrological evolution of these Archean sequences are less clear. These upper mantle rocks are more common in the upper Proterozoic ophiolites (Fig. 14).

We depict in Fig. 14 the igneous stratigraphy of three Phanerozoic ophiolites, together with an in-situ oceanic equivalent (the I-B-M) showing the typical lithological association and the structural architecture of subduction-related (suprasubduction), Penrose-type ophiolites (Fig. 14). Of the Precambrian greenstones shown in Fig. 14, all, except four (Kostomuksha, Taishan, the initial part of Wawa, and Jormua), are regarded to represent subduction-related sequences (Table 1).

## 4. Geochemistry

### 4.1. Selection of elements

In order to constrain the usage of geochemical data in a meaningful way, the secondary mobility of elements during low-temperature

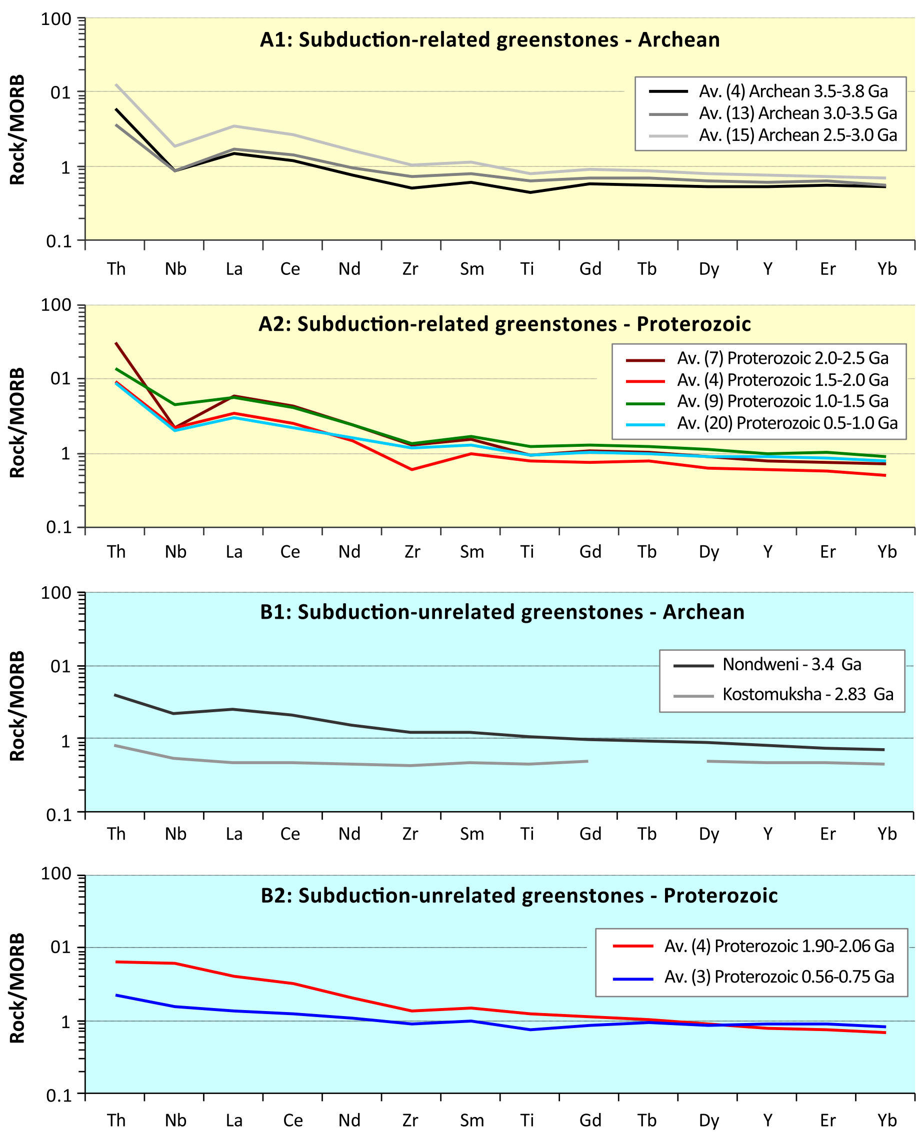


**Fig. 16.** MORB-normalized diagrams.
MORB values from Pearce and Parkinson (1993).

Please cite this article as: Furnes, H., et al., Precambrian greenstone sequences represent different ophiolite types, Gondwana Research (2013), http://dx.doi.org/10.1016/j.gr.2013.06.004

alteration and greenschist to amphibolite grade metamorphism of basaltic rocks has to be evaluated. This has been done in numerous studies before, and the general conclusion is that the elements Ti, Al, Cr, Ni, Co, V, Y, Zr, Nb, REE and Th are little affected (e.g. Scott and Hajash, 1976; Coish, 1977; Hellman et al., 1979; Staudigel and Hart, 1983; Seyfried et al., 1988; Gillis and Thompson, 1993; Komiya et al., 2004; Hofmann and Wilson, 2007; Dilek et al., 2008; Furnes et al., 2012). For the present study, we have used Al, Ti, Mg, Ni, V, Zr, Y, Nb, REE and Th in our evaluation of the geochemical characteristics of the Precambrian greenstones. Some of the above-mentioned studies show that MgO has been disturbed to variable degrees by post-eruptive alteration; however, its range in concentration is so large that it is still considered to be useful in the characterization of the rocks.

### 4.2. Age-related geochemical variations

The concentrations of $Al_2O_3$, $TiO_2$, MgO, Zr and Ni for all the geochemical data (from 3030 samples) used for this study have been plotted against age, and time averages for 250 m.y. intervals (Fig. 15). There is a large scatter in the element concentration at any age interval. For $Al_2O_3$, $TiO_2$ and Zr there is a general increase, and for MgO and Ni a decrease in the average concentrations from the oldest towards the youngest rocks.

To test whether they are subduction-related or subduction-unrelated, a powerful characterization of metabasaltic can be visualized by MORB-normalized trace element patterns, using immobile trace elements. The elements used here are: Th, Nb, La, Ce, Zr, Sm, Ti, Gd, Tb, Dy, Y, Er and Yb, and they are arranged in this order, from the most (Th) to the least (Yb) incompatible elements during mantle melting (Pearce and Parkinson, 1993). We have MORB-normalized the samples and have plotted them in multi-element diagrams that from the published literature, easily can be classified as either subduction-related or subduction-unrelated, particularly based on the behavior of Nb and/or Ta. The majority of the metabasalts are subduction-related. We show the average of the Archean and Proterozoic samples in Fig. 16A1 and A2, divided into time intervals of 500 million years. They all show the same pattern, i.e. a markedly increasing concentration towards the most incompatible elements, and a marked negative Nb-anomaly (for most of the samples). But, in general there is a shift towards higher element concentration from

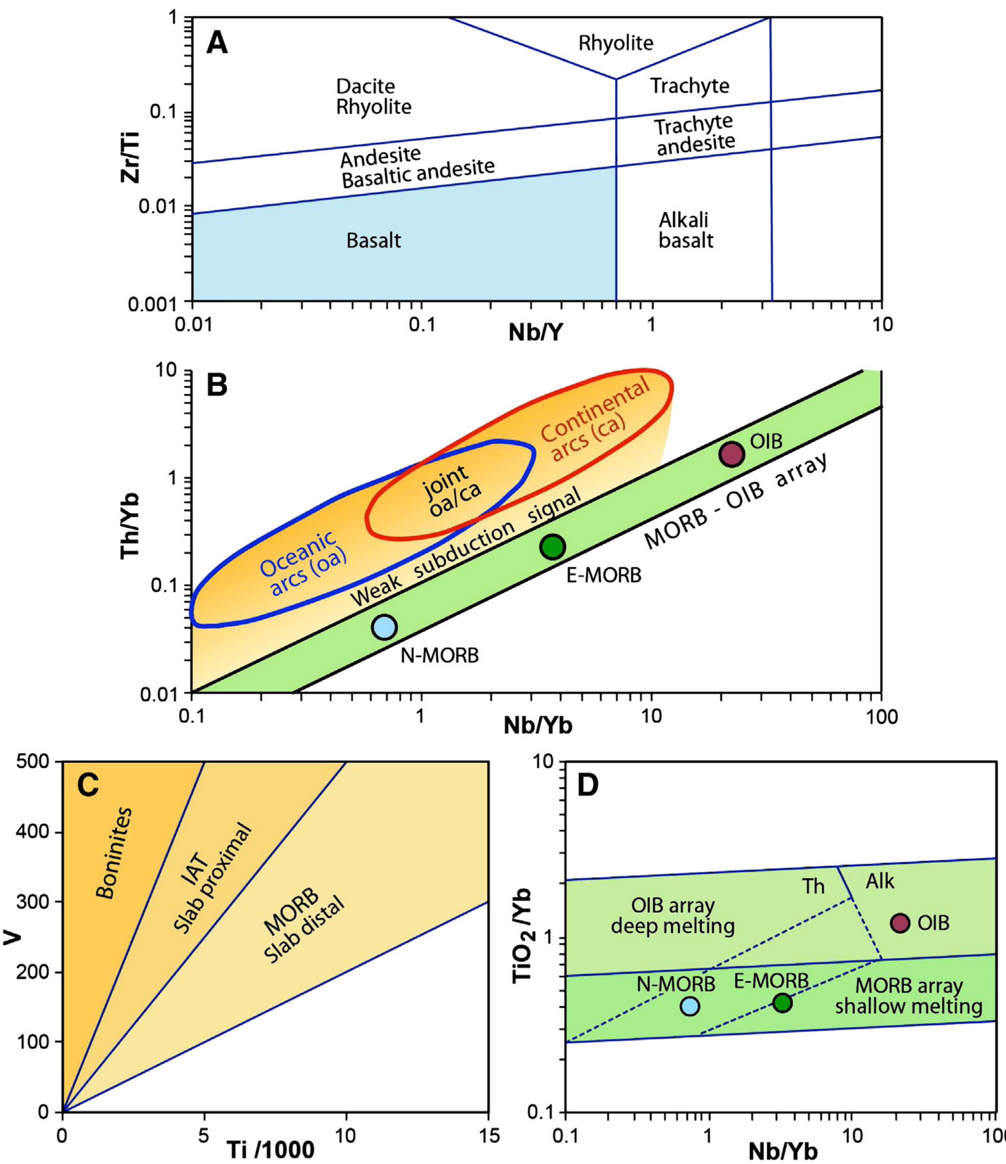


**Fig. 17.** Proxies (A: Zr/Ti–Nb/Y; B: Th/Yb–Nb/Yb; C: V–Ti/1000; D: $TiO_2$/Yb–Nb/Yb) for rock classification and tectonic setting. After Pearce (2008, in press).

the oldest to the youngest. In Fig. 16B1 and B2 the MORB-normalized patterns of the subduction-unrelated samples are shown, and these samples define nearly flat, to only slightly enriched (in the most incompatible elements) patterns, without negative Nb-anomalies.

### *4.3. Proxies for rock classification and tectonic setting*

The first geochemical diagram made to distinguish between basalts from different tectonic environments is the one based on Ti, Zr and Y (Pearce and Cann, 1971). Subsequently, more elements, such as Cr and V, found to be rather stable during alteration and metamorphism, were employed to further construct discrimination diagrams (Pearce, 1975; Shervais, 1982). Later, as access to more low-concentration, incompatible trace elements, such as REE, Th, Nb, Ta, and Hf became more common, further element combinations were used to constrain the tectonic environment in which basaltic rocks were formed. The patterns of MORB-normalized, multi-element diagrams have shown to be highly efficient to distinguish between subduction-related and subduction-unrelated basalts (Pearce et al., 2005; Pearce, 2008, in press).

#### *4.3.1. Rock classification*

Classification of magmatic rocks has traditionally been done by the total alkali-silica (TAS) diagram of Le Bas and Streckeisen (1991). However, the elements (K, Na and Si) used in this classification diagram are highly mobile (particularly K and Na) during alteration and metamorphism, and are therefore not suitable for classification of greenstones. A more suitable diagram for this purpose is the Zr/Ti–Nb/Y diagram of Floyd and Winchester (1975), in which the ratios of Zr/Ti and Nb/Y are proxies for $SiO_2$ and ($Na_2O + K_2O$), respectively (Fig. 17A). In our

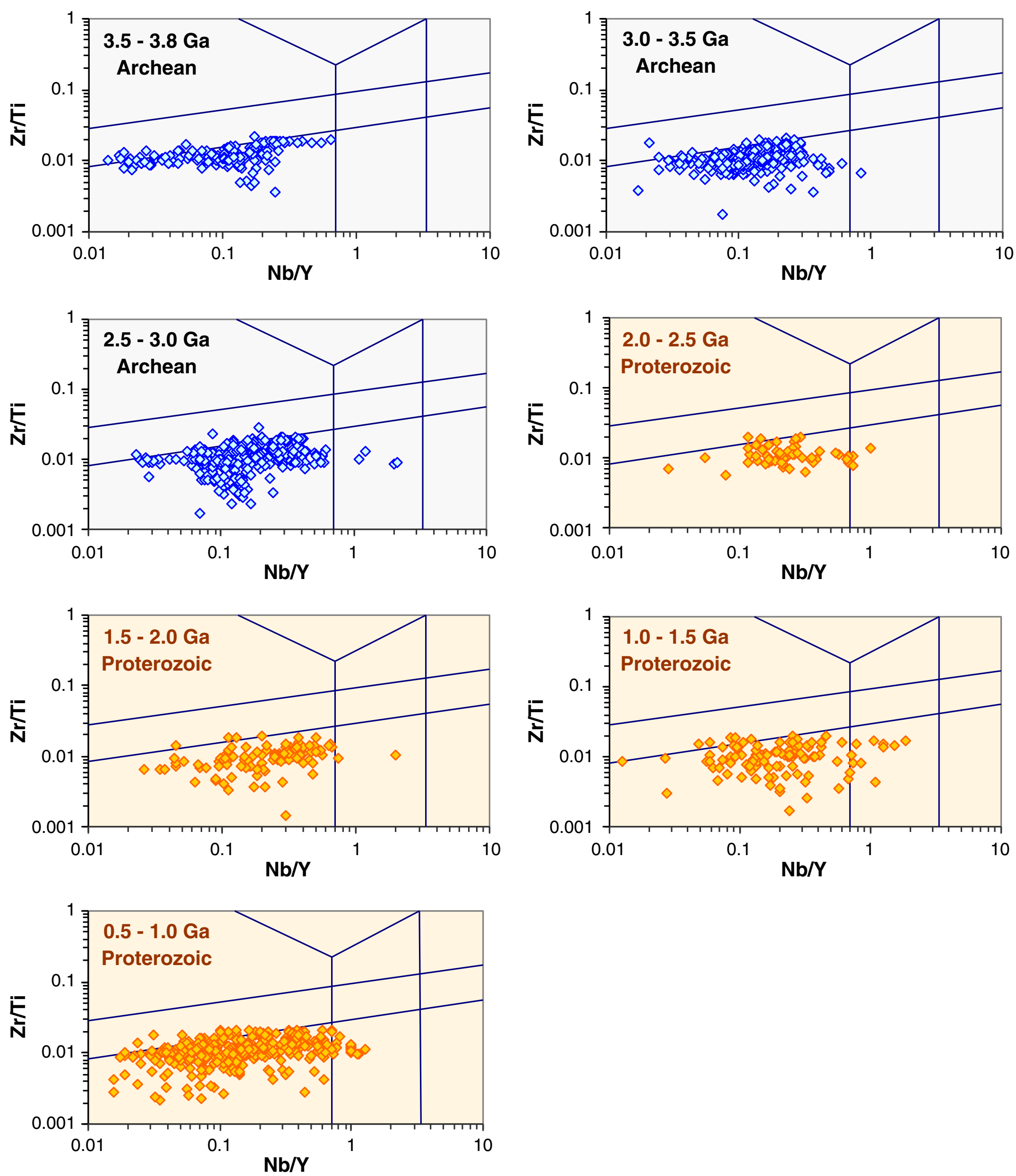


**Fig. 18.** All data plotted in Zr/Ti–Nb/Y diagrams.

Please cite this article as: Furnes, H., et al., Precambrian greenstone sequences represent different ophiolite types, Gondwana Research (2013), http://dx.doi.org/10.1016/j.gr.2013.06.004

treatment of the geochemical data, we used this diagram for all the data in order to decipher the data that plot only in the basalt field, and that straddle the field between basalt and basaltic andesite.

*4.3.2. Magma types and tectonic settings*

In further treating the data we have followed the proposed classification scheme of Pearce (in press), in which the first step is to plot the basaltic rocks in the Th/Yb–Nb/Yb diagram to distinguish between subduction-related and subduction-unrelated basalts (Fig. 17B). The mantle domains that were modified by subduction-derived fluids (e.g. Pearce, 2008), and that were hence enriched in Th, yield magmas with Th/Yb ratios that are displaced to higher values than those of the mantle array, e.g. they fall in the field defined by N-MORB through E-MORB and OIB (Fig. 17B). The samples that are displaced above the MORB-OIB array are further plotted in the V–Ti diagram (Fig. 17C). Whereas Ti is depleted in the source during melting above a subduction zone, Vanadium becomes enriched in the magma (Shervais, 1982). Water released from the subducting slab drives the melting process to become more oxidizing, which in turn increases the proportion of V in the higher oxidation state. Vanadium in the highest oxidation state ($V^{V}$) is more incompatible than in the lowest oxidation state ($V^{III}$). Thus, the more subduction-influenced a source region is, the higher the V/Ti ratio is in those magmas derived from such a source (Shervais, 1982). Therefore, the V/Ti ratio can be used as a proxy for supra-subduction zone melting, and the V–Ti diagram, as modified by Pearce (in press) can be subdivided into fields defined by boninites, island arc tholeiites, and MORB, the latter being the most slab-distal (Fig. 17C). The samples that only plot within the MORB-OIB array are further plotted in the $TiO_2$/Yb–Nb/Yb diagram, in which the $TiO_2$/Yb ratio is a proxy for the depth of melting. Since Yb is an element that is highly partitioned into garnet, the Ti/Yb ratio in a melt is sensitive to whether or not garnet is present in the residue after melting; it is high if garnet is present. Hence, the Ti/Yb ratio may function as a proxy for the depth of melting (Fig. 17D).

*4.4. Application of proxies to Precambrian greenstone sequences*

The literature-collected data have all been treated according to the method outlined above, and plotted in the diagrams as outlined in Fig. 17. The Archean and Proterozoic data have been

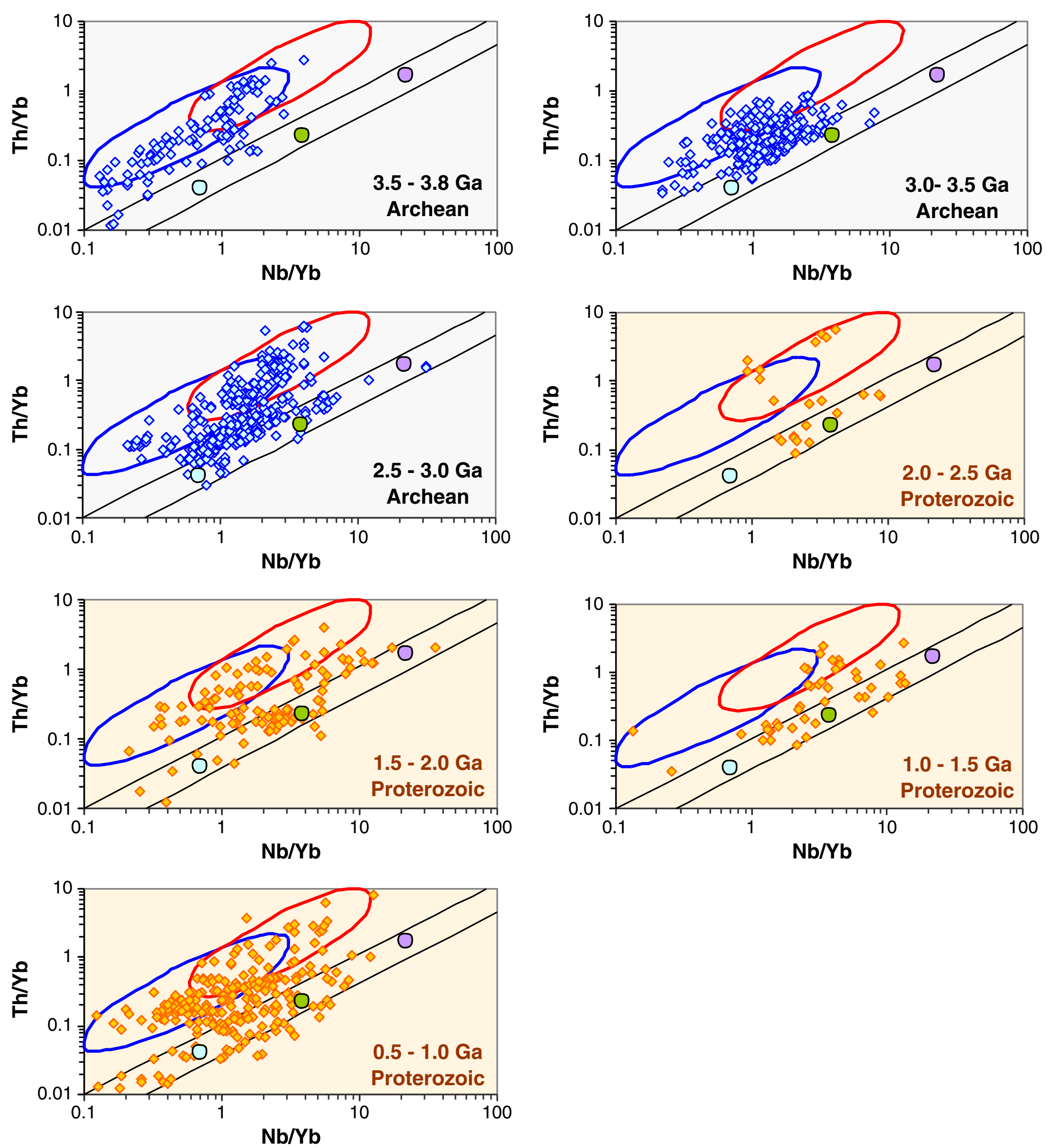


**Fig. 19.** All data plotted in Th/Yb–Nb/Yb diagrams.

divided into time intervals of 500 million-years, in order to test if there are noticeable differences in the data sets as a function of time.

*4.4.1. Zr/Ti versus Nb/Y*

The Zr/Ti–Nb/Y relationships for the samples with Zr/Ti < 0.02 (basalts) are shown in Fig. 18. For each of the time intervals there is a pronounced variation in the Nb/Y ratios, but by far the majority of the samples plot in the field of subalkaline basalt (referred to as "basalt" in Fig. 17A). A small proportion of the younger Proterozoic data have relatively high Nb/Y values (>0.7) and plot in the field of alkali basalts.

*4.4.2. Th/Yb versus Nb/Yb*

Fig. 19 shows all the data plotted in a Th/Yb–Nb/Yb diagram. For the oldest Archean (3.5–3.8 Ga) rocks, nearly all the samples plot above the MORB-OIB array, and in the field defined as oceanic arc and joint oceanic/continental arc. For the next billion years of the Archean Eon (3.5–2.5 Ga), the majority of the data also plot above the MORB-OIB array, but a significant part also plot within the mantle array. Throughout the Proterozoic there is a large scatter in the data, with about half plotting in the MORB-OIB field, and also a small part plotting in the field of continental arc.

*4.4.3. V versus Ti*

Fig. 20 shows all the data that plot above the MORB-OIB array (Fig. 19), plotted in the V–Ti diagram. The data from the earliest Archean spread equally between the fields defined as boninites, island arc tholeiites and MORB, whereas the 3.5–2.5 Ga data plot nearly exclusively in the field of island arc tholeiite and MORB. The data from the Proterozoic show large time-related variations. During the first 500-million years (2.5–2.0 Ga) the data plot nearly exclusively in the MORB field, or straddle the boundary between MORB and island arc tholeiites, whereas during the following 500-million years (though less amount of data) they plot mainly in the fields of boninites and island arc tholeiites. The data from the last billion years of the Proterozoic (1.5–0.5 Ga) define the largest spreads, though most of the data fall within the MORB field.

*4.4.4. $TiO_2$/Yb versus Nb/Yb*

Fig. 21 shows all the data that plot within the MORB-OIB array (Fig. 19), plotted in the $TiO_2$/Nb/Yb diagram. The data from the Archean and Proterozoic Eons show that the majority of these greenstones

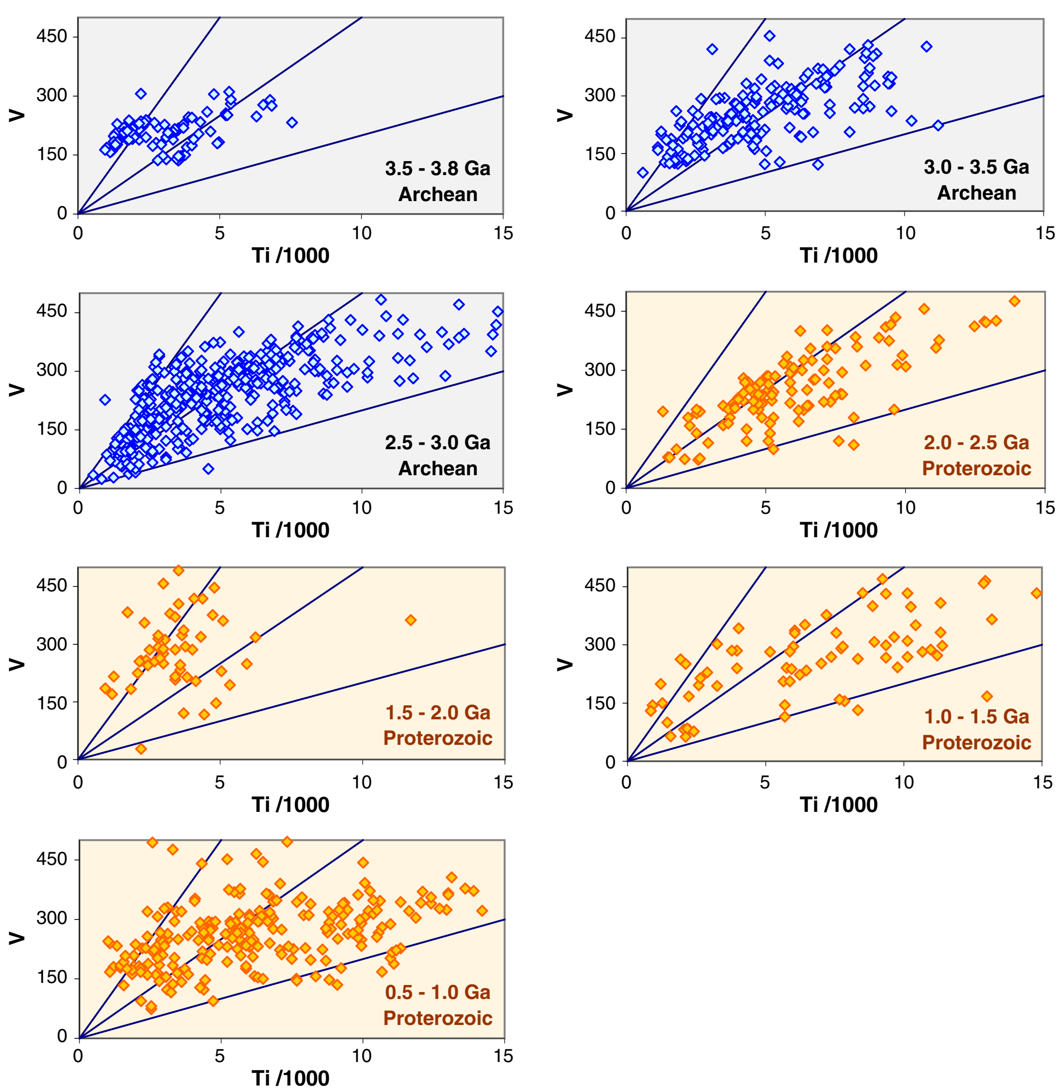


**Fig. 20.** All data plotted in V–Ti diagrams.

Please cite this article as: Furnes, H., et al., Precambrian greenstone sequences represent different ophiolite types, Gondwana Research (2013), http://dx.doi.org/10.1016/j.gr.2013.06.004

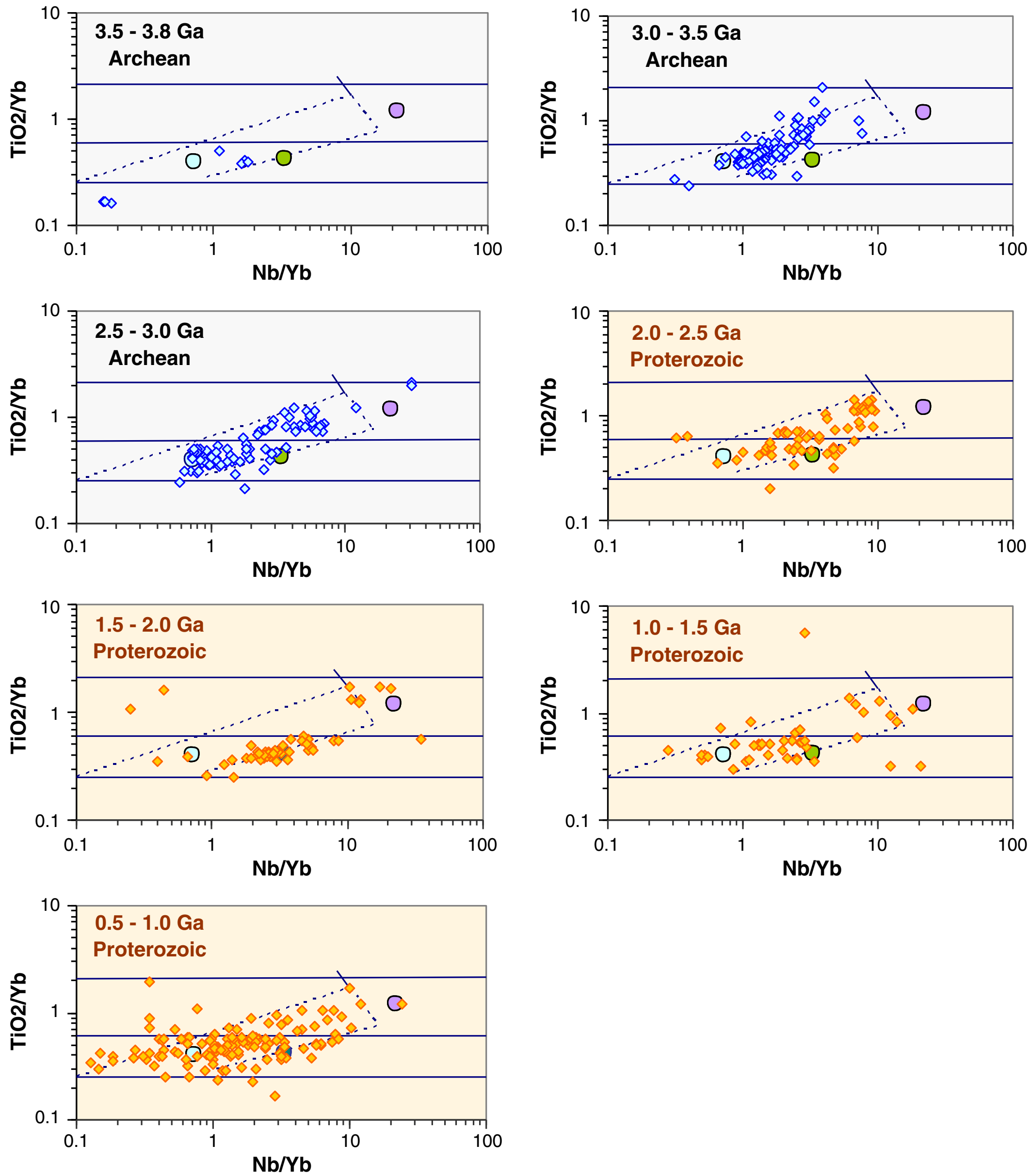


**Fig. 21.** All data plotted in $TiO_2$/Yb–Nb/Yb diagrams.

plot within the MORB field, indicating shallow melting processes in their magmatic evolution. The highest proportion of the data (about 40%) that plot in the OIB field of deep melting is the data from the time interval of 3.0–2.5 Ga.

#### 4.4.5. Nd-isotope geochemistry

Eight hundred and nineteen $\varepsilon^t_{Nd}$ ratios have been plotted against the age of the investigated samples (Fig. 22). The majority of the samples exhibit positive $\varepsilon^t_{Nd}$ values, except for those in the age range of 2.4 to 2.8 Ga, for which ca. 50% exhibit negative values. Most of the samples plot in the $\varepsilon_{Nd}$–age diagram above the CHUR reference line and between the depleted mantle growth curves of DePaolo (1980). For the younger sequences, most of the data plot below the depleted mantle growth curves and some exhibit highly negative $\varepsilon^t_{Nd}$ values, showing the involvement of continental material. However, even for the oldest rocks (3.0–3.7 Ga) substantial parts of the data plot above the depleted mantle growth curves, and others plot below the CHUR line, yielding negative values. These features suggest that depletion of the mantle and recycling of crustal material had occurred prior to their generation. This is in accordance with the results of a study by Adam et al. (2012) on the partial-melting experiments of the 4.3 Ga (Hadean) greenstones from Nuvvuagittuq complex (Canada) giving arc-like TTG melts. On this basis the authors (op.cit.) suggest crustal recycling whereby mafic crust and water were returned to the mantle to yield arc-like magmas.

### 4.5. Summary of data

On the basis of the data presented in Figs. 19–21, we have made an estimate (in percentage) of the proportion of each data set that plot within the MORB-OIB array, and the data that display subduction signatures, shown by the Th/Yb-proxy for subduction. The subduction-related data are further plotted on the V–Ti diagram, and subdivided into boninites, island arc tholeiites and MORB, and the data that plot with the MORB-OIB array are further subdivided

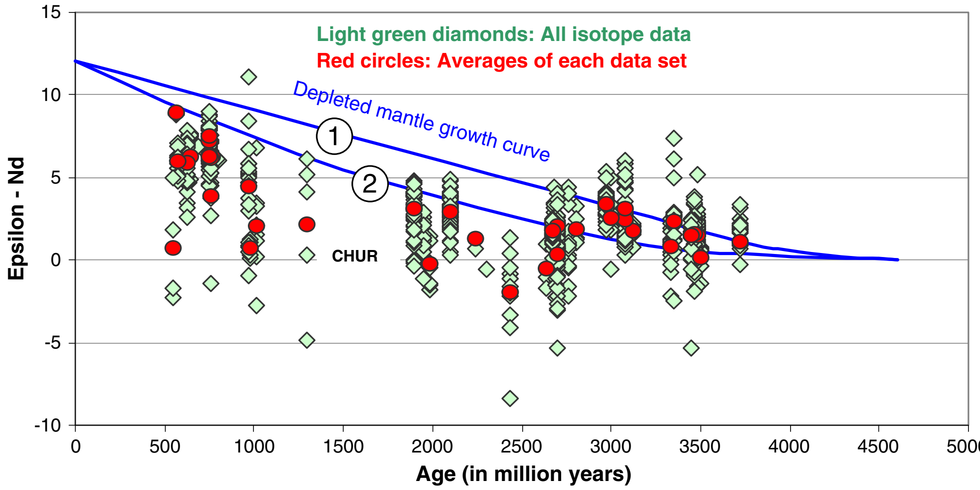


**Fig. 22.** Epsilon Nd values for some of the investigated greenstone sequences plotted against age. The mantle growth curves 1 and 2 from DePaolo (1980) are constrained to $\varepsilon_{Nd} = +12$ at T = 0 and are based on the assumptions of rapid early growth (1) and continuous linear growth (2) of the continental crust. Data locations (see Table 1) and sources are: SW Greenland: Isua (Hoffmann et al., 2010), Ivisaartoc (Polat et al., 2008), Tartoq (Szilas et al., 2013), Fiskenæsset (Polat et al., 2011). Africa: Barberton (Jahn et al., 1982; Lahaye et al., 1995; Chavagnac, 2004; Van Kranendonk et al., 2009; Furnes et al., 2012); Belingwe (Smith and Ludden, 1989); Birimian (Abouchami and Boher, 1990); Leerkrans Fm (Bailie et al., 2011); Tasriwine (Samson et al., 2004). Baltica and Kola: Vedlozero-Segzero (Svetov et al., 2001); Kostomuksha (Puchtel et al., 1998); North Karelia (Shchipansky et al., 2004); Kalikorva (Mil'kevich et al., 2007); Avarench (Vrevsky, 2011); Jeesiorova-Peuramaa (Hanski et al., 2001); Nuttio (Hanski and Huhma, 2005); Pilguyärvi (Skruf'in and Bayanova, 2006); Jormua (Peltonen et al., 1996). Polar Ural and Siberia: Olondo (Puchtel, 2004); Dunzhugur (Khain et al., 2002); Enganepe (Scarrow et al., 2001); Chaya Massif (Amelin et al., 1997). India: Sargur (Jayananda et al., 2008); Phulad (Volpe and Macdougall, 1990). Australia: Whundo (Smithies et al., 2005); Meekatharra-Cue (Wyman and Kerrich, 2012); Kalgoorlie (Bateman et al., 2001); Marlborough (Bruce et al., 2000). China: Taishan (Wang et al., 2013); Longsheng (Li, 1997); Anhui and Jiangxi (Li et al., 1997). Canada: Yellowknife (Cousens, 2000); Wawa (Polat and Kerrich, 2002); Flin Flon (Stern et al., 1995); Burin Group (Murphy et al., 2008). Nubian Shield, Egypt: Wadi Gerf (Zimmer et al., 1995); Wadi Ghadir (Basta et al., 2011); Wadi Kareim and Wadi El Dabbah (Ali et al., 2009). Mongolia: Bayankhongor (Jian et al., 2010); Agardagh Tes-Chem (Pfänder et al., 2002). South America: Pirapora (Tassinari et al., 2001). Bulgaria: Froloch/Struma (Kounov et al., 2012).

by the Ti/Yb proxy for melting conditions. All these data are shown in Table 2. On this basis we have first divided the investigated sequences into those which are *subduction-related* and *subduction-unrelated*, and further subdivided each type according to the division shown in Fig. 2. Thus, the subduction-related sequences have been classified as ophiolites of the *Volcanic Arc type*, and the suprasubduction-type (SSZ) into *SSZ-Forearc*, *SSZ-Backarc*, *SSZ-Backarc to forearc*, and *SSZ to Volcanic arc* (VA) subtypes. The subduction-unrelated type has been classified as *Rift-*, *Continental Margin-*, *MOR-* and *Plume-types*. This subdivision for the 111 data sets is shown in Table 3, and graphically displayed in Fig. 23. In the new ophiolite classification of Dilek and Furnes (2011), there is no example classified as Rift type. We consider the stages from rift–drift–seafloor spreading (Dilek et al., 2005) as a continuous development, from the incipient dyke intrusions into continental crust, to finally into an oceanic stage with a fully developed oceanic crust that also may show differences depending on the spreading rate (see MOR-type of Fig. 2). Thus, it may be difficult to define at what stage in the magmatic development of a sequence it qualifies to be classified as the first stage of ophiolite development, i.e. the Continental Margin-type ophiolite.

It is clear that the subduction-related type is by far the dominant, and that the SSZ-backarc and SSZ-backarc to forearc are the dominant subtypes (Fig. 23). The subdivision of the subduction-unrelated sequences show that the Plume-type is the main type, but this subdivision is based on a much smaller data base, and hence the subdivision is likely less well defined. It is also worth mentioning that the sequences classified as Continental Margin-type and Plume-type ophiolites are all from the Baltica region. The three typical MOR type ophiolites are represented from the Late Precambrian Nubian Shield (Gabal Gerf and Abu Meriewe), and the Bayankhongor ophiolite from Mongolia.

## 5. Discussion

Compilation of the data collected for this study, in terms of the abundance of greenstone sequences, the average concentration of incompatible and compatible elements, and the estimated subduction-influence, related to age, is displayed in Fig. 24.

### 5.1. Age distribution of greenstone sequences

With respect to the age distribution of the investigated greenstone sequences, there is an equal distribution in the time intervals of 1.0–1.5, 1.75–2.25, and 2.75–3.5 Ga, a much higher abundance in the time intervals 0.5–1.0, and 2.5–2.75 Ga, and very low in the time intervals 1.5–1.75, 2.25–2.5, and >3.5 Ga (Fig. 24A). This relationship may to some extent be fortuitous, since only greenstone sequences with easily accessible geochemical data, have been chosen. Alternatively, the minima defined by the age-greenstone frequency relationship (Fig. 24A), may reflect a preservation problem, i.e. time periods when less greenstone material were preserved. However, in relation to the compilation of some major Precambrian tectonic events, the two greenstone minima at 1.5–1.75, 2.25–2.5 Ga coincide with the time gaps for major periods of continental collision events (Fig. 24D).

### 5.2. Secular geochemical development

We have chosen Zr and Ni as representatives for incompatible and compatible elements, respectively. They are among some of the most stable trace elements during alteration and metamorphism, and are thus regarded to represent the best proxies to test for possible secular changes in ophiolite geochemistry that reflect magmatic processes. In general, there is a trend of decreasing Zr and increasing Ni contents with increasing age. This is a feature that probably reflects decreasing degrees of partial melting, as a consequence of secular mantle cooling. It is generally agreed on theoretical grounds that melting of the mantle was more extensive in the early Earth, and yielded thicker oceanic crust and hotter magmas (e.g. Foley et al., 2003; Komiya, 2004; Korenaga, 2006; Herzberg et al., 2010). According to Komiya (2004), the potential mantle temperature of the upper mantle was about 1480 °C in the Archean, i.e. 150–200 °C higher than in the modern

**Table 2**
Zr/Ti, Th/Yb, V–Ti and Ti/Yb proxies for geochemical classification of the selected greenstone sequences.

| | | Zr/Ti-proxy (%) | | Th/Yb-proxy for subduction (%) | | | | | V vs. Ti-proxy for SSZ melting (%) | | | Ti/Yb-proxy for plume melting (%) | | | | |
|---|---|---|---|---|---|---|---|---|---|---|---|---|---|---|---|---|
| | | | | None | Various subduction signal | | | | | | | MORB — shallow melting | | OIB — deep melting | | Av. Epsilon-Nd & stdev |
| Magmatic sequence | Age (Ga) | Mafic | Interm. & felsic | Mantle array | Weak | Oceanic arc(oa) | Cont. arc(ca) | Joint oa/ca | Bon. | IAT | MORB | N-MORB | E-MORB | Thol. | Alk. | |
| 1. Nuvvuagittuq (Canada) | 4.3?–3.8 | 100 | | 3 | 13 | 13 | 5 | 65 | | 92 | 8 | 100 | | | | |
| 2. Isua (Greenland) | 3.8 | 100 | | 5 | 15 | 60 | | 20 | 56 | 16 | 28 | 100 | | | | 1.72 ± 0.88 |
| 3. Pilbara–Warrawoona (NW Australia) | 3.53–3.43 | 100 | | | 68 | | | 32 | | 36 | 64 | | | | | |
| 4. Pilbara–Kelly (NW Australia) | 3.35–3.29 | 100 | | | | 50 | | 50 | | 100 | | | | | | |
| 5 Southern Iron Ore Group (India) | 3.51 | 70 | 30 | 38 | 12 | | | 50 | | 60 | 40 | | 100 | | | |
| 6. Barberton–Komati (South Africa) | 3.48 | 100 | | 79 | 21 | | | | | 100 | | 100 | | | | 1.58 ± 1.07 |
| 7. Barberton–Hooggenoeg (South Africa) | 3.47 | 100 | | 77 | 19 | 2 | | 2 | | 100 | | 90 | | 10 | | 1.53 ± 1.26 |
| 8. Barberton–Kromberg (South Africa) | 3.45 | 100 | | 6 | 94 | | | | | 60 | 40 | 100 | | | | 1.42 ± 0.90 |
| 9. Barberton–Mendon (South Africa) | 3.33 | 100 | | | 100 | | | | | 100 | | | | | | 0.75 ± 1.27 |
| 10 Nondweni (South Africa) | 3.4 | 100 | | 90 | 10 | | | | | | 100 | 55 | | 45 | | |
| 11. Pietersburg (South Africa) | 3.4 | | | | | | | | | | | | | | | |
| 12. Sargur Group (India) | 3.35 | 100 | | 29 | 43 | | | 28 | | 100 | | | | 100 | | 2.30 ± 2.09 |
| 13. Commondale (South Africa) | 3.33 | 100 | | | | | | | | | | 100 | | | | |
| 14. Regal Formation (W Australia) | 3.2 | 100 | | 50 | 50 | | | | | | | | | | | |
| 15. Whundo Group (Pilbara, Australia) | 3.12 | 63 | 37 | 3 | 59 | | | 38 | | 18 | 82 | | 100 | | | 1.76 ± 0.45 |
| 16. Ivisaartoc (SW Greenland) | 3.075 | 100 | | 26 | | 21 | | 53 | 35 | 65 | | 80 | | 20 | | 2.37 ± 1.29 |
| 17. Ujarassuit (SW Greenland) | 3.07 | 100 | | 8 | 52 | 36 | | 4 | 13 | 57 | 30 | 100 | | | | |
| 18. Storø–Lower (SW Greenland) | 3.06 | 100 | | | | | | 100 | | | 100 | | | | | |
| 19. Tartoq (SW Greenland) | 3.0 | 100 | | 19 | 33 | 17 | 31 | | | 50 | 50 | 100 | | | | 2.48 ± 1.45 |
| 20. Koolyanobbing greenstone (Australia) | 3.0 | 100 | | | 22 | 33 | | 45 | 20 | 80 | | | | | | |
| 21. Olondo, Siberia (Russia) | 3.0 | 100 | | 21 | 64 | 15 | | | | | | 100 | | | | |
| 22. Fiskenæsset (SW Greenland) | 2.97 | 100 | | 43 | 29 | 28 | | | | 50 | 50 | 100 | | | | 3.35 ± 0.64 |
| 23. Vedlozero–Segozero (Karelia, Russia) | 2.921 | 100 | | | | | | | | 44 | 56 | | | | | |
| 24. Belingwe (Zimbabwe) | 2.9–2.7 | 97 | 3 | 19 | 54 | | 8 | 19 | 5 | 43 | 52 | 100 | | | | |
| 25. Kostomuksha (Karelia, Russia) | 2.843 | 100 | | 100 | | | | | | | | 100 | | | | |
| 26. Storø, upper (SW Greenland) | 2.8 | 100 | | | | | | 100 | | | 100 | | | | | |
| 27. Khizovaara–Iringora (N Karelia, Russia) | 2.8 | 100 | | 16 | 81 | 3 | | | 35 | 53 | 12 | 100 | | | | 1.80 ± 0.88 |
| 28. Meekatharra–Cur (Yilgarn, Australia) | 2.8–2.76 | 67 | 33 | 6 | 34 | 20 | | 40 | | 60 | 40 | | | | | |
| 29. Tikshozero (Karelia, Russia) | 2.785 | 40 | 60 | 30 | | | 40 | 30 | | 30 | 70 | | 50 | 50 | | |
| 30. Rio das Velhas Gr.stone Belt (Brazil) | 2.77 | 100 | | | | | | 100 | | | | | | | | |
| 31. Carajas Greenstone Belt (Brazil) | 2.76 | 100 | | | | | 90 | 10 | | | | | | | | |
| 32. Taishan (China) | 2.747 | 100 | | 28 | 46 | 8 | | 18 | | | | | 50 | 50 | | |
| 33. Kushtagi–Hungund gr. st. (India) | 2.746 | 62 | 38 | 9 | 55 | | | 36 | 15 | 70 | 15 | 50 | | 50 | | |
| 34. Wawa 1 (Superior Province, Canada) | 2.75–2.65 | 100 | | 35 | 65 | | | | | 65 | 35 | 39 | | 48 | 13 | 1.76 ± 0.56 |
| Wawa 2 (Superior Province, Canada) | 2.75–2.65 | 52 | 48 | | | | 61 | 39 | | 20 | 80 | | | | | |
| 35. Abitibi (SE Canada) | 2.74–2.67 | 100 | | 39 | 53 | 5 | | 3 | 27 | 54 | 19 | | 75 | 25 | | |
| 36. Yellowknife (Slave Craton, Canada) | 2.72–2.66 | 76 | 24 | 10 | 28 | | | 62 | | 15 | 85 | | 30 | 70 | | 0.58 ± 1.75 |
| 37. Kalgoorlie (Yilgarn, Australia) | 2.71 | 93 | 7 | 37 | 33 | | 22 | 8 | 26 | 74 | | 30 | | 70 | | 2.01 ± 1.63 |
| 38. Gindalbie–Kurnalpi (Yilgarn, Australia) | 2.7 | 17 | 83 | | | | | 100 | | | 100 | | | | | |

(continued on next page)

**Table 2** (*continued*)

| | | Zr/Ti-proxy (%) | | Th/Yb-proxy for subduction (%) | | | | | V vs. Ti-proxy for SSZ melting (%) | | | Ti/Yb-proxy for plume melting (%) | | | | |
|---|---|---|---|---|---|---|---|---|---|---|---|---|---|---|---|---|
| | | | | None | Various subduction signal | | | | | | | MORB — shallow melting | | OIB — deep melting | | Av. Epsilon-Nd & stdev |
| Magmatic sequence | Age (Ga) | Mafic | Interm. & felsic | Mantle array | Weak | Oceanic arc(oa) | Cont. arc(ca) | Joint oa/ca | Bon. | IAT | MORB | N-MORB | E-MORB | Thol. | Alk. | |
| 39. Wind River (North America) | 2.7 | 100 | | | | | | | | 70 | 30 | | | | | |
| 40. Gadwal greenstone (S India) | 2.7–2.5 | 100 | | | | 82 | | 18 | | 60 | 40 | | | | | |
| 41. Suomussalmi (Karelia, Russia) | 2.65 | 75 | 25 | | | | | | | 70 | 30 | | | | | |
| 42. Kuhmo–Tipasjarvi (Karelia, Russia) | 2.65 | 100 | | | | | | | | 60 | 40 | | | | | |
| 43. Bastar greenstone (central E India) | 2.6 | 58 | 42 | | | | 37 | 63 | | 100 | | | | | | |
| 44. Hutti greenstone (S India) | 2.6 | 55 | 45 | 23 | 12 | | | 65 | | 30 | 70 | 100 | | | | |
| 45. Zanhuang Complex (China) | 2.5 | 100 | | 7 | 52 | | | 41 | | 10 | 90 | | 100 | | | |
| 46. Dongwanzi (China) | 2.5 | 30 | 70 | | | | | | | | 100 | 50 | | 50 | | |
| 47. Krasnaya Rechka & Semch structures (central Karelia, Russia) | 2.5 | 100 | | 100 | | | | | | | | | 50 | 50 | | |
| 49. Arvarench structure (Kola, Russia) | 2.429 | 50 | 50 | | | | | | | | | | | | | −2.01 ± 2.51 |
| 49. Kholodnikan gr.st. (Siberia, Russia) | 2.41 | 58 | 42 | | | | | | | 20 | 80 | 80 | | 20 | | |
| 50. Mazaruni/Barama greenstone (South America) | 2.25 | 50 | 50 | 50 | 50 | | | | | | | | | 100 | | |
| 51. Birimian Terrane (Western Africa) | 2.1 | 100 | | | | | | | | 31 | 69 | 95 | | 5 | | 2.92 ± 0.90 |
| 52. Karasjok belt (Baltica, Norway) | 2.1 | 100 | | | | | | | | | | | 40 | 60 | | |
| 53. Jeesiorova (Baltica, Finland) | 2.056 | 100 | | 13 | 74 | | 13 | | | 91 | 9 | 100 | | | | |
| 54. Peuramaa (Baltica, Finland) | 2.056 | 100 | | 100 | | | | | | | | | | 100 | | |
| 55. Narracoota Formation (Australia) | 2.0 | 88 | 12 | | 14 | | 14 | 72 | | 50 | 50 | | | | | |
| 56. Purtuniq (Cape Smith Belt, Canada) | 2.0 | 100 | | | 100 | | | | | | | | 50 | 50 | | |
| 57. Nuttio (Baltica, Finland) | 2.0 | 100 | | | | | 100 | | | 100 | | | | | | |
| 58. Pilgujärvi Fm. (Pechenga, Russia) | 1.97 | 100 | | 100 | | | | | | | | | 25 | | 75 | −0.29 ± 1.08 |
| 59. Jormua (Baltica, Finland) | 1.95 | 100 | | 100 | | | | | | | | | 100 | | | 1.22 ± 1.17 |
| 60. Birch Lake (Cape Smith Belt, Canada) | 1.9 | 40 | 60 | | | 100 | | | 100 | | | | | | | |
| 61. Flin Flon (Cape Smith Belt, Canada) | 1.9 | 91 | 9 | 2 | 17 | 15 | 6 | 60 | 42 | 42 | 16 | 100 | | | | 3.07 ± 1.30 |
| 62. Outokumpu (Baltica, Finland) | 1.9 | 100 | | 100 | | | | | | | | 25 | 75 | | | |
| 63. Kandra (SE India) | 1.85 | 85 | 15 | 54 | | | 38 | 8 | | 50 | 50 | | 70 | 30 | | |
| 64. Payson (North America) | 1.73 | 73 | 27 | 40 | 53 | | 7 | | | 100 | | | 100 | | | |
| 65. Chewore oph. (Kalahari–Congo, Africa) | 1.4 | 81 | 19 | | | | | | | | | 100 | | | | |
| 66. Bas Draa (Morocco) | 1.38 | 74 | 26 | 18 | 27 | | 55 | | | | 100 | 100 | | | | |
| 67. Fraser Complex (SW Australia) | 1.3 | 90 | 10 | 30 | 30 | | 10 | 30 | | | | | 100 | | | |
| 68. Leerkrans Formation (South Africa) | 1.3 | 100 | | 63 | 13 | | 12 | 12 | | | 100 | | 100 | | | 2.16 ± 4.49 |
| 69. Coal Creek Domain (Grenville, North America) | 1.33–1.28 | 100 | | | | | | | | | | | 75 | | 25 | |
| 70. Queensborough Complex (Grenville, North America) | 1.25 | 100 | | | | | | | | 20 | 80 | 80 | | 20 | | |
| 71. Pie de Palo (South America) | 1.118 | | | | | | | | | | | | | | | |
| 72. Phulad (NW India) | 1.012 | 92 | 8 | | | | | | 13 | 6 | 81 | | | | | 1.97 ± 2.78 |
| 73. Dunzhugur ophiolite (Siberia, Russia) | 1.02 | | | | | | | | 11 | 32 | 57 | | | | | |
| 74. Daba & Kui (NW India) | 1.00 | 100 | | 57 | 43 | | | | | 50 | 50 | | | 100 | | |
| 75. Miaowan (China) | 1.0 | 100 | | 73 | 18 | 9 | | | | 30 | 70 | 100 | | | | |
| 76. Longsheng ophiolite (China) | 0.977 | 100 | | | 100 | | | | | | 100 | | | | | 0.68 ± 0.34 |
| 77. Anhui & Jiangxi ophiolites (China) | 0.970 | ?? | | 13 | | 25 | 12 | 50 | | | | | | | | 4.12 ± 2.26 |
| 78. Jebel Thurwah (Arabian Shield) | 0.870 | 100 | | | | | | | | | | | | | | |
| 79. Darb Zubaydah (Arabian Shield) | 0.830 | 40 | 60 | | | | | | | | | | | | | |
| 80. Bir Umq (Arabian Shield) | 0.838 | 100 | | | | | | | | | | 34 | | 33 | 33 | |
| 81. Onib (Nubian Shield, Egypt) | 0.808 | 83 | 17 | | | | | | | 26 | 74 | | 100 | | | |
| 82. Manamedu Complex (India) | 0.800 | 92 | 8 | 18 | 17 | 17 | 8 | 50 | 36 | 74 | | | | | | |

Please cite this article as: Furnes, H., et al., Precambrian greenstone sequences represent different ophiolite types, Gondwana Research (2013), http://dx.doi.org/10.1016/j.gr.2013.06.004

**Table 2** (*continued*)

| Magmatic sequence | Age (Ga) | Zr/Ti-proxy (%) | | Th/Yb-proxy for subduction (%) | | | | | V vs. Ti-proxy for SSZ melting (%) | | | Ti/Yb-proxy for plume melting (%) | | | | Av. Epsilon-Nd & stdev |
|---|---|---|---|---|---|---|---|---|---|---|---|---|---|---|---|---|
| | | | | None | Various subduction signal | | | | | | | MORB — shallow melting | | OIB — deep melting | | |
| | | Mafic | Interm. & felsic | Mantle array | Weak | Oceanic arc(oa) | Cont. arc(ca) | Joint oa/ca | Bon. | IAT | MORB | N-MORB | E-MORB | Thol. | Alk. | |
| 83. Older Basement Unit (Republic of Georgia) | 0.800 | 100 | | 88 | | | 12 | | | | | | 100 | | | |
| 84. Fawakhir (Nubian Shield, Egypt) | 0.8–0.7 | 100 | | | | 96 | | 4 | | 62 | 38 | | | | | |
| 85. Southern Ethiopia i) Megado & ii) Moyale-El Kur | 0.79-0.66 | 100 | | | | | | | | | | | | | | |
| 86. Yanbu (Jabal Ess, Al 'Ays) (Arabian Shield) | 0.789 | 64 | 36 | 17 | | | 16 | 67 | | | | 100 | | | | |
| 87. Tasriwine (Morocco) | 0.762 | | | | | | | | | | | | | | | 6.20 ± 0.17 |
| 88. Burin Group (Newfoundland, Canada) | 0.760 | 73 | 27 | 50 | 8 | | 42 | | | 50 | 50 | | 100 | | | |
| 89. Gabal Gerf (Nubian Shield, Egypt) | 0.750 | 100 | | 100 | | | | | | | | 100 | | | | 7.20 ± 0.78 |
| 90. Wadi Ghadir (Nubian Shield, Egypt) | 0.750 | 100 | | 6 | 6 | | | 88 | | | 100 | 100 | | | | 6.32 ± 0.99 |
| 91. Wizer (Nubian Shield, Egypt) | 0.750 | 100 | | 67 | | | | 33 | 100 | | | 100 | | | | |
| 92. Abu Meriewa (Nubian Shield, Egypt) | 0.750 | 100 | | 100 | | | | | | | | 100 | | 25 | | |
| 93. Wadi Kareim (Nubian Shield, Egypt) | 0.750 | 67 | 33 | | 60 | 40 | | | | | 100 | | | | | 7.48 ± 0.77 |
| 94. Wadi El Dabbah (Nubian Shield, Egypt) | 0.750 | 80 | 20 | | | | | 100 | | 73 | 27 | | | | | 6.19 ± 0.73 |
| 95. Tulu Dimtu (Ethiopia) | 0.750 | 85 | 15 | 33 | 33 | | 34 | | | 30 | 70 | 50 | | 50 | | |
| 96. Siroua Massif (Morocco) | 0.743 | 100 | | | | | | | | 30 | 70 | | | | | |
| 97. Jabal al Wask (Saudi Arabia) | 0.743 | 100 | | | | | | | | | | | | | | |
| 98. Halaban (Arabian Shield) | 0.700 | 100 | | | | | 17 | 83 | | 67 | 33 | | | | | |
| 99. Bou Azzer ophiolite (Morocco) | 0.697 | 78 | 22 | | | | | | | 18 | 82 | | | | | |
| 100. Enganepe (Polar Urals, Russia) | 0.670 | 75 | 25 | 14 | | 57 | 29 | | 45 | 28 | 27 | | | 100 | | 3.84 ± 2.55 |
| 101. "Marich" ophiolite (Kenya) | 0.663 | 81 | 19 | | 50 | 50 | | | | | | | | | | |
| 102. Bayankhongor (Mongolia) | 0.647 | 88 | 12 | 100 | | | | | | | | | 100 | | | 6.20 ± 1.62 |
| 103. Pirapora (South America) | 0.628 | 100 | | 90 | | 10 | | | | | | | | | | |
| 104. Chaya Massif, Baikal–Muya (Siberia, Russia) | 0.627 | 100 | | 36 | 50 | 14 | | | | | | 100 | | | | 5.80 ± 1.33 |
| 105. Cele (Turkey) | >0.590 | 88 | 12 | | | | | | | 35 | 65 | | | | | |
| 106. Matchless greenstone (Namibia) | 0.600 | 100 | | | | | | | | | 100 | | | | | |
| 107. Agardagh Tes-Chem (Mongolia) | 0.569 | 90 | 10 | 75 | | 25 | | | | | | 70 | | 30 | | 5.91 ± 0.17 |
| 108. Tcherni Vrah & Deli Jovan massifs (Bulgaria/Serbia) | 0.563 | 100 | | | | | | | | | 100 | | | | | |
| 109. Marlborough (E Australia) | 0.560 | 80 | 20 | 100 | | | | | | | | 100 | | | | 8.88 ± 0.04 |
| 110. Frolosh/Struma (Bulgaria) | 0.560 | 83 | 17 | 55 | 27 | 9 | 9 | | | | | | 85 | 15 | | 0.71 ± 3.36 |
| 111. North Qilian Suture (China) | 0.517 | 100 | | 30 | 6 | 64 | | | 35 | 59 | 6 | 100 | | | | |

Interm. = intermediate; cont. = continental; Bon. = boninite; IAT = island arc tholeiite; MORB = mid-ocean-ridge basalt; Thol. = tholeiitic; Alk. = alkaline; stdev = standard deviation.

mantle, or even lower (ca. 100 °C) according to Grove and Parman (2004).

The trends on our plots are not linear, but rather define oscillatory patterns (Fig. 24B). In the time interval 0.5 to ca. 2.2 Ga, the trends defined by Zr and Ni are approximately parallel, whereas at older ages they diverge from each other, and define the mirror image of each other. However, these patterns, shown especially by the compatible elements (e.g. Ni) and to some extent by the incompatible elements (e.g. Zr), are likely to reflect a bias in selectivity; many studies of Precambrian magmatic rocks focus exclusively on the evolution of high-MgO rocks, i.e. komatiites. The true proportions between the actual magmatic components from selected literature-based data may not be truly representative. Thus, the maxima and minima, as shown by the Ni-curve (Fig. 24B), most probably represent over-representation of komatiites and basalts, respectively, and a linear magmatic evolutionary trend may be equally likely. However, Komiya (2004) has suggested that the temperature decrease of the upper mantle is not entirely linear, and hence the oscillatory patterns as shown in Fig. 24B should probably not be ignored. Similarly, Keller and Schoene (2012), in a comprehensive geochemical data synthesis of basalts through Phanerozoic and Precambrian times, demonstrate an irregularly increasing concentration of compatible elements and a decreasing concentration of incompatible elements when traced back in time. Interestingly, their identification of a geochemical discontinuity at around 2.5 Ga is not displayed in the data presented here.

In order to produce the subduction signatures, as demonstrated by the Th/Yb–Nb/Yb relationships (Fig. 19), the upper mantle peridotites must have undergone metasomatic processes to become enriched in Th (and other alkaline and LREE elements). This feature of Th-enrichment above the MORB-OIB array (Fig. 17B) is observed even in the oldest known sequences, as reported from Eoarchean–Hadean Nuvvuagittuq

**Table 3**
Proposed classification of the selected greenstone sequences according to the ophiolite classification of Dilek and Furnes (2011), based on Th/Yb, V/Ti, and Ti/Yb proxies.

| Magmatic sequence | Age (Ga) | Subd.rel. | Subd.unrel. | Suggested ophiolite type and tectonic environment on the basis of documented data in Table 2 *In italics: Suggested from literature* |
|---|---|---|---|---|
| 1. Nuvvuagittuq (Canada) | 4.3?–3.8 | X | | SSZ – Forearc to VA, |
| 2. Isua (Greenland) | 3.8 | X | | SSZ – Backarc to forearc |
| 3. Pilbara–Warrawoona Gp. (NW Australia) | 3.53–3.43 | X | | SSZ – Backarc to forearc |
| 4. Pilbara–Kelly Gp. (NW Australia) | 3.35–3.29 | X | | SSZ – Forearc |
| 5. Southern Iron Ore Group (India) | 3.51 | X | | SSZ – Backarc to forearc to VA |
| 6. Barberton–Komati (South Africa) | 3.48 | X | | SSZ – Backarc to forearc + major MOR component |
| 7. Barberton–Hooggenoeg (South Africa) | 3.47 | X | | SSZ – Backarc to forearc + major MOR component |
| 8. Barberton–Kromberg (South Africa) | 3.45 | X | | SSZ – Backarc to forearc |
| 9. Barberton–Mendon (South Africa) | 3.33 | X | | SSZ – Forearc |
| 10. Nondweni (South Africa) | 3.4 | X | | MOR-type, minor SSZ-backarc |
| 11. Pietersburg (South Africa) | 3.4 | | | *Oceanic-like crust* |
| 12. Sargur Group (India) | 3.35 | X | | SSZ-Forearc to deep MOR type |
| 13. Commondale (South Africa) | 3.33 | X | | *Subduction-related* |
| 14. Regal Formation (W Australia) | 3.2 | X | | SSZ-type or MORB-type |
| 15. Whundo Group (Pilbara, NW Australia) | 3.12 | X | | SSZ-Backarc to forearc |
| 16. Ivisaartoc (SW Greenland) | 3.075 | X | | SSZ-Forearc to VA + shallow MOR component |
| 17. Ujarassuit (SW Greenland) | 3.07 | X | | SSZ-Backarc to forearc |
| 18. Storø-Lower (SW Greenland) | 3.06 | X | | VA-type |
| 19. Tartoq (SW Greenland) | 3.0 | X | | SSZ-Backarc to forearc + shallow MOR component |
| 20. Koolyanobbing greenstone (SW Australia) | 3.0 | X | | SSZ-Forearc to VA |
| 21. Olondo (Siberia, Russia) | 3.0 | X | | SSZ-Backarc + major shallow MOR component |
| 22. Fiskenæsset (SW Greenland) | 2.97 | X | | SSZ-Backarc + major shallow MOR component |
| 23. Vedlozero-Segozero (Karelia, Russia) | 2.921 | | X | *Deep mantle plume* |
| 24. Belingwe (Zimbabwe) | 2.9–2.7 | X | | SSZ-Backarc to forearc + minor shallow MOR component |
| 25. Kostomuksha (Karelia, Russia) | 2.843 | | X | P-type + shallow MOR component |
| 26. Storø, upper (SW Greenland) | 2.8 | X | | SSZ-Backarc to VA |
| 27. Khizovaara-Iringora (N Karelia, Russia) | 2.8 | X | | SSZ-Backarc to forearc + minor shallow MOR component |
| 28. Meekatharra-Cur (Yilgarn, Australia) | 2.8–2.76 | X | | SSZ-Backarc to forearc, + minor shallow MOR component |
| 29. Tikshozero (Karelia, Russia) | 2.785 | X | | SSZ-Backarc to VA + significant shallow to deep MOR component |
| 30. Rio das Velhas Greenstone Belt (Brazil) | 2.772 | X | | SSZ-type or VA-type |
| 31. Carajas Greenstone Belt (Brazil) | 2.76 | X | | VA-type |
| 32. Taishan (China) | 2.747 | X | | SSZ-Backarc ? + significant shallow to deep MOR component |
| 33. Kushtagi-Hungund gr. st. (India) | 2.746 | X | | SSZ-Backarc to forearc + minor shallow to deep MOR component, P-type |
| 34. Wawa 1 (Superior Province, Canada) | 2.75–2.65 | X | | SSZ-Backarc + significant shallow to deep MOR component, P-type |
| Wawa 2 (Superior Province, Canada) | 2.75–2.65 | X | | VA-type |
| 35. Abitibi (SE Canada) | 2.74–2.67 | X | | SSZ-Backarc + major shallow to deep MOR component, P-type |
| 36. Yellowknife (Slave Craton, Canada) | 2.72–2.66 | X | | SSZ-VA type + minor significant deep MOR component, P-type |
| 37. Kalgoorlie (Yilgarn, SW Australia) | 2.71 | X | | SSZ-Forearc + significant deep MOR component, P-type |
| 38. Gindalbie-Kurnalpi (Yilgarn, SW Australia) | 2.7 | X | | VA-type |
| 39. Wind River (North America) | 2.7 | X | | SSZ-Backarc ? + significant shallow to deep MOR component |
| 40. Gadwal greenstone (Southern India) | 2.7–2.5 | X | | SSZ-Backarc |
| 41. Suomussalmi (Karelia, Russia) | 2.65 | X | | SSZ-Backarc ? |
| 42. Kuhmo-Tipasjarvi (Karelia, Russia) | 2.65 | X | | SSZ-Backarc ? |
| 43. Bastar greenstone (central eastern India) | 2.6 | X | | VA-type |
| 44. Hutti greenstone (Southern India) | 2.6 | X | | SSZ-Backarc to VA + significant shallow MOR component |
| 45. Zanhuang Complex (China) | 2.5 | X | | SSZ-Backarc + minor shallow MOR component |
| 46. Dongwanzi (China) | 2.5 | X | | *Suprasubduction* |
| 47. Krasnaya Rechka & Semch structures (Central Karelia, Russia) | 2.5 | | X | P-type, shallow to deep MOR component |
| 48. Arvarench structure (Kola, Russia) | 2.429 | | X | *Intracratonic rifting* |
| 49. Kholodnikan gr.stone (Siberia, Russia) | 2.41 | | X | *mantle plume* |
| 50. Mazaruni/Barama greenstone (South America) | 2.25 | X | | SSZ-type + shallow MOR component |
| 51. Birimian Terrane (Western Africa) | 2.1 | X | | SSZ-Backarc + shallow MOR component |
| 52. Karasjok belt (Baltica, Norway) | 2.1 | | X | CM-type, shallow to deep MOR component |
| 53. Jeesiorova (Baltica, Finland) | 2.056 | X | | SSZ-Backarc + shallow MOR component |
| 54. Peuramaa (Baltica, Finland) | 2.056 | | X | P-type, deep MOR component |
| 55. Narracoota Fm (W Australia) | 2.0 | X | | SSZ-Backarc |
| 56. Purtuniq (Cape Smith Belt, Canada) | 2.0 | X | | SSZ-Backarc + shallow to deep MOR component |
| 57. Nuttio (Baltica, Finland) | 2.0 | X | | VA-type |
| 58. Pilgujärvi Fm. (Pechenga, Russia) | 1.97 | | X | CM-type, shallow to deep MOR component |
| 59. Jormua (Baltica, Finland) | 1.95 | | X | CM/MOR-type, shallow MOR component |
| 60. Birch Lake (Cape Smith Belt, Canada) | 1.9 | X | | SSZ-Forearc |
| 61. Flin Flon (Cape Smith Belt, Canada) | 1.9 | X | | SSZ-Backarc to forearc |
| 62. Outokumpu (Baltica, Finland) | 1.9 | | X | CM-type, shallow MOR component |
| 63. Kandra (SE India) | 1.85 | X | | VA-type + shallow to deep MOR component |
| 64. Payson (North America) | 1.73 | X | | SSZ-Backarc + shallow MOR component |
| 65. Chewore oph. (Kalahari-Congo, Africa) | 1.4 | X | | SSZ-type ? |
| 66. Bas Draa (Morocco) | 1.38 | X | | CM-type, early stage |
| 67. Fraser Complex (SW Australia) | 1.3 | X | | SSZ-Backarc to forearc + shallow MOR component |
| 68. Leerkrans Formation (South Africa) | 1.3 | X | | SSZ-Backarc + major shallow MOR component |
| 69. Coal Creek Domain (Grenville, North America) | 1.33–1.28 | X | | *Island arc setting* |
| 70. Queensborough Complex (Grenville, North America) | 1.25 | X | | *Back-arc basin* |
| 71. Pie de Palo (South America) | 1.118 | X | | *Suprasubduction* |

Please cite this article as: Furnes, H., et al., Precambrian greenstone sequences represent different ophiolite types, Gondwana Research (2013), http://dx.doi.org/10.1016/j.gr.2013.06.004

**Table 3** (*continued*)

| Magmatic sequence | Age (Ga) | Subd.rel. | Subd.unrel. | Suggested ophiolite type and tectonic environment on the basis of documented data in Table 2 *In italics: Suggested from literature* |
|---|---|---|---|---|
| 72. Phulad (NW India) | 1.012 | X | | SSZ-Backarc to forearc |
| 73. Dunzhugur ophiolite (Siberia, Russia) | 1.02 | X | | SSZ-Backarc to forearc |
| 74. Daba & Kui (NW India) | 1.00 | X | | SSZ-Backarc + deep MOR component |
| 75. Miaowan (China) | 1.0 | X | | SSZ-Backarc + shallow MOR component |
| 76. Longsheng ophiolite (China) | 0.977 | X | | SSZ-Backarc |
| 77. Anhui & Jiangxi ophiolites (China) | 0.970 | X | | SSZ-? |
| 78. Jebel Thurwah (Arabian Shield) | 0.870 | X | | *Suprasubduction* |
| 79. Darb Zubaydah (Arabian Shield) | 0.830 | X | | *Intra-arc rifting* |
| 80. Bir Umq (Arabian Shield) | 0.838 | X | | *Suprasubduction* |
| 81. Onib (Nubian Shield, Egypt) | 0.808 | X | | *Suprasubduction* |
| 82. Manamedu Complex (India) | 0.800 | X | | SSZ-Forearc |
| 83. Older Basement Unit (Republic of Georgia) | 0.800 | X | | SSZ-? + major shallow MOR component |
| 84. Fawakhir (Nubian Shield, Egypt) | 0.8–0.7 | X | | SSZ-Backarc |
| 85. Southern Ethiopia i) Megado & ii) Moyale-El Kur | 0.70–0.66 | | | *SSZ-type, forearc* |
| 86. Yanbu (Jabal Ess, Al 'Ays) (Arabian Shield) | 0.789 | X | | SSZ/VA-type + minor shallow MOR component |
| 87. Tasriwine (Morocco) | 0.762 | X | | *Arc-related* |
| 88. Burin Group (Newfoundland, Canada) | 0.760 | | | |
| 89. Gabal Gerf (Nubian Shield, Egypt) | 0.750 | | X | MORB-type |
| 90. Wadi Ghadir (Nubian Shield, Egypt) | 0.750 | X | | SSZ-Backarc |
| 91. Wizer (Nubian Shield, Egypt) | 0.750 | X | | SSZ-Forearc + major shallow MOR component |
| 92. Abu Meriewa (Nubian Shield, Egypt) | 0.750 | | X | MORB-type |
| 93. Wadi Kareim (Nubian Shield, Egypt) | 0.750 | X | | SSZ-Backarc |
| 94. Wadi El Dabbah (Nubian Shield, Egypt) | 0.750 | X | | VA-type |
| 95. Tulu Dimtu (Ethiopia) | 0.750 | X | | SSZ-Backarc + shallow to deep MOR component |
| 96. Siroua Massif (Morocco) | 0.743 | X | | SSZ-? |
| 97. Jabal al Wask (Saudi Arabia) | 0.743 | X | | *Marginal sea/island arc* |
| 98. Halaban (Arabian Shield) | 0.700 | X | | SSZ/VA-type |
| 99. Bou Azzer ophiolite (Morocco) | 0.697 | X | | *Island arc/forearc* |
| 100. Enganepe (Polar Urals, Russia) | 0.670 | X | | SSZ-Backarc to forearc + minor shallow MOR component |
| 101. "Marich" ophiolite (Kenya) | 0.663 | X | | SSZ-Backarc |
| 102. Bayankhongor (Mongolia) | 0.647 | | X | MORB-type |
| 103. Pirapora (South America) | 0.628 | X | | MORB-type |
| 104. Chaya Massif, Baikal-Muya (Siberia, Russia) | 0.627 | X | | SSZ-Backarc |
| 105. Cele (Turkey) | >0.590 | X | | *Suprasubduction (arc to backarc)* |
| 106. Matchless greenstone (Namibia) | 0.600 | | X | *Rift-related – Red Sea type* |
| 107. Agardagh Tes-Chem (Mongolia) | 0.569 | X | | SSZ-Backarc + major shallow to deep MOR component |
| 108. Tcherni Vrah & Deli Jovan massifs (Bulgaria/Serbia) | 0.563 | X | | MORB-type |
| 109. Marlborough (E Australia) | 0.560 | X | | SSZ/MORB-type |
| 110. Frolosh/Struma (Bulgaria) | 0.560 | X | | SSZ-Backarc + major shallow to deep MOR component |
| 111. North Qilian Suture (China) | 0.517 | X | | SSZ-Backarc to forearc + shallow MOR component |

Subd.rel. = subduction-related; subd.unrel. = subduction-unrelated; SSZ = suprasubduction zone; VA = volcanic arc; CM = continental margin; MOR = mid-ocean-ridge; P = plume.

(O'Neil et al., 2011), the Eoarchean Isua (Furnes et al., 2009), and the Paleoarchean Barberton (Furnes et al., 2012) sequences. We consider this feature as the strongest evidence for metasomatic processes to yield Th-enrichment of the Paleoarchean mantle above subduction zones (Dilek and Polat, 2008), as also independently suggested by the geophysical data (Chen et al., 2009).

### *5.3. Greenstone sequences related to major global magmatic and tectonic events*

Fig. 24C shows pronounced variations in the estimated subduction-influence for the investigated greenstone belts. The largest variations, continuous from 0 to 100%, are observed in the sequences that formed during the time period ca. 500 to 750 Ma. The older subduction-related greenstones (750 Ma to 3800 Ma) generally define high subduction-influence (~50 to 100%). An exception is shown by part of the Barberton greenstone belt (Komati and Hooggenoeg Complexes) and the Nondweni greenstone that define only ~20% and 10% subduction-influence, respectively (Fig. 24C and Table 2).

Fig. 24D shows a compilation of major global tectonic and magmatic events in the Precambrian (Groves et al., 2005; Nance and Murphy, in press). Such compilation and related interpretations (Fig. 24D) are subject to modifications and discussions as new discoveries and observations come about; similarly, the density distribution pattern of subduction-influenced greenstone sequences, as shown in Fig. 24C, is also subject to change. However, albeit the present dataset is somewhat incomplete, we can still comment on some of the salient patterns seen in Fig. 24C and D. The two time periods for which there are a minimum number of subduction-related greenstone sequences are approximately 1300 to 1700 Ma, and 2100 to 2600 Ma. It is noteworthy to point out that these two time periods coincide with the supercontinent break-up events in the models of Groves et al. (2005) and Nance and Murphy (in press) (Fig. 24D). The youngest of these time periods is within the range of break-up of the inferred Columbia supercontinent that may have started at ~1.6 Ga, and completed by ~1.3 Ga (Zhao et al., 2011). The older of the two periods, i.e. 2100–2600 Ma, is within the time frame for the late Neoarchean to early Paleoproterozoic (2.5–2.1 Ga) break-up of the Neoarchean Kenorland (Strand and Köykkä, 2012), one of the Earth's speculative supercontinents that comprised the Laurentia, Baltica, Australia and Kalahari shields.

The 100% mantle derived sequences are shown by two clusters in the time intervals ca. 560–750 Ma and 1900–2056 Ma, and the two other single examples at 2500 and 2843 Ma (Fig. 24C). It is interesting to note that the ages of the two main 100% mantle-derived and

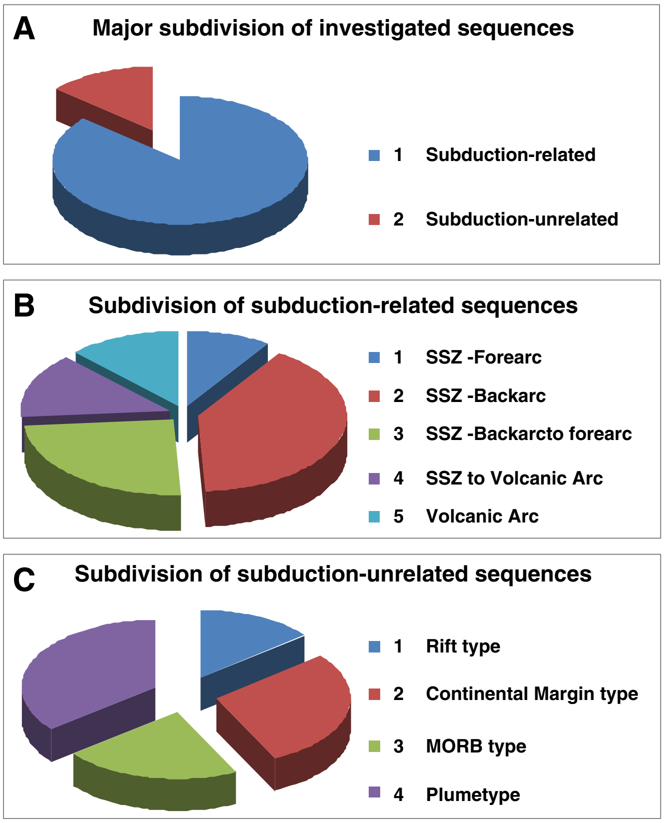


**Fig. 23.** Pie-diagram showing: (A) the proportion of subduction-related and subduction-unrelated Precambrian greenstone sequences; (B) subdivisions of the subduction-related, and (C) the subduction-unrelated investigated greenstone sequences.

subduction-unrelated sequences overlap with or are slightly younger than the two main Precambrian break-up periods (Fig. 24D). The two oldest subduction-unrelated sequences overlap closely in time with the two oldest super-plume records (Fig. 24D).

### 5.4. Precambrian plate tectonics

In light of the geological and geochemical data presented throughout Precambrian time, it is relevant to bring up the discussion about a controversial question, i.e. timing of the onset of plate tectonics in the early history of the Earth. The following time windows have been suggested: at ca. 3 to 3.2 Ga (Van Kranendonk, 2007; Wyman et al., 2008; Shirey and Richardson, 2011; Van Kranendonk, 2011); at 3.6 Ga (Nutman et al., 2007); at 3.8 Ga (Furnes et al., 2007; Dilek and Polat, 2008), at 4.0 Ga (de Wit, 1998; Friend and Nutman, 2010); and by 4.2 Ga (Cavosie et al., 2007). Proponents of the absence of ophiolites in the Archean greenstone belts and the late onset of Phanerozoic-like plate tectonics suggest that it did not commence until the Neoproterozoic (e.g. Bickle et al., 1994; Hamilton, 1998; Stern, 2005; Hamilton, 2007; Stern, 2008; Maurice et al., 2009; Hamilton, 2011).

Starting with the geological development of the selected Archean, Proterozoic and Phanerozoic greenstone sequences as outlined in this study, it is clear that pronounced differences exist both in terms of thickness, and the distribution of different volcanic and intrusive rocks. However, these differences notwithstanding, of the eighteen Archean and Proterozoic greenstone sequences, the majority are regarded to have been generated in a subduction-related tectonic environment; only four (Kostomuksha, Taishan, lower part of Wawa, and Jormua) are interpreted to represent subduction-unrelated greenstone sequences (Fig. 14, and Table 1).

The existence of sheeted dyke complexes in ophiolites has been conventionally interpreted as strong evidence for the origin of ancient oceanic crust via seafloor spreading (e.g. Moores and Vine, 1971; Gass, 1990). This feature is generally regarded as an essential component of those greenstone complexes classified as ophiolites. The implication of sheeted dykes is that their occurrence provides a clear sign of horizontal movement, which is an essential hallmark of plate tectonics. In the Archean examples shown in Fig. 14, three of the complexes, the 3.8 Ga Isua, 2.7 Ga Yellowknife, and 2.5 Ga Dongwanzi greenstone sequences include sheeted dyke complexes, although the case of Dongwanzi as an Archean ophiolite is questionable (Zhai et al., 2002). Also, at various stratigraphic levels of the Hooggenoeg Complex within the Barberton greenstones belt, there are distinctive dyke swarms and the Kromberg Complex contains a well-developed sheeted sill complex (Fig. 14). However, the generation of a sheeted dyke complex requires a delicate balance between the rates of spreading and magma supply for a sustained period such that sufficient melt is produced to keep pace with extension in the rift zone (Robinson et al., 2008). Thus, the rare occurrence or the absence of sheeted dyke complexes could be explained by higher spreading rate, higher magma production from a hotter and/or more vigorously convecting mantle in the Archean (e.g. Hargraves, 1986).

The geochemical signatures as summarized in Fig. 24B show that there has been a secular magmatic evolution (as shown by Ni and Zr). However, independent of this evolution for most of the sequences, even back to the oldest ones represented by the 3.8 Ga Isua and probably also the even older Nuvvuagittuq sequence (Table 1), there is a pronounced subduction-signature (Fig. 24C). Thus, on the basis of geology (rock associations and structural development) and geochemistry, it seems unavoidable that subduction was active, and that plate tectonic processes were operative in the early Archean, although possibly not in the same style and rates as today. At the transition stage between the Hadean into Eoarchean the plates may have been smaller, hotter, and hence more ductile compared to those of the present day (e.g. Abbott and Hoffman, 1984; Pollack, 1997; de Wit, 1998; Dilek and Polat, 2008; Ernst, 2009). This is consistent with the study of the greenstones from the Nuvvuagittuq complex, suggesting that the Hadean/Archean Earth was possibly organized into a larger number of smaller tectonic units than today (e.g. Pollack, 1997; Komiya, 2004) that drifted horizontally rather than by plume-driven tectonic activity (e.g. Adam et al., 2012). Based on lithological components and their field relationships, coupled with geochemical characteristics, the same conclusion was reached for the magmatic complex of the 3.8 Ga Isua supracrustal complex in SW Greenland (Komiya et al., 1999; Furnes et al., 2007, 2009), and by means of paleomagnetic observations for the 3.4–3.5 Ga Onverwacht Suite (Biggin et al., 2011).

## 6. Summary

In this literature-based, global study of one hundred-and-five Precambrian greenstone belts, we have applied a series of discrimination systematics to distinguish those with different geochemical fingerprints and tectonic origins. Plotting the data in a Zr/Ti–Nb/Y diagram helps us isolate the rocks with basaltic compositions in the first step. Producing a Th/Yb–Nb/Yb diagram is the essential next step to discriminate between those of subduction-unrelated (MORB-OIB array) and subduction-related origins of basaltic rock associations. Subduction-related rock units are then plotted in a V–Ti diagram to infer their proximity to a subduction zone during their mantle melt evolution. Subduction-unrelated rock units are plotted in a Ti/Yb–Nb/Yb diagram to deduce the depth of partial melting. Based on this geochemical sorting and using the available geological information, we then classify each of the sequences according to the new and expanded ophiolite classification (Dilek and Furnes, 2011). This systematic survey of the Precambrian greenstone belts shows that they appear to include all the ophiolite types classified in Dilek and Furnes (2011). However, the number of greenstone belts we have

Please cite this article as: Furnes, H., et al., Precambrian greenstone sequences represent different ophiolite types, Gondwana Research (2013), http://dx.doi.org/10.1016/j.gr.2013.06.004

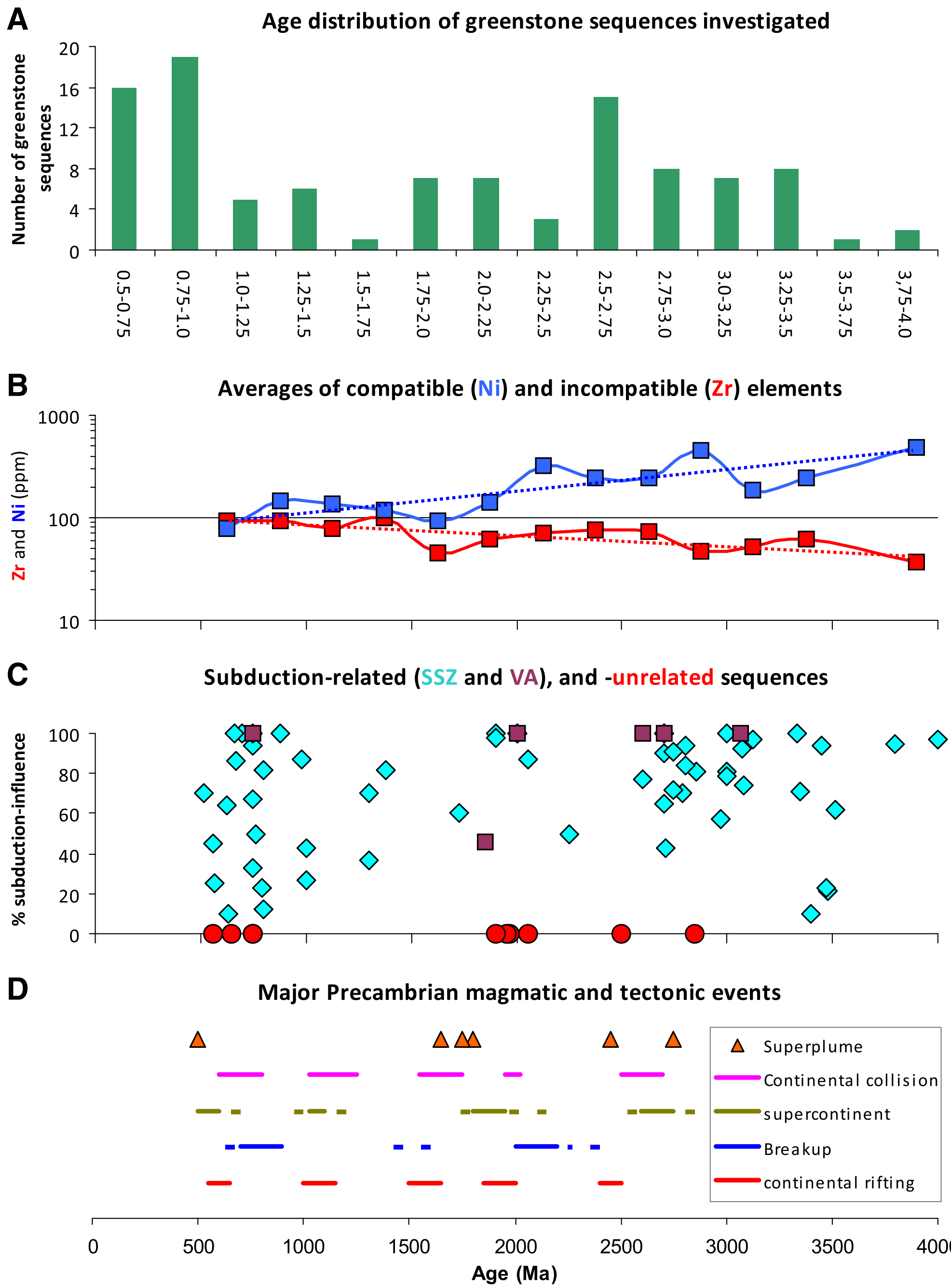


**Fig. 24.** Summary diagram of the data showing: (A) age distribution of investigated greenstone sequences through Precambrian time; (B) average concentrations (at 250 million-years intervals) for two of the most stable elements during alteration and metamorphism, i.e. the compatible element Cr, and the incompatible element Zr; (C) calculated percentage subduction-influence plotted against age of the investigated greenstone sequences; and (D) some of the major tectonic and magmatic events that were likely responsible for the magmatic evolution of the investigated greenstone sequences. The time constraints for: Super continents, Superplume, Breakup (Groves et al., 2005); Continental rifting; Continental collision (Nance and Murphy, in press).

examined represent less than half (42%) of the known greenstone belts worldwide (ca. 250; de Wit and Ashwal, 1997a,b), but for which little or no geochemistry is yet available, leaving much room for further exploration.

We further conclude that:

- The vast majority (85%) of the Precambrian ophiolites for which geochemical data is available, are subduction-related (various suprasubduction (SSZ) types, and volcanic arc type), and 15% are subduction-unrelated.
- The subduction-related type has further been subdivided into SSZ-backarc (40%), SSZ-forearc (9%), SSZ-backarc to forearc (25%), SSZ to volcanic arc (14%), and Volcanic Arc (12%) subtypes.
- The subduction-unrelated can be subdivided into Rift (14%), Continental Margin (28%), MORB (22%) and Plume (36%) subtypes.
- The subduction-related complexes extend back to the oldest known sequences, i.e. the Nuvvuagittuq (3.8–4.3? Ga), Isua (3.8 Ga) and Barberton (3.5–3.2 Ga) sequences.
- The corollary of this conclusion is that plate tectonics with plate subduction had to be operative during the Eoarchean.

## Acknowledgments

We express our sincere thanks to the Editor-in-Chief, M. Santosh, for inviting this contribution to the Special Issue of Ophiolites as a Focus Review Paper. Financial support over many years of field work in Phanerozoic ophiolites and Precambrian greenstone belts has been provided by the Norwegian Research Council and the Meltzer Foundation at the University of Bergen (HF), the National Research Foundation of South Africa (MdeW), and Miami University, USA (YD). Jane Ellingsen helped with most of the illustrations. We acknowledge the insightful and constructive reviews for the journal by Brian F. Windley and Jingen Dai that helped us improve the paper. We also thank Marcia Zucchetti for generously letting us have access to her PhD thesis, and the geochemical data from the Carajas Greenstone Belt of the Amazonian Craton. This is AEON publication No. 114.

## References

Abbott, D.H., Hoffman, S.E., 1984. Archaean plate tectonics revisited 1. Heat flow, spreading rate, and the age of subducting oceanic lithosphere and their effects on the origin and evolution of continents. Tectonics 3 (4), 429–448.

Abd El-Rahman, Y., Polat, A., Dilek, Y., Fryer, B.J., El-Sharkawy, M., Sakran, S., 2009. Geochemistry and tectonic evolution of the Neoproterozoic incipient arc–forearc crust in the Fawakhir area, Central Eastern Desert of Egypt. Precambrian Research 175, 116–134.

Abdelsalam, M.G., Liegeois, J.-P., Stern, R.J., 2002. The Saharan Metacraton. Journal of African Earth Sciences 34, 119–136.

Abdelsalam, M.G., Abdel-Rahman, El-S.M., El-Faki, El-F.M., Al-Hur, B., El-Bashier, F.-R.M., Stern, R.J., Thurmond, A.K., 2003. Neoproterozoic deformation in the northeastern part of the Saharan Metacraton, northern Sudan. Precambrian Research 123, 203–221.

Abouchami, W., Boher, M., 1990. A major 2.1 Ga event of mafic magmatism in West Africa: an early stage of crustal accretion. Journal of Geophysical Research 95 (B11), 17605–17629.

Adam, J., Rushmer, T., O'Neil, J., Francis, D., 2012. Hadean greenstones from the Nuvvuagittuq fold belt and the origin of the Earth's early continental crust. Geology 40 (4), 363–366.

Ahmed, Z., Hariri, M.M., 2008. Neoproterozoic ophiolites as developed in Saudi Arabia and their oceanic and pericontinental domains. Arabian Journal for Science and Engineering 33 (1C), 17–54.

Ali, K.A., Stern, R.J., Manton, W.I., Kimura, J.-I., Khamees, H.A., 2009. Geochemistry, Nd isotopes and U–Pb SHRIMP zircon dating of Neoproterozoic volcanic rocks from the Central Eastern Desert of Egypt: new insight into the 750 Ma crust-forming event. Precambrian Research 171, 1–22.

Al-Saleh, A.M., Boyle, A.P., 2001. Neoproterozoic ensialic back-arc spreading in the eastern Arabian Shield: geochemical evidence from the Halaban Ophiolite. Journal of African Earth Sciences 33 (1), 1–15.

Amelin, Y.V., Ritsk, E.Yu., Neymark, L.A., 1997. Effects of interaction between ultramafic tectonite and mafic magma on Nd–Pb–Sr isotopic systems in the Neoproterozoic Chaya Massif, Baikal-Muya ophiolite belt. Earth and Planetary Science Letters 148, 299–316.

Angerer, T., Kerrich, R., Hagemann, S.G., 2013. Geochemistry of a komatiitic, boninitic, and tholeiitic basalt association in the Mesoarchean Koolyanobbing greenstone belt, Southern Cross Domain, Yilgarn craton: implications for mantle sources and geodynamic setting of banded iron formation. Precambrian Research 224, 110–128.

Anonymous, 1972. Penrose field conference on ophiolites. Geotimes 17, 24–25.

Armstrong, R.A., Compston, W., de Wit, M.J., Williams, I.S., 1990. The stratigraphy of the 3.5–3.2 Ga Barberton Greenstone Belt revisited: a single zircon ion microprobe study. Earth and Planetary Science Letters 101, 90–106.

Arndt, N.T., Lesher, C.M., Barnes, S., 2008. Komatiite. Cambridge University Press (488 pp.).

Baars, F.J., 1997. The São Francisco Craton. In: de Wit, M.J., Ashwal, L.D. (Eds.), Greenstone Belts. Oxford University Press, Oxford, pp. 529–557.

Bailie, R., Gutzmer, J., Rajesh, H.M., 2011. Petrography, geochemistry and geochronology of gthe metavolcanic rocks of the Mesoproterozoic Leerkrans Formation, Wilgenhoutsdrif Group, South Africa — back-arc basin to the Areachap volcanic arc. South African Journal of Geology 114 (2), 167–194.

Bakor, A.R., Gass, I.G., Neary, C.R., 1976. Jabal Al Wask, northwest Saudi Arabia: an Eocambrian back-arc ophiolite. Earth and Planetary Science Letters 30, 1–9.

Baltazar, O.F., Zucchetti, M., 2007. Lithofacies associations and structural evolution of the Archean Rio das Velhas greenstone belt, Quadrilátero Ferrífero, Brazil: a review of the setting of gold deposits. Ore Geology Reviews 32, 471–499.

Barley, M.E., Brown, S.J.A., Krapež, B., Kositcin, N., 2008. Physical volcanology and geochemistry of a Late Archaean volcanic arc: Kurnalpi and Gindalbie Terranes, Eastern Goldfields Superterrane, Western Australia. Precambrian Research 161, 53–76.

Basta, F.F., Maurice, A.E., Bakhit, B.R., Ali, K.A., Manton, W.I., 2011. Neoproterozoic contaminated MORB of Wadi Ghadir ophiolite, NE Africa: geochemical and Nd and Sr isotopic constraints. Journal of African Earth Sciences 59, 227–242.

Bateman, R., Costa, S., Swe, T., Lambert, D., 2001. Archaean mafic magmatism in the Kalgoorlie area of the Yilgarn Craton, Western Australia: a geochemical and Nd isotopic study of the petrogenetic and tectonic evolution of a greenstone belt. Precambrian Research 108, 75–112.

Begg, G.C., Griffin, W.L., Natapov, L.M., O'Reilly, S.Y., Grand, S.P., O'Neill, C.J., Hronsky, J.M.A., Poudjom Djomani, Y., Swain, C.J., Deen, T., Bowden, P., 2009. The lithospheric architecture of Africa: seismic tomography, mantle petrology, and tectonic evolution. Geosphere 5 (1), 23–50.

Bickle, M.J., Nesbit, E.G., Martin, A., 1994. Archean greenstone belts are not oceanic crust. Journal of Geology 102, 121–128.

Biggin, A., de Wit, M.J., Langerijs, C., Zegers, T.E., Voûte, S., Dekkers, M.J., Drost, K., 2011. Palaeomagnetism of Archaean rocks of the Onverwacht Group, Barberton Greenstone Belt (southern Africa): evidence for a stable and potentially reversing geomagnetic field at ca. 3.5 Ga. Earth and Planetary Science Letters 302, 314–328.

Blewitt, R., 2002. Archean tectonic processes: a case for horizontal shortening in the north Pilbara granite-greenstone terrane, Western Australia. Precambrian Research 113, 87–120.

Bolhar, R., Woodhead, J.D., Hergt, J.M., 2003. Continental setting inferred for emplacement of the 2.9–2.7 Ga Belingwe Greenstone Belt, Zimbabwe. Geology 31 (4), 295–298.

Bozkurt, E., Winchester, J.A., Yiğitbaş, E., Ottley, C.J., 2008. Proterozoic ophiolites and mafic-ultramafic complexes marginal to the Istanbul Block: an exotic terrane of Avalonian affinity in NW Turkey. Tectonophysics 461, 240–251.

Breitkoff, J.H., Maiden, K.J., 1988. Tectonic setting of the Matchless Belt pyrite copper deposits, Namibia. Economic Geology 83, 710–723.

Bruce, M.C., Niu, Y., Harbort, T.A., Holcombe, R.J., 2000. Petrological, geochemical and geochronological evidence for a Neoproterozoic ocean basin recorded in the Marlborough terrane of the northern New England Fold Belt. Australian Journal of Earth Sciences 47, 1053–1064.

Buchan, C., Cunningham, D., Windley, B.F., Tomurhuu, D., 2001. Structural and lithological characteristics of the Bayankhongor Ophiolite Zone, Central Mongolia. Journal of the Geological Society of London 158, 445–460.

Buchan, C., Pfänder, J., Kröner, A., Brewer, T.S., Tomurtogoo, O., Tomurchuu, D., Cunningham, D., Windley, B.F., 2002. Timing of accreation and collisional deformation in the Central Asian Orogenic Belt: implications of granite geochronology in the Bayankhongor Ophiolite Zone. Chemical Geology 192 (1–2), 23–45.

Byerly, G.R., 1999. Komatiites of the Mendon Formation: late-stage ultramafic volcanism in the Barberton Greenstone Belt. In: Lowe, D.R., Byerly, G.R. (Eds.), Geologic Evolution of the Barberton Greenstone Belt, South Africa: Boulder, Colorado. Geological Society of America Special Paper, vol. 329, pp. 189–211.

Cates, N.L., Ziegler, K., Schmitt, A.K., Mojzsis, S.J., 2013. Reduced, reused and recycled: detrital zircons define a maximum age for the Eoarchean (ca. 3750–3780 Ma) Nuvvuagittuq Supracrustal Belt, Québec (Canada). Earth and Planetary Science Letters 362, 283–293.

Cavosie, A.J., Valley, J.W., Wilde, S.A., 2007. The oldest terrestrial mineral record: a review of 4400–4000 Ma detrital zircons from Jack Hills, Western Australia. In: Van Kranendonk, M.J., Smithies, R.H., Bennet, V.C. (Eds.), Earth's Oldest Rocks. Development in Precambrian Geology, vol. 15. Elsevier B.V., pp. 91–111.

Cawood, P.A., Tyler, I.M., 2004. Assembling and reactivating the Proterozoic Capricorn Orogen: lithotectonic elements, orogenesis, and significance. Precambrian Research 128, 201–218.

Chavagnac, V., 2004. A geochemical and Nd isotopic study of Barberton komatiites (South Africa): implication for the Archean mantle. Lithos 75, 253–281.

Chen, C.-W., Rondenay, S., Evans, R.L., Snyder, D.B., 2009. Geophysical detection of relict metasomatism from an Archean (3.5 Ga) subduction zone. Science 326, 1089–1091.

Coish, R.A., 1977. Ocean floor metamorphism in the Betts Cove Ophiolite, Newfoundland. Contributions to Mineralogy and Petrology 60, 277–302.

Condie, K.C., 1994. Archean crustal evolution. In: Windley, B.F. (Ed.), Developments in Precambrian Geology. Elsevier (528 pp.).

Condie, K.C., Myers, J.S., 1999. Mesoproterozoic Fraser Complex: geochemical evidence for multiple subduction-related sources of lower crustal rocks in the Albany-Fraser Orogen, Western Australia. Australian Journal of Earth Sciences 46, 875–882.

Corcoran, P.L., Mueller, W.U., Kusky, T.M., 2004. Inferred ophiolites in the Archean Slave Craton. In: Kusky, T.M. (Ed.), Precambrian Ophiolites and Related Rocks. Development in Precambrian Geology, vol. 13, pp. 363–404.

Cordani, U.G., Sato, K., Texeira, W., Tassinari, C.G., Basei, M.A.S., 2000. Crustal evolution of the South American Platform. In: Cordani, U.G., Milani, E.J., Thomaz Filho, A., Campos, D.A. (Eds.), Tectonic Evolution of South America, 31st IGC, Rio de Janeiro, Brazil, Special Publication, pp. 19–40.

Cordani, U.G., Teixeira, W., D'Agrella-Filho, M.S., Trindade, R.I., 2009. The position of the Amazonian Craton in supercontinents. Gondwana Research 15, 396–407.

Corfu, F., 1993. The evolution of the southern Abitibi greenstone belt in light of precise U–Pb geochronology. Economic Geology 88, 1323–1340.

Cousens, B., 2000. Geochemistry of the Archean Kam Group, Yellowknife Greenstone Belt, Slave Province, Canada. Journal of Geology 108, 181–197.

Czarnota, K., Champion, D.C., Goscombe, B., Blewett, R.S., Cassidy, K.F., Henson, P.A., Groenewald, P.B., 2010. Geodynamics of eastern Yilgarn Craton. Precambrian Research 183, 175–202.

Dann, J.C., 1991. Early Proterozoic ophiolite, central Arizona. Geology 19, 590–593.

Dann, J.C., 1992. The Origin and Emplacement of the Early Proterozoic Payson Ophiolite, Central Arizona. (PhD thesis) Washington University (340 pp.).

Dann, J.C., 1997. Pseudostratigraphy and origin of the Early Proterozoic Payson ophiolite, central Arizona. Geological Society of America Bulletin 209 (3), 347–365.

Dann, J.C., 2000. The 3.5 Ga Komati Formation, Barberton Greenstone Belt, South Africa, Part I: new maps and magmatic architecture. South African Journal of Geology 103 (1), 47–68.

Dann, J.C., Bowring, S.A., 1997. The Payson ophiolite and Yavapai–Mazatzal orogenic belt, central Arizona. In: de Wit, M.J., Ashwal, L.D. (Eds.), Greenstone Belts. Oxford University Press, Oxford, U.K., pp. 781–790.

Dann, J.C., Grove, T.L., 2007. Volcanology of the Barberton greenstone Belt, South Africa: inflation and evolution of flow fields. In: Van Kranendonk, M.J., Smithies, R.H., Bennett, V.C. (Eds.), Earth's Oldest Rocks. Developments in Precambrian Geology, vol. 15, pp. 527–570.

de Wit, M.J., 1998. On Archean granites, greenstones, cratons and tectonics: does the evidence demand a verdict? Precambrian Research 91, 181–226.

de Wit, M.J., 2004. Archean greenstone belts do contain fragments of ophiolites. In: Kusky, T.M. (Ed.), Precambrian Ophiolites and Related Rocks. Development in Precambrian Geology, vol. 13, pp. 599–614.

de Wit, M.J., Ashwal, L.D., 1995. Greenstone belts: what are they? South African Journal of Geology 98, 504–519.

de Wit, M.J., Ashwal, L.D., 1997a. Convergence towards divergent models of greenstone belts. In: de Wit, M.J., Ashwal, L.D. (Eds.), Greenstone Belts. Oxford University Press, Oxford, U.K., pp. ix–xvii.

de Wit, M.J., Ashwal, L.D. (Eds.), 1997b. Greenstone Belts. Clarendon Press, Oxford (809 pp.).

de Wit, M.J., Hart, R.A., Hart, R.J., 1987. The Jamestown Ophiolite Complex, Barberton mountain belt: a section through 3.5 Ga oceanic crust. Journal of African Earth Sciences 6, 681–730.

de Wit, M.J., Roering, C., Hart, R.J., Armstrong, R.A., de Ronde, C.E.J., Green, R.E., Tredoux, M., Peberdy, E., Hart, R.A., 1992. Formation of an Archean continent. Nature 357, 553–562.

de Wit, M.J., Furnes, H., Robins, B., 2011. Geology and tectonostratigraphy of the Onverwacht Suite, Barberton Greenstone Belt, South Africa. Precambrian Research 186, 1–27.

Deng, H., Kusky, T., Polat, A., Wang, L., Wang, J., Wang, S., 2013. Geochemistry of Neoarchean mafic volcanic rocks and late mafic dikes and sills in the Zanhuang Complex, Central Orogenic Belt, North China Craton: Implications for geodynamic setting. Lithos 175–176, 193–212.

DePaolo, D.J., 1980. Crustal growth and mantle evolution: inferred from models of element transport and Nd and Sr isotopes. Geochimica et Cosmochimica Acta 44, 1185–1196.

Dharma Rao, C.V., Santosh, M., Wu, Y.-B., 2011. Mesoproterozoic ophiolitic melange from the SE periphery of the Indian plate: U–Pb zircon ages and tectonic implications. Gondwana Research 19, 384–401.

Dilek, Y., 2003. Ophiolite concept and its evolution. In: Dilek, Y., Newcomb, S. (Eds.), Ophiolite Concept and the Evolution of Geological Thought. Geological Society of America Special Paper, 373, pp. 1–16.

Dilek, Y., 2006. Collision tectonics of the Eastern Mediterranean region: causes and consequences. Geological Society of America Special Paper 409, 1–13. http://dx.doi.org/10.1130/2006.2409(1).

Dilek, Y., Ahmed, Z., 2003. Proterozoic ophiolites of the Arabian Shield and their significance in Precambrian tectonics. In: Dilek, Y., Robinson, P.T. (Eds.), Ophiolites in Earth History. Geological Society, London, Special Publications, vol. 218, pp. 685–700.

Dilek, Y., Eddy, C.A., 1992. The Troodos and Kizaldag ophiolites as structural models for slow-spreading ridge segments. Journal of Geology 100, 305–322.

Dilek, Y., Flower, M.F.J., 2003. Arc-trench rollback and forearc accretion: 2. Model template for Albania, Cyprus, and Oman. In: Dilek, Y., Robinson, P.T. (Eds.), Ophiolites in Earth History. Geological Society of London Special Publication, 218, pp. 43–68.

Dilek, Y., Furnes, H., 2009. Structure and geochemistry of Tethyan ophiolites and their petrogenesis in subduction rollback systems. Lithos 113, 1–20.

Dilek, Y., Furnes, H., 2011. Ophiolite genesis and global tectonics: geochemical and tectonic fingerprinting of ancient oceanic lithosphere. Geological Society of America Bulletin 123 (3/4), 387–411.

Dilek, Y., Polat, A., 2008. Suprasubduction zone ophiolites and Archean tectonics. Geology 36 (5), 431–432.

Dilek, Y., Robinson, P.T., 2003. Ophiolites in Earth History: introduction. In: Dilek, Y., Robinson, P.T. (Eds.), Ophiolites in Earth History. Geological Society of London Special Publication, 218, pp. 1–8.

Dilek, Y., Thy, P., 2009. Island arc tholeiite to boninitic melt evolution of the Cretaceous Kizildag (Turkey) ophiolite: model for multi-stage early arc-forearc magmatism in Tethyan subduction factories. Lithos 113, 68–87. http://dx.doi.org/10.1016/j.lithos.2009.05.044.

Dilek, Y., Shallo, M., Furnes, H., 2005. Rift–drift, seafloor spreading, and subduction tectonics of Albanian ophiolites. International Geology Review 47, 147–176.

Dilek, Y., Furnes, H., Shallo, M., 2008. Geochemistry of the Jurassic Mirdita ophiolite (Albania) and the MORB to SSZ evolution of a marginal basin oceanic crust. Lithos 100, 174–209. http://dx.doi.org/10.1016/j.lithos.2007.06.026.

Dostal, J., Mueller, W.U., 2013. Deciphering an Archean mantle plume: Abitibi greenstone belt, Canada. Gondwana Research 23, 493–505.

El Bahat, A., Ikenne, M., Søderlund, U., Cousens, B., Youbi, N., Ernst, R., Soulaimani, A., El Janati, M., Hafid, A., 2013. U–Pb baddelyite ages and geochemistry of dolerite dikes in the Bas Draa Inlier of the Anti-Atlas of Morocco: newly identified 1380 Ma event in the West African Craton. Lithos 174, 85–98.

El Boukhari, A., Chabane, A., Rocci, G., Tane, J.-L., 1992. Upper Proterozoic ophiolites of the Siroua Massif (Anti-Atlas, Morocco) a marginal sea and transform fault system. Journal of African Earth Sciences 14 (1), 67–80.

Eriksson, P.G., Alterman, W., Nelson, D.R., Mueller, W.U., Catuneanu, O. (Eds.), 2004. The Precambrian Earth: Tempos and Events. Condie, K.C. (Ed.), 2004. Developments in Precambrian Geology, vol. 12. Elsevier, Amsterdam (941 pp.).

Ernst, W.G., 2009. Archean plate tectonics, rise of Proterozoic supercontinentality and onset of regional, episodic stagnant-lid behavior. Gondwana Research 15, 243–253.

Farahat, E.S., 2010. Neoproterozoic arc-back-arc system in the Central Eastern Desert of Egypt: evidence from supra-subduction zone ophiolites. Lithos 120, 293–308.

Fitzsimons, I.C.W., 2003. Proterozoic basement provinces of southern and south-western Australia, and their correlation with Antarctica. In: Yoshida, M., Windley, B.F., Dasgupta, S. (Eds.), Proterozoic East Gondwana: Supercontinent Assembly and Breakup. Geological Society, London, Special Publications, vol. 206, pp. 93–130.

Flower, M.F.J., Dilek, Y., 2003. Arc-trench rollback and accretion: 1. A collision induced mantle flow model for Tethyan ophiolites. In: Dilek, Y., Robinson, P.T. (Eds.), Ophiolites in Earth history. Geological Society of London Special Publication, 218, pp. 21–41.

Floyd, P.A., Winchester, J.A., 1975. Magma type and tectonic setting discrimination using immobile elements. Earth and Planetary Science Letters 27, 211–218.

Foley, S.F., Buhre, S., Jacob, D.E., 2003. Evolution of the Archaean crust by lamination and shallow subduction. Nature 421, 249–252.

Friend, C.R.L., Nutman, A.P., 2010. Eoarchean ophiolites? New evidence for the debate on the Isua supracrustal belt, Southern West Greenland. American Journal of Science 310, 826–861.

Furnes, H., Pedersen, R.B., Stillman, C.J., 1988. The Leka Ophiolite Complex, central Norwegian Caledonides: field characteristics and geotectonic significance. Journal of the Geological Society of London 145, 401–412.

Furnes, H., de Wit, M., Staudigel, H., Rosing, M., Muehlenbachs, K., 2007. A vestige of Earth's oldest ophiolite. Science 315, 1704–1707.

Furnes, H., Rosing, M., Dilek, Y., de Wit, M., 2009. Isua supracrustal belt (Greenland) — a vestige of a 3.8 Ga suprasubduction zone ophiolite, and implications for Archean geology. Lithos 113, 115–132.

Furnes, H., de Wit, M.J., Robins, B., Sandstå, N.R., 2011. Volcanic evolution of the upper Onverwacht Suite, Barberton Greenstone Belt, South Africa. Precambrian Research 186, 28–50.

Furnes, H., Robins, B., de Wit, M.J., 2012. Geochemistry and petrology of lavas in the upper Onverwacht Suite, Barberton Mountain Land, South Africa. South African Journal of Geology 115 (2), 171–210.

Furnes, H., de Wit, M.J., Robins, B., 2013. A review of new interpretations of the tectonostratigraphy, geochemistry and evolution of the Onverwacht Suite, Barberton Greenstone Belt, South Africa. Gondwana Research 23, 403–428.

Furnes, H., de Wit, M.J., Dilek, Y., 2013. Precambrian greenstone belts host different ophiolite types. In: Dilek, Y., Furnes, H. (Eds.), Archean Earth and Early Life. Springer Science (in press).

Garrison Jr., J.R., 1981. Metabasalts and metagabbros from the Llano Uplift, Texas: petrologic and geochemical characterization with emphasis on tectonic setting. Contributions to Mineralogy and Petrology 78, 459–475.

Garrison Jr., J.R., 1985. Petrology, geochemistry, and origin of the Big Branch and Red Mountain Gneisses, southeastern Llano uplift, central Texas. American Mineralogist 70, 1151–1163.

Gass, I.G., 1990. Ophiolites and oceanic lithosphere. In: Malpas, J., Moores, E.M., Panayiotou, A., Xenophontos, C. (Eds.), Ophiolites, Oceanic Crustal Analogues. Proceedings of the Symposium "Troodos 1987". The Geological Survey Department, Nicosia, Cyprus, pp. 1–10.

Gillis, K.M., Thompson, G., 1993. Metabasalts from the Mid-Atlantic Ridge: new insight into hydrothermal systems in slow-spreading crust. Contributions to Mineralogy and Petrology 113, 502–523.

Glen, R.A., 2005. The Tasmanides of eastern Australia. In: Vaughan, A.P.M., Leat, P.T., Pankhurst, R.J. (Eds.), Terrane Processes at the Margins of Gondwana. Geological Society, London, Special Publications, vol. 246, pp. 23–96.

Goodwin, A.M., 1996. Principles of Precambrian Geology. Academic Press, London (327 pp.).

Grove, T.L., Parman, S.W., 2004. Thermal evolution of the Earth as recorded by komatiites. Earth and Planetary Science Letters 219, 173–187.

Groves, D.I., Condie, K.C., Goldfarb, R.J., Hronsky, J.M.A., Vielreicher, R.M., 2005. Secular changes in global tectonic processes and their influence on the temporal distribution of gold-bearing mineral deposits. Economic Geology 100, 203–224.

Hamilton, W.B., 1998. Archean magmatism and deformation were not the products of plate tectonics. Precambrian Research 91, 109–142.

Hamilton, W.B., 2007. Earth's first two billion years — the era of internally mobile crust. Geological Society of America, Memoir 200, 233–296.

Hamilton, W.B., 2011. Plate tectonics began in Neoproterozoic time, and plumes from deep mantle have never operated. Lithos 123, 1–20.

Hanski, E.S., 1997. The Nuttio sepentinite belt, Central Lapland: an example of Paleoproterozoic ophiolitic mantle rocks in Finland. Ofioliti 22 (1), 35–46.

Hanski, E., Huhma, H., 2005. Central Lapland greenstone belt. In: Lehtinen, M., Nurmi, P.A., Ramø, O.T. (Eds.), Precambrian Geology of Finland – Key to the Evolution of the Fennoscandian Shield. Elsevier B.V., Amsterdam, pp. 139–194.

Hanski, E., Huhma, H., Rastas, P., Kamenetsky, V.S., 2001. The Palaeoproterozoic komatiite–picrite association of Finnish Lapland. Journal of Petrology 52 (5), 855–876.

Hargraves, R.B., 1986. Faster spreading or greater ridge length in the Archean? Geology 14, 750–752.

Harms, U., Darbyshire, D.P.F., Denkler, T., Hengst, M., Schandelmeier, H., 1994. Evolution of the Neoproterozoic Delgo suture zone and crustal growth in northern Sudan: geochemical and radiogenic isotope constraints. Geologische Rundschau 83, 591–603.

Harper, G.D., 1985. Dismembered Archean ophiolite, Wind River Mountains, Wyoming (U.S.A.). Ofioliti 10 (2/3), 297–306.

Heilimo, E., Halla, J., Höllä, P., 2010. Discrimination and origin of the sanukitoid series: geochemical constraints from the Neoarchean western Karelian Province (Finland). Lithos 115, 27–39.

Hellman, P.L., Smith, R.E., Henderson, P., 1979. The mobility of the rare earth elements: evidence and implications from selected terrains affected by burial metamorphism. Contributions to Mineralogy and Petrology 71, 23–44.

Henriksen, N., Higgins, A.K., Kalsbeek, F., Pulvertaft, T.C.R., 2009. Greenland from Archean to Quaternary. Descriptive text to the 1995 Geological map of Greenland, 1:2500000. Geological Survey of Denmark and Greenland Bulletin 18, 126 pp. + map.

Please cite this article as: Furnes, H., et al., Precambrian greenstone sequences represent different ophiolite types, Gondwana Research (2013), http://dx.doi.org/10.1016/j.gr.2013.06.004

Herzberg, C., Condie, K., Korenaga, J., 2010. Thermal history of the Earth and its petrological expression. Earth and Planetary Science Letters 292, 79–88.
Hickman, A.H., 2004. Two contrasting granite–greenstone terranes in the Pilbara Craton, Australia: evidence for vertical and horizontal tectonic regimes prior to 2900 Ma. Precambrian Research 131, 153–172.
Hickman, A.H., 2012. Review of the Pilbara Craton and Fortescue Basin, Western Australia: crustal evolution providing environments for early life. Island Arc 21, 1–31.
Hoffmann, J.E., Münker, C., Polat, A., König, S., Mezger, K., Rosing, M.T., 2010. Highly depleted Hadean mantle reservoirs in the sources of early Archean arc-like rocks, Isua supracrustal belt, southern West Greenland. Geochimica et Cosmochimica Acta 74, 7236–7260.
Hofmann, A., Kusky, T., 2004. The Belingwe greenstone belt: ensialic or oceanic? In: Kusky, T.M. (Ed.), Precambrian Ophiolites and Related Rocks. In: Condie, K.C. (Ed.), Developments in Precambrian Geology, vol. 13, pp. 486–536.
Hofmann, A., Wilson, A.H., 2007. Silicified basalts, bedded cherts and other sea floor alteration phenomena of the 3.4 Ga Nondweni greenstone belt, South Africa. In: Van Kranendonk, M.J., Smithies, R.H., Bennett, V.C. (Eds.), Earth's Oldest Rocks. Developments in Precambrian Geology, vol. 15, pp. 571–605.
Hunter, D.R., Stove, C.W., 1997. A historical review of the origin, composition, and setting of Archean greenstone belts. In: de Wit, M.J., Ashwal, L.D. (Eds.), Greenstone Belts. Oxford University Press, Oxford, U.K., pp. 5–30.
Huson, R., Kusky, T.M., Li, J.H., 2004. Geochemical and petrological characteristics of the central belt of the Archean Dongwanzi ophiolite complex. In: Kusky, T.M. (Ed.), Precambrian Ophiolites and Related Rocks. Development in Precambrian Geology, vol. 13, pp. 283–320.
Hussein, I.M., Kröner, A., Reismann, T., 2004. The Wadi Onib mafic-ultramafic complex: a Neoproterozoic supra-subduction zone ophiolite in the northern Red Sea Hills of the Sudan. In: Kusky, T.M. (Ed.), Precambrian Ophiolites and Related Rocks. Developments in Precambrian Geology, vol. 13, pp. 163–206.
Isachsen, C.E., Bowring, S.A., 1994. Evolution of the Slave craton. Geology 22, 917–920.
Isachsen, C.E., Bowring, S.A., 1997. The Bell Lake group and Anton Complex: a basement-cover sequence beneath the Archean Yellowknife greenstone belt revealed and implicated in greenstone belt formation. Canadian Journal of Earth Sciences 34, 169–189.
Ishizuka, O., Tani, K., Reagan, M.K., 2013. Izu-Bonin-Mariana forearc crust as a modern ophiolite analogue. Elements (in press).
Jahn, B.M., 2004. The Central Asian Orogenic Belt and growth of the continental crust in the Phanerozoic. In: Malpas, J., Fletcher, C.J.N., Ali, R.R., Aitchison, J.C. (Eds.), Aspects of the Tectonic Evolution of China. Geological Society, London, Special Publications, vol. 226, pp. 73–100.
Jahn, B.M., Auvray, B., Blais, S., Capdevila, R., Cornichet, J., Vidal, F., Hameurt, J., 1980. Trace element geochemistry and petrogenesis of Finnish greenstone belts. Journal of Petrology 21 (2), 201–244.
Jahn, B.M., Gruau, G., Glikson, A.Y., 1982. Komatiites of the Onverwacht Group, S. Africa: REE geochemistry, Sm/Nd age, and mantle evolution. Contributions to Mineralogy and Petrology 80, 25–40.
Jayananda, M., Kano, T., Peucat, J.-J., Channabasappa, S., 2008. 3.35 Ga komatiite volcanism in the western Dharwar craton, southern India: constraints from Nd isotopes and whole-rock geochemistry. Precambrian Research 162, 160–179.
Jian, P., Kröner, A., Windley, B.F., Shi, Y., Zhang, F., Miao, L., Tomurhuu, D., Zhang, W., Liu, D., 2010. Zircon ages of the Bayankhongor ophiolite melange and associated rocks: time constraints on Neoproterozoic to Cambrian accretionary and collisional orogenesis in Central Mongolia. Precambrian Research 177, 162–180.
Johnson, S.P., Oliver, G.J.H., 2000. Mesoproterozoic oceanic subduction, island-arc formation and the initiation of back-arc spreading in the Kibaran Belt of central, southern Africa: evidence from the Ophiolite Terrane, Chevore Inliers, northern Zimbabwe. Precambrian Research 103, 125–146.
Johnson, P.R., Andresen, A., Collins, A.S., Fowler, A.R., Fritz, H., Ghebreab, W., Kusky, T., Stern, R.J., 2011. Late Cryogenian-Ediacaran history of the Arabian-Nubian Shield: a review of depositional, plutonic, structural and tectonic events in the closing stages of the northern East African Orogen. Journal of African Earth Sciences 61, 167–232.
Keller, C.B., Schoene, B., 2012. Statistical geochemistry reveals disruption in secular lithospheric evolution about 2.5 Gyr ago. Nature 585, 490–495.
Kemp, A.I.S., Hawkesworth, C.J., Collins, W.J., Gray, C.M., Blevin, P.L., EIMF, 2009. Isotopic evidence for rapid continental growth in an extensional accretionary orogen: the Tasmanides, eastern Australia. Earth and Planetary Science Letters 284, 455–466.
Kerrich, R., Wyman, D., Fan, J., Bleeker, W., 1998. Boninite series: low Ti-tholeiite associations from the 2.7 Ga Abitibi greenstone belt. Earth and Planetary Science Letters 164, 303–316.
Khain, E.V., Bibikova, E.V., Kröner, A., Zhuravlev, D.Z., Sklyarov, E.V., Fedotova, A.A., Kravchenko-Berezhnoy, I.R., 2002. The most ancient ophiolite of the Central Asian fold belt: U–Pb and Pb–Pb zircon ages for the Dunzhugur Complex, Eastern Sayan, Siberia, and geodynamic implications. Earth and Planetary Science Letters 199, 311–325.
Klemd, R., Maiden, K.J., Okrusch, M., Richter, P., 1989. Geochemistry of the Matchless metamorphosed massive sulfide deposits, South West Africa/Namibia: wall–rock alteration during submarine ore-forming processes. Economic Geology 84, 603–617.
Kloppenburg, A., White, S.H., Zegers, T.E., 2001. Structural evolution of the Warrawoona Greenstone Belt and adjoining granitoid complexes, Pilbara Craton, Australia: implications for Archean tectonic processes. Precambrian Research 112, 107–147.
Komiya, T., 2004. Material circulation model including chemical differentiation within the mantle and secular variation of temperature and composition of the mantle. Physics of the Earth and Planetary Interiors 146, 333–367.
Komiya, T., Maruyama, S., Masuda, T., Nohda, S., Hayashi, M., Okamoto, K., 1999. Plate tectonics at 3.8–3.7 Ga: field evidence from the Isua accretionary complex, Southern West Greenland. Journal of Geology 107, 515–554.
Komiya, T., Maruyama, S., Hirata, T., Yurimoto, H., Nohda, S., 2004. Geochemistry of the oldest MORB and OIB in the Isua Supracrustal Belt, southern West Greenland: implications for the composition and temperature of early Archean upper mantle. Island Arc 13 (1), 47–72.
Kontinen, A., 1987. An early Proterozoic ophiolite — the Jormua mafic-ultramafic complex, northeastern Finland. Precambrian Research 35, 313–334.
Korenaga, J., 2006. Archean geodynamics and the thermal evolution of Earth. In: Benn, K., Mareschal, J.-C., Condie, K. (Eds.), Archean Geodynamics and Environments. AGU Geophysical Monograph Series, vol. 164. AGU, Washington DC, pp. 7–32.
Kounov, A., Graf, J., von Quadt, A., Bernoulli, D., Burg, J.-P., Seward, D., Ivanov, Z., Fanning, M., 2012. Evidence for a "Cadomian" ophiolite and magmatic-arc complex in SW Bulgaria. Precambrian Research 212–213, 275–295.
Kröner, A. (Ed.), 1981. Precambrian Plate Tectonics. Developments in Precambrian Geology, 4. Elsevier, Amsterdam (781 pp.).
Kröner, A., Hegner, E., Wendt, J.L., Byerly, G.R., 1996. The oldest part of the Barberton granitoid–greenstone terrain, South Africa: evidence for crust formation between 3.5 and 3.7 Ga. Precambrian Research 78, 105–124.
Kusky, T.M. (Ed.), 2004. Precambrian Ophiolites and Related Rocks. Developments in Precambrian Geology, vol. 13 (772 pp.).
Kusky, T.M., Kidd, W.S.F., 1992. Remnants of an Archaean oceanic plateau, Belingwe Greenstone Belt, Zimbabwe. Geology 20, 43–46.
Kusky, T.M., Li, J.-H., 2002. Is the Donwanzi Complex an Archean ophiolite? Response to Zhai, M.G., Zhao, G., Zhang, Q. Science 295, 923a.
Kusky, T.M., Zhai, M., 2012. The Neoarchean ophiolite in the North China Craton: Early Precambrian plate tectonics and scientific debate. Journal of Earth Science 23 (3), 277–284.
Kusky, T.M., Li, J.-H., Tucker, R.D., 2001. The Archean Dongwanzi ophiolite complex, north China craton: 2.505-billion-year-old oceanic crust and mantle. Science 292, 1142–1145.
Küster, D., Liégeois, J.-P., 2001. Sr, Nd isotopes and geochemistry of the Bayuda Desert high grade metamorphic basement (Sudan): an early Pan African oceanic convergent margin, not the edge of the east Saharan ghost craton? Precambrian Research 109, 1–23.
Lahaye, Y., Arndt, N., Byerly, G., Chauvel, C., Fourcade, S., Gruau, G., 1995. The influence of alteration on the trace-element and Nd isotopic compositions of komatiites. Chemical Geology 126, 43–64.
Lavrik, S.N., Mishkin, M.A., 2010. Geochemistry of metamorphosed volcanic rocks in the Kholodnikan greenstone belt, southern Aldan Shield. Geochemistry International 48 (6), 593–605.
Le Bas, M.J., Streckeisen, A.L., 1991. The IUGS systematics of igneous rocks. Journal of the Geological Society of London 148, 825–833.
Li, X.-H., 1997. Geochemistry of the Longsheng Ophiolite from the southern margin of Yangtze Craton, SE China. Geochemical Journal 31, 323–337.
Li, X.-H., Zhao, J.-x., McCulloch, M.T., Zhou, G.-q., Xing, F.-m., 1997. Geochemical and Sm–Nd isotopic study of Neoproterozoic ophiolites from southeastern China: petrogenesis and tectonic implications. Precambrian Research 814, 129–144.
Li, J., Kusky, T.M., Huang, X., 2002. Archean podiform chromitites and mantle tectonites in ophiolitic melange, North China Craton, A record of early oceanic mantle processes. GSA Today 12 (7), 4–11.
Lopez- Martinez, M., York, D., Hanes, J.A., 1992. $^{40}Ar/^{39}Ar$ geochronology study of Komatiites and komatiitic basalts form the lower Onverwacht Volcanics, Barberton Mountain Land, South Africa. Precambrian Research 57, 91–119.
Lowe, D.R., Byerly, G.R., 1999. Stratigraphy of the west-central part of the Barberton Greenstone Belt, South Africa. In: Lowe, D.R., Byerly, G.R. (Eds.), Geologic Evolution of the Barberton Greenstone Belt, South Africa: Boulder, Colorado. Geological Society of America Special Paper, vol. 329, pp. 1–36.
Lowe, D.R., Byerly, G.R., 2007. An overview of the geology of the Barberton Greenstone Belt: implications for early crustal development. In: Van Kranendonk, M.J., Smithies, R.H., Bennett, V.C. (Eds.), Earth's Oldest Rocks. Developments in Precambrian Geology, vol. 15, pp. 481–526.
Lowe, D.R., Byerly, G.R., Heubeck, C., 1999. Structural divisions and development of the west-central part of the Barberton Greenstone Belt. In: Lowe, D.R., Byerly, G.R. (Eds.), Geologic Evolution of the Barberton Greenstone Belt, South Africa: Boulder, Colorado. Geological Society of America Special Paper, vol. 329, pp. 37–82.
Lucas, S.B., Stern, R.A., Syme, E.C., Reilly, B.A., Thomas, D.J., 1996. Intraoceanic tectonics and the development of continental crust: 1.92–1.84 Ga evolution of the Flin Flon Belt, Canada. Geological Society of America Bulletin 108 (5), 602–629.
Manikyamba, C., Naqvi, S.M., Subba Rao, D.V., Ram Mohan, M., Khanna, T.C., Rao, T.C., Reddy, G.L.N., 2005. Boninites from the Neoarchaean Gadwal Greenstone belt, Eastern Dharwar Craton, India: implications for Archaean subduction processes. Earth and Planetary Science Letters 230, 65–83.
Manikyamba, C., Kerrich, R., Khanna, T.C., Satyanayanan, M., Keshav Krishna, A., 2009. Enriched and depleted arc basalts, with Mg-andesites and adakites: a potential paired arc-back-arc of the 2.6 Ga Hutti greenstone terrane, India. Geochimica et Cosmochimica Acta 73, 1711–1736.
Marshak, S., 2005. Earth: Portrait of a Planet. W.W. Norton & Company, New York (747 pp.).
Maurice, C., David, J., Bedard, J.H., Francis, D., 2009. Evidence for a mafic cover sequence and its implications for continental growth in the northeastern Superior Province. Precambrian Research 168, 45–65.
Meert, J.G., Pandit, M.K., Pradhan, V.R., Banks, J., Sirianni, R., Stroud, M., Newstead, B., Gifford, J., 2010. Precambrian crustal evolution of Peninsular India: a 3.0 billion year odyssey. Journal of Asian Earth Sciences 39, 483–515.
Mil'kevich, R.I., Myskova, T.A., Glebovitsky, V.A., L'vov, A.B., Berezhnaya, N.G., 2007. Kalikorva structure and its position in the system of the Northern Karelian

greenstone belts: geochemical and geochronological data. Geochemistry International 45 (5), 428–450.

Miyashiro, A., 1973. The Troodos ophiolite complex was probably formed in an island arc. Earth and Planetary Science Letters 19, 218–224.

Moores, E.M., Vine, F.J., 1971. The Troodos massif, Cyprus, and other ophiolites as oceanic crust: Evaluation and implications. Philosophical Transactions of the Royal Society of London 268A, 443–466.

Mueller, W.U., Stix, J., Corcoran, P.L., Daigneault, R., 2009. Subaqueous calderas in the Archean Abitibi greenstone belt: an overview and new ideas. Ore Geology Reviews 35, 4–46.

Mukhopadhyay, J., Ghosh, G., Zimmermann, U., Guha, S., Mukherjee, T., 2012. A 3.51 Ga bimodal volcanics-BIF-ultramafic succession from Singhbhum Craton: implications for Palaeoarchaean geodynamic processes from the oldest greenstone succession of the Indian subcontinent. Geological Journal 47, 284–311.

Murphy, J.B., McCausland, P.J.A., O'Brien, S.J., Pisarevsky, S., Hamilton, M.A., 2008. Age, geochemistry and Sm–Nd isotopic signature of the 0.76 Ga Burin Group: compositional equivalent of Avalonian basement? Precambrian Research 165, 37–48.

Naidoo, D.D., Bloomer, S.H., Saquaque, A., Hefferan, K., 1991. Geochemistry and significance of metavolcanic rocks from the Bou Azzer-El Graara ophiolite (Morocco). Precambrian Research 53, 79–97.

Nance, R.D., Murphy, J.B., 2013. Origins of the supercontinent cycle. Geoscience Frontiers. http://dx.doi.org/10.1016/j.gsf.2012.12.007 (in press).

Naqvi, S.M., Rogers, J.J.W., 1987. Precambrian Geology of India. Oxford University Press, New York (223 pp.).

Naqvi, S.M., Khan, R.M.K., Manikyamba, C., Ram Mohan, M., Khanna, T.C., 2006. Geochemistry of the NeoArchaean high-Mg basalts, boninites and adakites from the Kushtagi-Hungund greenstone belt of the Eastern Dharwar Craton (EDC); implications for tectonic setting. Journal of Asian Earth Sciences 27, 25–44.

Nassief, M.O., Macdonald, R., Gass, I.G., 1984. The Jebel Thurwah Upper Ophiolite Complex, western Saudi Arabia. Journal of the Geological Society of London 141, 537–546.

Noce, C.M., Tassinari, C.G., Lobato, L.M., 2007. Geochronological framework of the Quadrilátero Ferrífero, with emphasis on the age of gold mineralization hosted in Archean greenstone belts. Ore Geology Reviews 32, 500–510.

Nutman, A.P., Bennett, V.C., Friend, C.R.L., Rosing, M.T., 1997. 3710 and ≥ 3790 Ma volcanic sequences in the Isua (Greenland) supracrustal belt; structural and Nd isotope implications. Chemical Geology 141, 271–287.

Nutman, A.P., Friend, C.R.L., Horie, K., Hidaka, H., 2007. The Itsaq Gneiss complex of southern west Greenland and the construction of Eoarchean crust at convergent plate boundaries. In: Van Kranendonk, M.J., Smithies, R.H., Bennet, V.C. (Eds.), Earth's Oldest Rocks. Development in Precambrian Geology, vol. 15. Elsevier B.V., pp. 187–218.

O'Neil, J., Carlson, R.W., Francis, D., Stevenson, R.K., 2008. Neodymium-142 evidence for Hadean mafic crust. Science 321, 1828–1831.

O'Driscoll, C.F., Dean, M.T., Wilton, D.H.C., Hinchey, J.G., 2001. The Burin Group: a Late Neoproterozoic ophiolite containing shear zone-hosted mesothermal-style gold mineralization in the Avalon Zone, Burin Peninsula, Newfoundland. Current Research. Geol. Surv. Branch Rept., 1. Dept. Mines Energy, Nfld, pp. 229–246.

Ohta, H., Maruyama, S., Takahashi, E., Watanabe, Y., Kato, Y., 1996. Field occurrence, geochemistry and petrogenesis of the Archean Mid-Oceanic Ridge basalts (AMORBs) of the Cleaverville area, Pilbara Craton, Western Australia. Lithos 37, 199–221.

Okay, A.I., Bozkurt, E., Satir, M., Yiğitbaş, E., Crowley, Q.G., Shang, C.K., 2008. Defining the southern margin of Avalonia in the Pontides: geochronological data from the Late Proterozoic and Ordovician granitoids from NW Turkey. Tectonophysics 461, 252–264.

O'Neil, J., Francis, D., Carlson, R.W., 2011. Implications of the Nuvvuagittuq greenstone belt for the formation of Earth's early crust. Journal of Petrology 52 (5), 985–1009.

Ordóñez-Calderon, J.C., Polat, A., Fryer, B.J., Apple, P.W.U., van Gool, J.A.M., Dilek, Y., Gagnon, J.E., 2009. Geochemistry and geodynamic origin of the Mesoarchean Ujarassuit and Ivisaartoq greenstone belts, SW Greenland. Lithos 113, 133–157.

Ordóñez-Calderon, J.C., Polat, A., Fryer, B.J., Gagnon, J.E., 2011. Field and geochemical characteristics of Mesoarchean to Neoarchean volcanic rocks in the Storö greenstone belt, SW Greenland: evidence for accretion of intra-oceanic volcanic arcs. Precambrian Research 184, 24–42.

Oyhantçabal, P., Siegesmund, S., Wemmer, K., 2011. The Río de Plata Craton: a review of units, boundaries, ages and isotopic significance. International Journal of Earth Sciences 100, 201–220.

Pandit, M.K., de Wall, H., Daxberger, H., Just, J., Bestmann, M., Sharma, K.K., 2011. Mafic rocks from Erinpura gneiss terrane in the Sirohi region: possible ocean-floor remnants in the foreland of the Delhi Fold Belt, NW India. Journal of Earth System Science 120 (4), 627–641.

Parman, S.W., Grove, T.L., 2004. Petrology and geochemistry of Barberton komatiites and basaltic komatiites: evidence of Archean fore-arc magmatism. In: Kusky, T.M. (Ed.), Precambrian Ophiolites and Related Rocks. Developments in Precambrian Geology, vol. 13, pp. 539–565.

Parman, S.W., Dann, J.C., Grove, T.L., de Wit, M.J., 1997. Emplacement conditions of komatiitic magmas from the 3.49 Ga Komati Formation, Barberton Greenstone Belt, South Africa. Earth and Planetary Science Letters 150, 303–323.

Pawley, M.J., Wingate, M.T.D., Kirkland, C.L., Wyche, S., Hall, C.E., Romano, S.S., Doublier, M.P., 2012. Adding pieces to the puzzle: episodic growth and a new terrane in the northeast Yilgarn Craton, Western Australia. Australian Journal of Earth Sciences 59, 603–623.

Pearce, J.A., 1975. Basalt geochemistry used to investigate past tectonic environments on Cyprus. Tectonophysics 25, 41–67.

Pearce, J.A., 1982. Trace element characteristics of lavas from destructive plate boundaries. In: Thorpe, J.S. (Ed.), Andesites. John Wiley, New York, pp. 525–548.

Pearce, J.A., 2008. Geochemical fingerprinting of oceanic basalts with implications for the classification of ophiolites and search for Archean oceanic crust. Lithos 100, 14–48.

Pearce, J.A., 2013. Immobile elements fingerprinting of ophiolites. Elements (in press).

Pearce, J.A., Cann, J.R., 1971. Ophiolite origin investigated by discriminant analysis using Ti, Zr and Y. Earth and Planetary Science Letters 12, 339–349.

Pearce, J.A., Parkinson, I.J., 1993. Trace element models for mantle melting: application to volcanic arc petrogenesis. In: Prichard, H.M., Alabaster, T., Harris, N.B.W., Neary, C.R. (Eds.), Magmatic Processes and Plate Tectonics. Geological Society of London, Special Publication, vol. 76, pp. 373–403.

Pearce, J.A., Lippard, S.J., Roberts, S., 1984. Characteristics and tectonic significance of supra-subduction zone ophiolites. In: Kokelaar, B.P., Howells, M.F. (Eds.), Marginal Basin Geology. Geological Society Special Publications, 13, pp. 74–94.

Pearce, J.A., Stern, R.J., Bloomer, S.H., Fryer, P., 2005. Geochemical mapping of the Mariana arc-basin system: implications for the nature and distribution of subduction components. Geochemistry, Geophysics, Geosystems 6 (7). http://dx.doi.org/10.1029/2004GC000895.

Peltonen, P., Kontinen, A., Huhma, H., 1996. Petrology and geochemistry of metabasalts from the 1.95 Ga Jormua ophiolite, Northeastern Finland. Journal of Petrology 37 (6), 1359–1383.

Peltonen, P., Kontinen, A., Huhma, H., 1998. Petrogenesis of the mantle sequence of the Jormua ophiolite (Finland): melt migration in the upper mantle during Palaeoproterozoic continental break-up. Journal of Petrology 39, 297–329.

Peltonen, P., Kontinen, A., Huhma, H., Kuronen, U., 2008. Outokumpu revisited: new mineral deposit model for the mantle peridotite-associated Cu–Co–Zn–Ni–Ag–Au sulphide deposits. Ore Geology Reviews 33, 559–617.

Peng, S., Kusky, T.M., Jiang, X.F., Wang, L., Wang, J.P., Deng, H., 2012. Geology, geochemistry, and geochronology of the Miaowan ophiolite, Yangtze craton: implications for South China's amalgamation history with the Rodinian supercontinent. Gondwana Research 21, 577–594.

Pfänder, J.A., Jochum, K.P., Kozakov, I., Kröner, A., Todt, W., 2002. Central Asia: evidence from trace element and Sr–Nd–Pb isotope data. Contributions to Mineralogy and Petrology 143, 154–174.

Pharaoh, T.C., Warren, A., Walsh, N.J., 1987. Early Proterozoic metavolcanic suites of the northernmost part of the Baltic Shield. In: Pharaoah, T.C., Beckinsale, R.D., Rickard, D. (Eds.), Geochemistry and Mineralization of Proterozoic Volcanic Rocks. Geological Society, Special Publication, vol. 33, pp. 41–58.

Pirajno, F., Occhipinti, S.A., 2000. Three Palaeoproterozoic basins – Yellida, Bryah and Padbury – Capricorn Orogen, Western Australia. Australian Journal of Earth Sciences 47, 675–688.

Pirajno, F., Occhipinti, S.A., Swager, C.P., 1998. Geology and tectonic evolution of the Palaeoproterozoic Bryah, Padbury and Yerrida Basins (formerly Glengarry Basin), Western Australia: implications for the history of the south-central Capricorn Orogen. Precambrian Research 90, 119–140.

Polat, A., 2009. The geochemistry of Neoarchean (ca. 2700 Ma) tholeiitic basalt, transitional to alkaline basalts, and gabbros, Wawa Subprovince, Canada: implications for petrogenetic and geodynamic processes. Precambrian Research 168, 83–105.

Polat, A., Hofmann, A.W., 2003. Alteration and geochemical patterns in the 3.7–3.8 Ga Isua greenstone belt, West Greenland. Precambrian Research 126, 197–218.

Polat, A., Kerrich, R., 2000. Archean greenstone belt magmatism and the continental growth-mantle evolution connection: constraints from Th–U–Nb–LREE systematics of the 2.7 Ga Wawa subprovince, Superior Province, Canada. Earth and Planetary Science Letters 175, 41–54.

Polat, A., Kerrich, R., 2002. Nd-isotopic systematics of 2.7 Ga adakites, magnesian andesites, and arc basalts, Superior Province: evidence for shallow crustal recycling at Archean subduction zones. Earth and Planetary Science Letters 202, 345–360.

Polat, A., Kerrich, R., Wyman, D.A., 1998. The late Archean Schreiber – Hemlo and White River – Dayohessarah greenstone belts, Superior Province: collages of oceanic plateaus, oceanic arcs, and subduction–accretion complexes. Tectonophysics 289, 295–326.

Polat, A., Kerrish, R., Wyman, D.A., 1999. Geochemical diversity in oceanic komatiites and basalts from the late Archean Wawa greenstone belts, Superior Province, Canada: trace element and Nd isotope evidence for a heterogeneous mantle. Precambrian Research 94, 139–173.

Polat, A., Hofmann, A.W., Rosing, M., 2002. Boninite-like volcanic rocks in the 3.7–3.8 Ga Isua greenstone belt, West Greenland: geochemical evidence of intra-oceanic subduction processes in the early Earth. Chemical Geology 184, 231–254.

Polat, A., Li, J., Fryer, B., Kusky, T., Gagnon, J., Zhang, S., 2006. Geochemical characteristics of the Neoarchean (2800–2700 Ma) Taishan greenstone belt, North China Craton: evidence for plume-craton interaction. Chemical Geology 230, 60–87.

Polat, A., Frei, R., Apple, P.W.U., Dilek, Y., Fryer, B., Ordóñez-Calderon, J.C., Yang, Z., 2008. The origin and compositions of Mesoarchean oceanic crust: evidence from the 3075 Ma Ivisaartoq greenstone belt, SW Greenland. Lithos 100 (1–4), 293–321.

Polat, A., Fryer, B.J., Apple, P.W.U., Kalvig, P., Kerrich, R., Dilek, Y., Yang, Z., 2011. Geochemistry of anorthositic differentiated sills in the Archean (2900 Ma) Fiskenæsset Complex, SW Greenland: implications for parental magma compositions, geodynamic setting, and secular heat flow in arcs. Lithos 123, 50–72.

Pollack, N.H., 1997. Thermal characteristics of the Archean. In: de Wit, M.J., Ashwal, L.D. (Eds.), Greenstone Belts. Oxford University Press, Oxford, pp. 223–232.

Puchtel, I.S., 2004. 3.0 Ga Olondo greenstone belt in the Aldan Shield, E. Siberia. In: Kusky, T.M. (Ed.), Precambrian Ophiolites and Related Rocks. Developments in Precambrian Geology, vol. 13, pp. 425–486.

Puchtel, I.S., Hofmann, A.W., Mezger, K., Jochum, K.P., Shchipansky, A.A., Samsonov, A.V., 1998. Oceanic plateau model for continental crustal growth in the Archaean: a case study from the Kostomuksha greenstone belt, NW Baltic Shield. Earth and Planetary Science Letters 155, 57–74.

Please cite this article as: Furnes, H., et al., Precambrian greenstone sequences represent different ophiolite types, Gondwana Research (2013), http://dx.doi.org/10.1016/j.gr.2013.06.004

Quick, J.E., 1990. Geology and origin of the Late Proterozoic Darb Zubaydah ophiolite, Kingdom of Saudi Arabia. Geological Society of America Bulletin 102, 1007–1020.

Ramos, V.A., Escayola, M., Mutti, D.I., Vujovich, G.I., 2000. Proterozoic-early Paleozoic ophiolites of the Andean basement of southern South America. In: Dilek, Y., Moores, E.M., Elthon, D., Nicolas, A. (Eds.), Ophiolites and Oceanic Crust: New Insights from Field Studies and the Ocean Drilling Program. Boulder, Colorado, Geological Society of America, Special Paper, vol. 349, pp. 331–349.

Rasilainen, K., 1996. Alteration geochemistry of gold occurrences in the late Archean Hattu schist belt, Ilomantsi, Eastern Finland. Geological Survey of Finland, Bulletin 388 (88 pp.).

Renner, R., Gibbs, A.K., 1987. Geochemistry and petrology of metavolcanic rocks of the early Proterozoic Mazaruni greenstone belt, northern Guyana. In: Pharaoh, T.C., Beckinsale, R.D., Rickard, D. (Eds.), Geochemistry and Mineralization of Proterozoic Volcanic Rocks. Geological Society, Special Publication, vol. 33, pp. 289–309.

Ries, A.C., Vearncombe, J.R., Price, R.C., Shackleton, R.M., 1992. Geochronology and geochemistry of the rocks associated with a Late Proterozoic ophiolite in West Pokot, NW Kenya. Journal of African Earth Sciences 14 (1), 25–36.

Robinson, P.T., Malpas, J., Dilek, Y., Zhou, M.-F., 2008. The significance of sheeted dike complexes in ophiolites. GSA Today 18 (11), 4–10. http://dx.doi.org/10.1130/GSAT22A.1.

Rosing, M.T., Rose, N.M., Bridgwater, D., Thomsen, S., 1996. Earliest part of Earth's stratigraphic record: a reappraisal of the >3.7 Ga Isua (Greenland) supracrustal sequence. Geology 24, 43–46.

Samson, S.D., Inglis, J.D., D'Lemos, R.S., Admou, H., Blichert-Toft, J., Hefferan, K., 2004. Geochronological, geochemical, and Nd–Hf isotopic constraints on the origin of Neoproterozoic plagiogranites in the Tasriwine ophiolite, Anti-Atlas orogen, Morocco. Precambrian Research 135, 133–147.

Santosh, M., Sajeev, K., 2006. Anticlockwise evolution of ultrahigh-temperature granulites within continental collision zone in southern India. Lithos 92, 447–464.

Sato, K., Siga Jr., O., Nutman, A.P., Basei, M.A.S., McReath, I., Kaulfuss, G., 2003. The Atuba Complex, Southern American Platform: Archean components and Paleoproterozoic to Neoproterozoic tectonothermal events. Gondwana Research 6 (2), 251–263.

Savov, I., Ryan, J., Haydoutov, I., Schijf, J., 2001. Late Precambrian Balkan–Carpathian ophiolite — a slice of the Pan-African ocean crust?: geochemical and tectonic insights from the Tcherni Vrah and Deli Jovan massifs, Bulgaria and Serbia. Journal of Volcanology and Geothermal Research 110, 299–318.

Scarrow, J.H., Pease, V., Fleutelot, C., Dushin, V., 2001. The late Neoproterozoic Enganepe ophiolite, Polar Urals, Russia: an extension of the Cadomian arc. Precambrian Research 110, 255–275.

Scott, R.B., Hajash Jr., A., 1976. Initial submarine alteration of basaltic pillow lavas: a microprobe study. American Journal of Science 276, 480–501.

Scott, D.J., St-Onge, M.R., Lucas, S.B., Helmstaedt, H., 1991. Geology and chemistry of the Early Proterozoic Purtuniq ophiolite, Cape Smith Belt, Northern Quebec, Canada. In: Peters, Tj, Nicolas, A., Coleman, R.G. (Eds.), Ophiolite Genesis and Evolution of the Oceanic Lithosphere. Ministry of Petroleum and Minerals, Sultanate of Oman, pp. 817–849.

Scott, D.J., Helmstaedt, H., Bickle, M.J., 1992. Purtuniq ophiolite, Cape Smith belt, northern Quebec, Canada: a reconstructed section of Early Proterozoic oceanic crust. Geology 20, 173–176.

Scott, C.R., Mueller, W.U., Pilote, P., 2002. Physical volcanology, stratigraphy, and lithogeochemistry of an Archean volcanic arc: evolution from plume-related volcanism to arc rifting of SE Abitibi Greenstone Belt, Val d'Or, Canada. Precambrian Research 115, 223–260.

Şengör, A.M.C., Yilmaz, Y., Sungurlu, O., 1984. Tectonics of the Mediterranean Cimmerides: nature and evolution of the western termination of Palaeo-Tethys. Geological Society of London, Special Publications 17, 77–112.

Seyfried, W.E., Berndt, M.E., Seewald, J.S., 1988. Hydrothermal alteration processes at mid-ocean ridges: constraints from diabase alteration experiments, hot-spring fluids and composition of the oceanic crust. Canadian Mineralogist 26, 787–804.

Shamim Khan, M., Smith, T.E., Raza, M., Huang, J., 2005. Geology, geochemistry and tectonic significance of mafic–ultramafic rocks of Mesoproterozoic Phulad ophiolite suite of South Delhi Fold Belt, NW Indian Shield. Gondwana Research 8 (4), 553–566.

Shchipansky, A.A., Samsonov, A.V., Bibikova, E.V., Babarina, I.I., Konilov, A.N., Krylov, K.A., 2004. 2.8 Ga boninite-hosting partial suprasubduction zone ophiolite sequences from the North Karelian Greenstone Belt, NE Baltic Shield, Russia. In: Kusky, T.M. (Ed.), Precambrian Ophiolites and Related Rocks. Developments in Precambrian Geology, vol. 13, pp. 405–423.

Shervais, J.W., 1982. Ti–V plots and the petrogenesis of modern and ophiolitic lavas. Earth and Planetary Science Letters 32, 114–120.

Shirey, S.B., Richardson, S.H., 2011. Start of the Wilson Cycle at 3 Ga shown by diamonds from subcontinental mantle. Science 333, 434–436.

Skruf'in, P.K., Bayanova, T.B., 2006. Early Proterozoic central-type volcano in the Pechenga structure and its relation to the ore-bearing gabbro-wehrlite complex of the Kola Peninsula. Petrology 14 (6), 609–627.

Skruf'in, P.K., Theart, H.F.J., 2005. Geochemical and tectono-magmatic evolution of the volcano-sedimentary rocks of Pechenga and other greenstone fragments within the Kola Greenstone Belt, Russia. Precambrian Research 141, 1–48.

Smith, T.E., Harris, M.J., 1996. The Queensborough mafic–ultramafic complex: a fragment of a Meso-Proterozoic ophiolite? Grenville Province, Canada. Tectonophysics 265, 53–82.

Smith, A.D., Ludden, J.N., 1989. Nd isotopic evolution of the Precambrian mantle. Earth and Planetary Science Letters 93, 14–22.

Smithies, R.H., Champion, D.C., Van Kranendonk, M.J., Howard, H.M., Hickman, A.H., 2005. Modern-style subduction processes in the Mesoarchaean: geochemical evidence from the 3.12 Ga Whundo intra-oceanic arc. Earth and Planetary Science Letters 231, 221–237.

Spaggiari, C.V., Kirkland, C.L., Pawley, M.J., Smithies, R.H., Wingate, M.T.D., Doyle, M.G., Blenkinsop, T.G., Clark, C., Oorschot, C.W., Fox, L.J., Savage, J., 2011. The geology of the East Albany-Fraser Orogen — a field guide. Geological Survey of Western Australia, Record 2011/23 (106 pp.).

Sprole, R.A., Lesher, C.M., Ayer, J.A., Thurston, P.C., Herzberg, C.T., 2002. Spatial and temporal variations in the geochemistry of komatiites and komatiitic basalts in the Abitibi greenstone belt. Precambrian Research 115, 153–186.

Srivastava, R.K., Singh, R.K., Verma, S.P., 2004. Neoarchaean volcanic rocks from the southern Bastar greenstone belt, Central India: petrological and tectonic significance. Precambrian Research 131, 305–322.

Staudigel, H., Hart, R., 1983. Alteration of basaltic glass: mechanism and significance for the oceanic crust-seawater budget. Geochimica et Cosmochimica Acta 47, 37–50.

Stern, R.J., 1994. Arc assembly and continental collision in the Neoproterozoic East African orogen: implications for the consolidation of Gondwanaland. Annual Review of Earth and Planetary Sciences 22, 319–351.

Stern, R.J., 2002. Crustal evolution in the East African Orogen: a neodymium isotopic perspective. Journal of African Earth Sciences 34, 109–117.

Stern, R.J., 2005. Evidence from ophiolites, blueschists, and ultra-high pressure metamorphic terranes that the modern episode of subduction tectonics began in Neoproterozoic time. Geology 33, 557–560.

Stern, R.J., 2008. Modern-style plate tectonics began in Neopreoterozoic time: an alternative interpretation of Earth's tectonic history. In: Condie, K.C., Pease, V. (Eds.), When Did Plate Tectonics Begin on Planet Earth? Geological Society of America, Special Paper, vol. 440, pp. 265–280.

Stern, R.J., Johnson, P., 2010. Continental lithosphere of the Arabian Plate: a geologic, petrologic, and geophysical synthesis. Earth-Science Reviews 101, 29–67.

Stern, R.J., Nielsen, K.C., Best, E., Sultan, M., Arvidson, R.E., Kröner, A., 1990. Orientation of late Precambrian sutures in the Arabian–Nubian Shield. Geology 18, 1103–1106.

Stern, R.A., Syme, E.C., Bailes, A.H., Lucas, S.B., 1995. Paleoproterozoic (1.90–1.86 Ga) arc volcanism in the Flin Flon Belt, Trans-Hudson Orogen, Canada. Contributions to Mineralogy and Petrology 119, 117–141.

St-Onge, M.R., Lucas, S.B., Scott, D.J., 1997. The Ungava orogen and the Cape Smith thrust belt. In: de Wit, M.J., Ashwal, L.D. (Eds.), Greenstone Belts. Oxford University Press, Oxford, U.K., pp. 772–780.

Strand, K., Köykkä, J., 2012. Early Paleoproterozoic rift volcanism in the eastern Fennoscandian Shield related to the breakup of the Kenorland supercontinent. Precambrian Research 214–215, 95–105.

Svetov, S.A., Svetova, A.I., Huhma, H., 2001. Geochemistry of the komatiite–tholeiite rock association in the Vedlozero–Sehozero Archean greenstone belt, central Karelia. Geochemistry International 39 (Suppl. 1), s24–s38.

Svetov, S.A., Golubev, A.I., Svetova, A.I., 2004. Geochemistry of Sumian basaltic andesites of Central Karelia. Geochemistry International 42 (7), 630–640.

Svetov, S.A., Svetova, A.I., Nazarova, T.N., 2009. Do Sumian high-Mg andesite–basalts belong to the bajaite series? Geology and Useful Minerals of Karelia (2), 112–124.

Sylvester, P.J., Attoh, K., 1992. Lithostratigraphy and composition of 2.1 Ga greenstone belts of West African craton and their bearing on crustal evolution of the Archean–Proterozoic boundary. Journal of Geology 100, 377–393.

Sylvester, P.J., Harper, G.D., Byerly, G.R., Thurston, P.C., 1997. Volcanic aspects of greenstone belts. In: de Wit, M.J., Ashwal, L.D. (Eds.), Greenstone Belts. Oxford University Press, Oxford, U.K., pp. 55–90.

Szilas, K., Van Hinsberg, V.J., Kisters, A.F.M., Hoffmann, J.E., Windley, B.F., Kokfelt, T.F., Schersten, A., Frei, R., Rosing, M.T., Munker, C., 2013. Remnants of arc-related Mesoarchaean oceanic crust in the Tartoq Group of SW Greenland. Gondwana Research 23 (2), 436–451.

Tadesse, G., Allen, A., 2005. Geology and geochemistry of the Neoproterozoic Tuludimtu Ophiolite suite, western Ethiopia. Journal of African Earth Sciences 41, 192–211.

Tassinari, C.C.G., 1997. The Amazonian Craton. In: de Wit, M.J., Ashwal, L.D. (Eds.), Greenstone Belts. Oxford University Press, Oxford, pp. 558–566.

Tassinari, C.C.G., Macambira, M.J.B., 1999. Geochronological provinces in the Amazonian Craton. Episodes 22 (3), 174–182.

Tassinari, C.C.G., Munha, J.M.U., Ribeiro, A., Correia, C.T., 2001. Neoproterozoic oceans in the Ribeira Belt (southeastern Brazil): the Pirapora do Bom Jesus ophiolitic complex. Episodes 24 (4), 245–251.

Van Kranendonk, M.J., 2007. Tectonics of early Earth. In: Van Kranendonk, M.J., Smithies, R.H., Bennet, V.C. (Eds.), Earth's Oldest Rocks. Development in Precambrian Geology, vol. 15. Elsevier B.V., pp. 1105–1116.

Van Kranendonk, M.J., 2011. Cool greenstone drips and the role of partial convective overturn in Barberton greenstone belt evolution. Journal of African Earth Sciences 60, 346–352.

Van Kranendonk, M.J., Pirajno, P., 2004. Geochemistry of metabasalts and hydrothermal alteration zones associated with *c.* 3.45 Ga chert and barite deposits: implications for the geological setting of the Warrawoona Group, Pilbara Craton, Australia. Geochemistry: Exploration, Environment, Analysis 4, 253–278.

Van Kranendonk, M.J., Hickman, A.H., Williams, I.R., Nijman, W., 2001. Archaen geology of the East Pilbara granite–greenstone terrane, western Australia — a field guide. Geological Survey of Western Australia, Record 2001/9 (134 pp.).

Van Kranendonk, M.J., Smithies, R.H., Bennett, V.C. (Eds.), 2007a. Earth's Oldest Rocks. Condie, K.C. (Ed.), 2007a. Developments in Precambrian Geology, vol. 15. Elsevier, Amsterdam (1307 pp.).

Van Kranendonk, M.J., Smithies, R.H., Hickman, A.H., Champion, D.C., 2007b. Review: secular tectonic evolution of Archean continental crust: interplay between horizontal and vertical processes in the formation of the Pilbara Craton, Australia. Terra Nova 19 (1), 1–38.

Please cite this article as: Furnes, H., et al., Precambrian greenstone sequences represent different ophiolite types, Gondwana Research (2013), http://dx.doi.org/10.1016/j.gr.2013.06.004

Van Kranendonk, M.J., Kröner, A., Hegner, E., Connelly, J., 2009. Age, lithology and structural evolution of the c. 3.53 Ga Theespruit Formation in the Tjakastad area, southwestern Barberton Greenstone Belt, South Africa, with implications for Archaean tectonics. Chemical Geology 261 (1–2), 115–139.

Vidal, M., Alric, G., 1994. The Palaeoproterozoic (Birimian) of Haute-Comoé in the West Africa Craton, Ivory Coast: a transtensional back-arc basin. Precambrian Research 65, 207–229.

Vijaya Kumar, K., Ernst, W.G., Leelanandam, C., Wooden, J.L., Grove, M.J., 2010. First Paleoproterozoic ophiolite from Gondwana: geochronological–geochemical documentation of ancient oceanic crust from Kandra, SE India. Tectonophysics 487, 22–32.

Viljoen, M.J., Viljoen, R.P., 1969. An introduction to the geology of the Barberton granite–greenstone terrain. Geological Society of South Africa Special Publication 2, 9–28.

Volpe, A.M., Macdougall, J.D., 1990. Geochemistry and isotope characteristics of mafic (Phulad Ophiolite) and related rocks in the Delhi Supergroup, Rajasthan, India: implications for rifting in the Proterozoic. Precambrian Research 48, 167–191.

Vrevsky, A.B., 2011. Petrology, age, and polychronous sources of the initial magmatism of the Imandra-Varzuga paleorift, Fennoscandian Shield. Petrology 19 (5), 521–547.

Vujovich, G.I., Kay, S.M., 1998. A Laurentian? Grenville-age oceanic arc/back-arc terrane in the Sierra de Pie de Palo, Western Sierras Pampeanas, Argentina. In: Pankhurst, R.J., Rapela, C.W. (Eds.), The Proto-Andean Margin of Gondwana. Geological Society, London, Special Publications, vol. 142, pp. 159–179.

Walker, J.D., Geissman, J.W., Bowring, S.A., Babcock, L.E., 2013. The Geological Society of America Geologic Time Scale. Geological Society of America Bulletin 125 (3/4), 259–272.

Wang, W., Yang, E., Zhai, M., Wang, S., Santosh, M., Du, L., Xie, H., Lv, B., Wan, Y., 2013. Geochemistry of 2.7 Ga basalts from Taishan area: constraints on the evolution of early Neoarchean granite-greenstone belt in western Shandong Province, China. Precambrian Research 224, 94–109.

Whitmeyer, S.J., Karlstrom, K.E., 2007. Tectonic model for the Proterozoic growth of North America. Geosphere 3 (4), 220–259.

Wilhem, C., Windley, B.F., Stampfli, G.M., 2012. The Altaids of Central Asia: a tectonic and evolutionary innovative review. Earth-Science Reviews 113, 303–341.

Wilks, M.E., Harper, G.D., 1997. Wind River Range, Wyoming Craton. In: de Wit, M.J., Ashwal, L.D. (Eds.), Greenstone Belts. Clarendon Press, Oxford, pp. 508–516.

Wilson, A.H., 2003. A new class of silica enriched, highly depleted komatiites in the southern Kaapvaal Craton, South Africa. Precambrian Research 127 (1–3), 125–141.

Windley, B.F., 1995. The Evolving Continents. John Wiley & Sons, Chichester 544.

Wyman, D.A., 1999a. A 2.7 Ga depleted tholeiitic suite: evidence of plume-arc interaction in the Abitibi Greenstone Belt, Canada. Precambrian Research 97, 27–42.

Wyman, D.A., 1999b. Paleoproterozoic boninites in an ophiolite-like setting, Trans-Hudson orogen, Canada. Geology 27 (5), 455–458.

Wyman, D.A., Kerrich, R., 2012. Geochemical and isotopic characteristics of Youanmi terrane volcanism: the role of mantle plumes and subduction tectonics in the eastern Yilgarn Craton. Australian Journal of Earth Sciences 59, 671–694.

Wyman, D.A., O'Neill, C., Ayer, J.A., 2008. Evidence for modern-style subduction to 3.1 Ga: a plateau-adakite-gold (diamond) association. In: Condie, K.C., Pease, V. (Eds.), When Did Plate Tectonics Begin on Planet Earth? . Geological Society of America, Special Paper, vol. 440, pp. 129–148.

Xia, X., Song, S., Niu, Y., 2012. Tholeiite-Boninite terrane in the North Qilian suture zone: implications for subduction initiation and back-arc basin development. Chemical Geology 328, 259–277.

Xie, Q., Kerrich, R., Fan, J., 1993. HFSE/REE fractionations recorded in three komatiite-basalt sequences, Archean Abitibi greenstone belt: implications for multiple plume sources and depths. Geochimica et Cosmochimica Acta 57, 4111–4118.

Yellappa, T., Chetty, T.R.K., Tsunogae, T., Santosh, M., 2010. The Manamedu Complex: geochemical constraints on Neoproterozoic suprasubduction zone ophiolite formation within the Gondwana suture in southern India. Journal of Geodynamics 50, 268–285.

Yibas, B., Reimold, W.U., Anhaeusser, C.R., Koeberl, C., 2003. Geochemistry of the mafic rocks of the ophiolitic fold and thrust belts of southern Ethiopia: constraints on the tectonic regime during the Neoproterozoic (900–700 Ma). Precambrian Research 121, 157–183.

Yiğitbaş, E., Kerrich, R., Yilmaz, Y., Elmas, A., Xie, Q., 2004. Characteristics and geochemistry of Precambrian ophiolites and related volcanics from the Istanbul-Zonguldak Unit, Northwestern Anatolia, Turkey: following the missing chain of the Precambrian South European suture zone to the east. Precambrian Research 132, 179–206.

Zakariadze, G.S., Dilek, Y., Adamia, S.A., Oberhansli, R.E., Karpenko, S.F., Bazylev, B.A., Solov'eva, N., 2007. Geochemistry and geochronology of the Neoproterozoic Pan-African Transcaucasian Massif (Republic of Georgia) and implications for island arc evolution of the late Precambrian Arabian-Nubian Shield. Gondwana Research 11, 92–108.

Zhai, M., Zhao, G., Zhang, Q., 2002. Is the Dongwanzi Complex an Archean ophiolite? Science 295, 923a.

Zhao, G., Cawood, P.A., 2012. Precambrian geology of China. Precambrian Research 222–223, 13–54.

Zhao, G., Wilde, S.A., Li, S., Sun, M., Grant, M.L., Li, X., 2007. U-Pb zircon age constraints on the Dongwanzi ultramafic-mafic body, North China, confirm that it is not an Archean ophiolite. Earth and Planetary Science Letters 255, 85–93.

Zhao, G., Li, S., Sun, M., Wilde, S.A., 2011. Assembly, accretion, and break-up of the Palaeo-Mesoproterozoic Columbia supercontinent: record in the North China revisited. International Geology Review 53 (11–12), 1331–1356.

Zhou, G., 1989. The discovery and significance of the northeastern Jiangxi Province ophiolite (NEJXO), its metamorphic peridotite and associated high temperature-high pressure metamorphic rocks. Journal of Southeast Asian Sciences 3 (1–4), 237–247.

Zimmer, M., Kröner, A., Jochum, K.P., Reishmann, T., Todt, W., 1995. The Gabal Gerf complex: a Precambrian N-MORB ophiolite in the Nubian Shield, NE Africa. Chemical Geology 123, 29–81.

Zucchetti, M., 2007. Rochas máficas do Grupo Grão pará e sua relação com a mineralizão de ferro dos depósitos N4eN5, Carajás, PA. (PhD thesis) (125 pp.).

Zucchetti, M., Lobato, L.M., Baars, F.J., 2000. Genetically diverse basalt geochemical signatures developed in the Rio das Velhas Greenstone Belt, Quadrilátero Ferrífero, Minas Gerais, Brazil. Revista Brasileira de Geociências 30 (3), 397–402.

**Harald Furnes** is professor at the Department of Earth Science, University of Bergen, Norway, since 1985. He received his D.Phil. at the University of Oxford, UK, in 1978. His main research interest has been connected to volcanic rocks. This involves physical volcanology, geochemistry and petrology of volcanic rocks, mainly connected to ophiolites and island arc development of various ages. During the last 10 years much focus has been on Precambrian greenstone belts and the Paleoarchean Barberton Greenstone Belt in particular. Another research focus has been related to the alteration of volcanic glass, which again led to a long-term study on the interaction between micro-organisms and glassy rocks, and the search for traces of early life. On these topics he has published a number of refereed papers in international journals.

**Yildirim Dilek** is a *Distinguished Professor of Geology* at Miami University (USA), where he teaches structural geology, global tectonics and geopolitics. He received his PhD from the University of California. He was a Senior Research Fellow at the Getty Conservation Institute in Los Angeles and a professor at Vassar College in New York before he joined the faculty at Miami University. He is affiliated with the China University of Geosciences-Beijing and the Chinese Academy of Geosciences-Beijing, China, and with the University of Torino, Italy. He has been a Visiting Professor at Ecole Normal Superieur in Paris-France, University of Bergen-Norway, University of Tsukuba-Japan, and University of Kanazawa-Japan. He served as the Editor of the Geological Society of America Bulletin and on the Editorial Boards of Geology, Lithos, Tectonophysics, and Journal of the Geological Society of London. He has served as a member of the UNESCO Science Board, and the U.S. Science Advisory Committee. Professor Dilek has worked extensively on the Phanerozoic ophiolites around the world, particularly those in the Alpine-Himalayan, North American Cordilleran and Caledonian ophiolites. His other research interests and activities include Precambrian tectonics and early life, collisional and post-collisional tectonics and magmatism in young orogenic belts, extensional tectonics and core complex development, and mélange-forming processes and the evolution of subduction–accretion complexes in convergent margin settings. He has published over 150 peer-reviewed journal papers and has edited/co-edited 22 books and special volumes.

**Maarten Johan de Wit** was born in Holland, went to school in Holland and Ireland, and completed his BSc/MA in Ireland (Trinity College, Dublin), PhD in England (Cambridge University), and was a postdoc at the Lamont Doherty Earth Observatory, Columbia University, USA. Presently he holds the chair of Earth Stewardship Science at the Nelson Mandela Metropolitan University in Port Elizabeth, South Africa. He was the Founding Director of AEON (Africa Earth Observatory Network), a transdisciplinary research institute (www.aeon.org.za). His scientific interests lie in how the Earth works (particular in its youthful stage); in global tectonics; the evolution of Africa and Gondwana; the origin of continents, life and mineral resources; and in the economics of natural-resources and sharing of the 'commons'. He has mapped in the Barberton Greenstone Belt since 1979.

Please cite this article as: Furnes, H., et al., Precambrian greenstone sequences represent different ophiolite types, Gondwana Research (2013), http://dx.doi.org/10.1016/j.gr.2013.06.004